Coordination Chemistry Reviews, 13 (1974) 339–406

PRINCIPLES OF STRUCTURE, BONDING, AND REACTIVITY FOR METAL NITROSYL COMPLEXES*

J.H. ENEMARK and R.D. FELTHAM

Department of Chemistry, University of Arizona, Tucson, Arizona 85721, USA

(Received October 9th, 1973; Revised January 21st, 1974)

CONTENTS

* Presented in part at the ACS–CIC Summer Symp. on Inorganic Chemistry, *Coordination and Activation of Small Molecules*, Buffalo, N.Y., June 19–21, 1972.

ABBREVIATIONS

acacen	*N,N'*-ethylenebis(acetylacetoneiminato)-
benacen	*N,N'*-ethylenebis(benzoylacetoneiminato)-
bipy	bipyridyl
das	*o*-phenylenebis (dimethylarsine)
diphos	1,2-diphenylphosphinoethane
dmpe	1,2-dimethylphosphinoethane
dtc	dithiocarbamate
en	ethylenediamine
EPR	electron paramagnetic resonance
EPA	ether–isopentane–alcohol
$f_6$fos	$(C_6H_5)_2PC=CP(C_6H_5)_2(CF_2)_2CF_2$
IR	infrared
l.h.s.	left-hand side
mnt	maleonitriledithiolate
r.h.s.	right-hand side
r.m.s.	root-mean-square
SCCC-MO	self consistent charge molecular orbitals
SCV	stereochemical control of valence
TBP	trigonal bipyramid
tep	$CH_3C[CH_2P(C_2H_5)_2]_3$
TP	tetragonal pyramid
TPP	tetraphenylporphine dianion
UV	ultraviolet

I. INTRODUCTION

The structure, bonding, and reactivity of transition metal nitrosyls have been provocative subjects for many years. There have been several reviews of metal nitrosyls[1,2], but no unified description of the bonding in metal nitrosyl complexes which adequately accounts for all their known structural, physical, and chemical properties has yet been provided. Sidgwick[1] initially classified metal nitrosyls as derivatives of either NO^+ or NO^-. This classification was continued by others[2] and is still extant. However, research has demonstrated that transition metal nitrosyls are highly covalent entities. Consequently, attempts to correlate their structures, physical properties, and reactivity with the formal oxidation state of the nitrosyl group have not been successful. Therefore, in writing this review, we have developed an alternative description of the bonding in metal nitrosyl complexes utilizing the molecular orbital correlation method.

The molecular orbital correlation method, developed by Hund[118] and Mulliken[119] for diatomic molecules, has proven extremely useful for unifying and understanding large areas of seemingly diverse chemistry. Walsh[3] successfully applied the correlation method in his pioneering analysis of the structures of triatomic species of the non-transition elements. More recently, Woodward and Hoffmann[120] utilized this method to provide a framework for understanding concerted reactions of olefins. Both of these applications showed that the nature of the highest occupied molecular orbital is of paramount importance in understanding the chemistry of the respective systems.

Although molecular orbital correlation diagrams have been constructed for several specific classes of metal nitrosyl complexes[5,6], a general analysis of the structure, bonding, and reactivity of metal nitrosyls based upon this approach has not appeared previously. The qualitative molecular orbital diagrams in this review are based upon previous molecular orbital studies[8,9], but take into account the ambiguities in ordering the energies of the molecular orbitals of the metal nitrosyl complexes. The molecular orbital correlation diagrams were obtained by: (1) treating each $M(NO)_x$ moiety as a covalently bound functional group which is perturbed by the coordination of additional ligands to the metal; (2) correlating all reasonable orderings of the molecular orbitals of the complex in its various geometries; (3) examining the nature of the highest occupied molecular orbital and ascertaining the structural consequences for the $M(NO)_x$ moiety.

Our results show that the properties of nitrosyl complexes are primarily determined by the nature of the highest occupied molecular orbital. In this respect, these results are similar to those obtained for other systems[3,120]. Our diagrams provide for the occurrence of metal nitrosyl complexes with intermediate geometries and define the circumstances for their existence. The diagrams also delineate the pathways whereby metal nitrosyl complexes with differing geometries may be interconverted. Finally, it is our hope that the conclusions regarding the relationships among structure, bonding, and reactivity of metal nitrosyl complexes obtained from these diagrams will stimulate detailed studies of the electronic properties of metal nitrosyls, investigations of the mechanisms of nitrosyl reactions, and syntheses of new classes of metal nitrosyl complexes.

II. MONONITROSYL COMPLEXES

The triatomic species MNO forms a large group of complexes whose properties and geometries have been investigated extensively. The bonding is dominated by covalent interaction of the metal with a single nitrosyl group. For this reason, it has proved instructive to compare the triatomic MNO group with triatomic molecules of the main group elements for which structural and electronic data are available.

A. Triatomic MNO

The geometries of triatomic species were considered in detail by Walsh[3]. Although Walsh's study was concerned with triatomic species which had only *s* and *p* orbitals in the

valence shells of the atoms, he did suggest that the concepts should be generally applicable. Mingos and Ibers[4] have pointed out that Walsh's concepts may be applicable to understanding the M–N–O angles in metal nitrosyl complexes, and Pierpont and Eisenberg[5] and Mingos[6] have utilized these concepts in attempts to interpret the geometries of tetragonal metal nitrosyl complexes. In order to determine whether the MNO group can be correctly described as a triatomic species perturbed by attaching ligands to the metal, Walsh's procedure will be applied to the MNO group. We will first investigate the behavior of the $O–N–O^m$ group ($m = +1, 0, -1$) and then ascertain the effects of replacing one of the oxygen atoms of this group by a metal atom.

In the series NO_2^+, NO_2, and NO_2^- the O–N–O bond angles are 180°, 134°, and 115°, respectively. Figure 1 shows a modified version[7] of Walsh's diagram which accounts for this behavior of the NO_2^m species. In linear NO_2^+ the 16 valence electrons in the 2*s* and 2*p* orbitals will fill the molecular orbitals through $1\pi_g$. The orbital $1\pi_g$ is a non-bonding molecular orbital which is destabilized by decreasing the O–N–O angle. Therefore, NO_2^+ remains linear. For linear NO_2 and NO_2^-, however, one and two electrons, respectively, must go into the $2\pi_u$

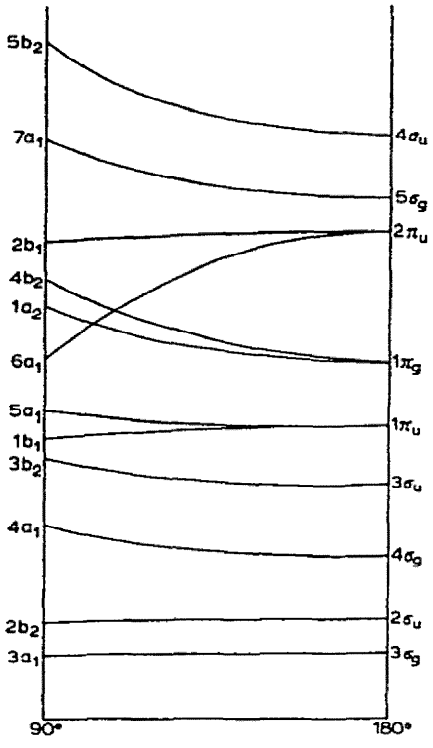

Fig. 1. Walsh diagram for XY_2 molecules. The order of the orbitals at right and left is not uniquely determined from theory. The 1*s* orbitals of X and Y are omitted but have been taken into account in the numbering of the orbitals. From G. Herzberg, *Molecular Spectra and Molecular Structure*, Vol. III: *Electronic Spectra and Electronic Structure of Polyatomic Molecules.* © 1966, Reprinted by permission of Van Nostrand Reinhold Company.

molecular orbital. *This orbital is anti-bonding with respect to all three atoms.* Figure 1 shows that bending the triatomic species greatly stabilizes the $6a_1$ component, a non-bonding orbital localized on the central atom. Thus, the formal addition of two electrons to the NO_2^+ ion to form the NO_2^- ion results in a decrease in the O–N–O bond angle from 180° to 115° and the localization of a pair of electrons in an sp^2-type orbital on the nitrogen atom.

The replacement of one of the terminal oxygen atoms of ONO by a metal possessing *d* orbitals results in several modifications of the molecular orbital scheme and its interpretation (Fig. 2). If *z* is taken as the molecular axis of the linear triatomic species MNO, then 4σ is an anti-bonding orbital (d_{z^2}) corresponding to $5\sigma_g$ of NO_2^+; $2\pi(d_{xz}, d_{yz}, \pi^*$ (NO)) corresponds to $1\pi_g$ of NO_2^+; and δ ($d_{x^2-y^2}$) is non-bonding with respect to the NO group and has no counterpart in NO_2^+. Therefore, the formal replacement of an O atom of the NO_2^+ group with a metal atom results in a triatomic species which requires a total of 18 electrons to fill all of the bonding and non-bonding orbitals (through δ).

Any additional electrons must occupy 3π which is antibonding with respect to all three atoms of MNO and which has a large contribution from the nitrogen atom. This 3π orbital corresponds to the $2\pi_u$ orbital of Fig. 1 and hence, population of 3π should give rise to a bent MNO species if Walsh's arguments apply.

The possibility that 4σ is lower in energy than 3π must also be considered. The 4σ orbital is antibonding with respect to M and N, and is composed primarily of d_{z^2} located on the terminal metal atom (cf. NO_2^+). If the 4σ orbital lies lower than 3π, additional electrons (over eighteen) will populate 4σ and the triatomic species will distort to

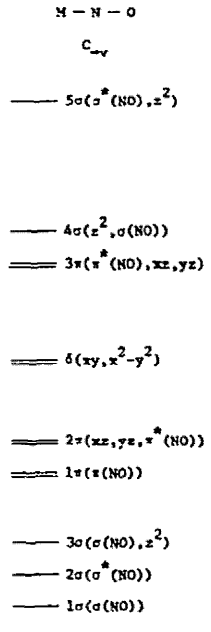

Fig. 2. The molecular orbital diagram proposed for the linear triatomic species, MNO.

localize non-bonding electrons on the terminal metal atom. Simple triatomic metal nitrosyl compounds are currently unknown. Therefore, the applicability of the triatomic model of mononitrosyl complexes will be first examined for six-coordinate compounds.

B. Six-coordination

In a six-coordinate complex of the MNO group the maximum symmetry is C_{4v}, and the molecular orbitals of the triatomic species (Fig. 2) are modified accordingly. The degeneracy of the two delta orbitals is lifted because $1b_1$ ($d_{x^2-y^2}$) is now strongly antibonding with respect to the four equatorial ligands of the complex, while $1b_2$(d_{xy}) is still non-bonding. The $4a_1$ orbital (d_{z^2}) is still antibonding and now of energy comparable to $1b_1$($d_{x^2-y^2}$). These modifications result in molecular orbital energies (Fig. 3) which are in agreement with those usually utilized for describing six-coordinate mononitrosyl complexes[2].

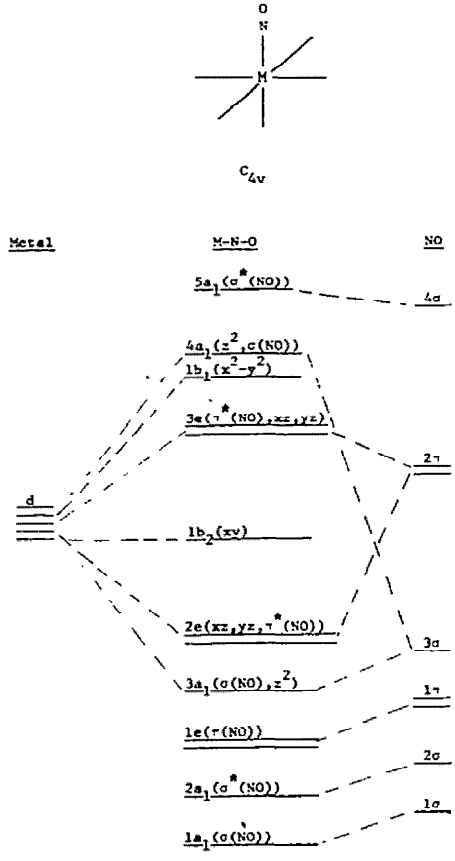

Fig. 3. The molecular orbital diagram for six-coordinate complexes with linear MNO groups. The z axis is coincident with the M–N bond.

Recently, Fenske and DeKock[8] have presented the results of detailed molecular orbital calculations in C_{4v} symmetry for the series of six-coordinate mononitrosyl complexes, $M(CN)_5NO^{m-}$. Their results are in general agreement with the conclusions reached earlier by Manoharan and Gray[9] from their studies of the electronic spectra of $Cr(CN)_5NO^{3-}$, $Mn(CN)_5NO^{3-}$, and $Fe(CN)_5NO^{2-}$. The essential difference between the results of Fenske and DeKock's calculations and the molecular orbitals in Fig. 3 is that only the energy levels of the triatomic species, MNO, in a field of C_{4v} symmetry have been considered. The orbital $3a_1$ is primarily localized on the N atom of the NO ligand and is σ-bonding with respect to the MNO group. The degenerate $2e$ orbital, consisting primarily of the metal d_{xz}, d_{yz} and the π^* orbitals of the NO ligand, is bonding with respect to M and N and is antibonding between N and O. The $1b_2$ orbital is localized on the metal (d_{xy}) and is non-bonding. Thus, an MNO complex with the electron configuration $(3a_1)^2(2e)^4$ has three bonding interactions between the metal and the NO group. This situation corresponds to the usual "back-bonding" model used in describing the bonding of NO^+ or CO with transition metals. The presence or absence of electrons in the $1b_2$ orbital will be of minor consequence as far as the MNO group is concerned.

It is convenient to classify MNO complexes by the number of d-type electrons present in the complex. Thus, an MNO complex with the electron configuration $(3a_1)^2(2e)^4$ would be written as $\{MNO\}^4$, one with an electron configuration $(3a_1)^2(2e)^4(1b_2)^2$ would be $\{MNO\}^6$ and so forth. This method of designating the number of d-type electrons present in MNO complexes corresponds to the familiar number of d electrons on the metal when the nitrosyl ligand is formally considered to be $N{\equiv}O^+$. This classification scheme will be used throughout the remainder of this review.

The structures of $Cr(CN)_5NO^{3-}$, $Mn(CN)_5NO^{3-}$ and $Fe(CN)_5NO^{2-}$ have all been determined by X-ray methods (Table 1)[10–12]. These complexes, $\{CrNO\}^5$, $\{MnNO\}^6$, and $\{FeNO\}^6$, all have essentially linear MNO groups (175–180°) and short M–N distances (1.63–1.71 Å). Several spectroscopic techniques have proved valuable for investigating the electronic structures of these complexes. Several groups[9,13–20] have investigated the EPR spectrum of $Cr(CN)_5NO^{3-}$. While there is not complete agreement on the interpretation of the EPR data for this complex, the important experimental results can be summarized as follows: (1) the g tensor and chromium hyperfine tensor have axial symmetry; (2) the nitrogen hyperfine tensor has near axial symmetry, the maximum deviation from axial symmetry (9°) being comparable to the observed deviation from linearity of the CrNO group (4.4°); (3) $g_\perp > g_\parallel$ and the nitrogen hyperfine tensor is highly anisotropic. Using their molecular orbital wave functions and spin–orbit coupling, Manoharan and Gray[9] obtained satisfactory agreement between the observed values for $g_\parallel$, $g_\perp$, and $|A-B|$ (Cr) and those calculated for the $^2B_2$ ground state expected from the electron configuration, $(2e)^4(1b_2)^1$, for $Cr(CN)_5NO^{3-}$. However, since $1b_2$ is non-bonding with respect to the NO group, the observation of large ^{14}N hyperfine coupling represents a significant deviation from an ^{14}N hyperfine coupling of zero expected from the one-electron molecular orbital configuration. Manoharan and Gray[9] suggested that configuration interaction between the electronic states with $^2B_2$ symmetry could account for the observed ^{14}N hyperfine coupling, while Goodman

TABLE 1
Data for representative six-coordinate mononitrosyl complexes

Complex	ν_{NO} (cm^{-1})	N–1s (eV)	M–N (A)	M–N–O (deg)	Electron configuration[a]
$[V(CN)_5(NO)]^{3-}$	1530 [b]	–	1.79 [b,c]	176	{VNO}[4]
$[Cr(CN)_5(NO)]^{3-}$	1660 [d]	400.7 [e]	1.71(1) [d]	176(1)	{CrNO}[5]
$[Mn(CN)_5(NO)]^{3-}$	1700 [f]	401.0 [g]	1.66(1) [h]	174(1)	{MnNO}[6]
$[Fe(CN)_5(NO)]^{2-}$	1939 [i]	403.3 [j]	1.63(2) [k]	178(1)	{FeNO}[6]
$[Fe(das)_2(NO)Cl]^{2+}$	1883 [l]	402.9 [j]	–	–	{FeNO}[6]
$[Fe(das)_2(NO)Cl]^{+}$	1620 [m]	400.0 [j]	1.7 [n]	148(2) [n]	{FeNO}[7]
$[Co(NH_3)_5(NO)]^{2+}$	1620 [o]	400.7 [j]	1.871(6) [p]	119(1)	{CoNO}[8]
$[Co(en)_2(NO)Cl]^{+}$	1611 [q]	–	1.82(1) [r]	124(1)	{CoNO}[8]
$[Co(en)_2(NO)(OClO_3)]^{+}$	1663 [q]	–	1.86 [s]	122	{CoNO}[8]
$[Co(das)_2(NO)(NCS)]^{+}$	1587, 1561 [q,t]	400.5 [j,u]	1.87(2) [v]	134(2)	{CoNO}[8]

a See text.
b S. Jagner and N.G. Vannerberg, *Acta Chem. Scand.*, 22 (1968) 3330.
c Average of an NO group and a CN group statistically disordered.
d See ref. 10.
e D. Hendrickson, J.M. Hollander and W.L. Jolly, *Inorg. Chem.*, 8 (1969) 2642.
f P. Gans, A. Sabatini and L. Sacconi, *Inorg. Chem.*, 5 (1966) 1877.
g R.D. Feltham, unpublished results.
h See ref. 11.
i See ref. 40.
j See ref. 21.
k See ref. 12.
l See ref. 87.
m W. Silverthorn and R.D. Feltham, *Inorg. Chem.*, 6 (1967) 1662.
n Data for $[Fe(das)_2(NO)Br][ClO_4]$, see ref. 26.
o E.P. Bertin, S. Mizushima, T.J. Lane and J.V. Quagliano, *J. Amer. Chem. Soc.*, 81 (1959) 3821.
p See ref. 29.
q See ref. 32.
r See ref. 30.
s J.H. Enemark and R.D. Feltham, *Abstr. Amer. Crystallogr. Ass.*, 2 (1974) 107.
t The two frequencies presumably result from *cis* and *trans* isomers (see ref. 32).
u Data for *trans*-$[Co(das)_2(NO)Cl]Cl$.
v See ref. 31.

et al.[17] have suggested that spin-polarization of the electrons in the 2e orbitals by the $1b_2$ electron is the source of the large anisotropic ^{14}N hyperfine coupling. However, the small deviation of the Cr–N–O angle from 180° could also account for the observed ^{14}N hyperfine interaction, since any non-linearity of the CrNO group will introduce non-zero overlap between the $1b_2$ orbital of the chromium and the π orbitals of nitrogen. This non-linearity of the CrNO group will also cause the ^{14}N hyperfine tensor to be quantized along an axis which is not coincident with either the Cr–N axis, the *g tensor*, or the ^{53}Cr hyperfine tensor.

Although there is ambiguity in interpreting the ^{14}N hyperfine coupling, the successful explanation of the g values, the ^{53}Cr and ^{13}C coupling constants, and the results of both sets of molecular orbital calculations are all consistent with the assignment of a $^2B_2$ ground state for $Cr(CN)_3NO^{3-}$ with the ordering of the molecular orbital energy levels given in Fig. 3.

Wide use has also been made of visible–UV spectroscopy for investigating the excited electronic states of the MNO complexes. Manoharan and Gray[9] investigated the visible–UV spectrum of $Cr(CN)_5NO^{3-}$ between 77 and 298°K and assigned the observed transitions on the basis of the one-electron molecular orbital diagram given in Fig. 3. The molecular orbital wave functions obtained from their SCCC-MO calculations were utilized to calculate the energies of the one-electron transitions and also the EPR parameters mentioned above. Although the agreement obtained by Manoharan and Gray between the observed electronic transition energies and the calculated one-electron energies is possibly fortuitous, the fact that the model can accomodate such a wide variety of experimental facts is encouraging.

Assessment of the molecular orbital scheme for $Fe(CN)_5NO^{2-}$ and $Mn(CN)_5NO^{3-}$, $((2e)^4(1b_2)^2)$, is experimentally more difficult, since few direct probes have been utilized in investigating the ground states of these diamagnetic complexes. Manoharan and Gray[9] did study the low-lying excited electronic states of these two complexes in solution and in single crystals of $Na_2Fe(CN)_5NO \cdot 2H_2O$. From the known crystal structure of $Na_2Fe(CN)_5NO \cdot 2H_2O$, the observed electronic transitions and their polarizations were interpreted using the same ordering of molecular orbitals outlined in Fig. 3. The electronic transitions

TABLE 2
Electronic and EPR spectra of some six-coordinate mononitrosyl complexes

Complex	Electron configuration	Magnetic properties	Absorption maxima (kK), (ϵ, (M^{-1} cm^{-1}))
$[Cr(CN)_5(NO)]^{3-}$	$\{CrNO\}^5$	$g_{\parallel} = 1.9922$;[a] $g_{\perp} = 2.0311$	13.7(8); 15.4(1.5; 22.2(72); 27.3(59); 37.3(1100); 43.5(3600)
$[Fe(CN)_5(NO)]^{2-}$	$\{FeNO\}^6$	diamagnetic[a]	20.8(8); 25.4(25); 30.3(sh); 37.8(900); 42.0(700); 50.0(24,000)
$[Mn(CN)_5(NO)]^{3-}$	$\{MnNO\}^6$	diamagnetic[a]	18.5(22); 24.7(66); 29.0(111); 37.9(1000); 42.6(4500x); 45.5(5000)
$[Fe(CN)_5(NO)]^{3-}$	$\{FeNO\}^7$	$g_x = 1.999$; $g_y = 1.970$; $g_z = 1.956$[b]	not reported
$[Fe(das)_2(NO)Cl]^+$	$\{FeNO\}^7$	$\mu = 1.8$BM[c]	10.6(170); 13.5(sh); 17.3(190); 24.0(sh)
$[Co(en)_2(NO)Cl]^+$	$\{CoNO\}^8$	diamagnetic[d]	9.0; 13.5; 18.0; 22.7; 28.0
$[Co(das)_2(NO)Cl]^+$	$\{CoNO\}^8$	diamagnetic[d]	8–9(sh); 12.5; 19.2

a Ref. 9.
b Ref. 25.
c Refs. 34–36.
d Ref. 32.

which have been observed and assigned for these pentacyanonitrosyl complexes are listed in Table 2.

Fenske and DeKock[8] have utilized their molecular orbital calculations to obtain the electron populations of the various orbitals of the metal and ligand basis set. They have shown that there is a linear relationship between the square of the observed ν_{NO} and the electronic occupation of the π^* orbital of the nitrosyl group. While such a correlation is not a direct test of the calculated *energies* of the one-electron molecular orbitals, such a relationship does indicate that the changes in the coefficients of the one-electron eigenvectors are rather well accounted for by their calculations.

At this point it is important to reemphasize that the energies of the metal *d* orbitals and the π^* orbitals of the NO ligand are similar. Consequently, the relative distribution of electrons between metal and NO in the 2*e* molecular orbital can vary markedly among isoelectronic complexes, and relatively minor changes in the metal atom and/or the other ligands coordinated to the metal may result in dramatic differences in physical properties. The isoelectronic complexes $Fe(CN)_5NO^{2-}$ and $Mn(CN)_5NO^{3-}$ provide a good example of such differences. Both compounds have linear MNO groups. However, ν_{NO} values for the two complexes differ by 200 cm^{-1}, and the N–1*s* binding energies of the nitrosyl group differ by 2.3 eV. These differences correlate well with the change in the metal *d* character of the 2*e* orbital. Thus, the N–1*s* binding energy and ν_{NO} are related to the *effective charge* on the NO group, but not necessarily to its *geometry*. Conversely, the M–N distance and the M–N–O angle describe the geometry of the complex, but in themselves do not provide sufficient information concerning the distribution of charge in the MNO group. Consequently, it is quite misleading to describe all linear complexes as derivatives of NO^+ and all bent complexes as derivatives of NO^-. It is equally tenuous to deduce the geometry of the MNO grouping from ν_{NO} and the N–1*s* binding energy alone†.

Further evidence regarding large changes in electron distribution between the metal and the NO group has recently been obtained from the photoelectron spectra of these compounds (Table 1). For example, both $Fe(CN)_5NO^{2-}$ and $Cr(CN)_5NO^{3-}$ possess essentially linear MNO groups, but the N–1*s* binding energy of the nitrosyl group in the chromium complex is lower than that of the iron complex. This difference in binding energy is substantiated by the calculated occupancies of the π^* orbitals of the NO groups in these two complexes which were found to be 1.1 and 1.6 e^- for the Fe and Cr complexes, respectively[8]. Moreover, Finn and Jolly[21] have found a roughly linear relationship between the N–1*s* photoelectron binding energy and ν_{NO}. Thus, for this isostructural series both the changes in binding energy of the N–1*s* photoelectrons from

† Possible exceptions to this statement are complexes that have both high NO stretching frequencies and high N–1*s* binding energies. In these cases, the π^* orbitals of the (NO^+) ligand are relatively little perturbed by the metal so that linear coordination is expected. From an examination of Tables 1 and 4, it appears that complexes with $\nu_{NO} > 1850$ cm^{-1} and/or N–1*s* binding energies greater than 402 eV always have a linear MNO grouping. Most complexes, however, do not exhibit frequencies and binding energies in these ranges.

the nitrosyl group and the changes in υ_{NO} are consistent with the molecular orbital scheme of Fig. 3.

Thus far, only linear complexes with $\{MNO\}^5$ or $\{MNO\}^6$ configurations have been discussed. However, as pointed out in the analysis of triatomic MNO, electron configurations which place electrons into anti-bonding orbitals will cause distortion of the MNO group. In six-coordinate $\{MNO\}^6$ complexes all of the bonding and non-bonding orbitals are filled. An $\{MNO\}^7$ complex, therefore, must have one electron in an anti-bonding orbital. If the molecular orbital scheme in Fig. 3 applies then the addition of an electron to $Fe(CN)_5NO^{2-}$ would result in an $\{FeNO\}^7$ complex with one electron in the $3e$ orbital. A brown complex having the stoichiometry $[N(C_2H_5)_4]_3$ $[Fe(CN)_5NO]$ with ν_{NO} = 1568 cm^{-1} has been isolated[22], but its structure is unknown. EPR studies of the brown species generated by one-electron reduction of $[Fe(CN)_5NO]^{2-}$ in basic solutions have been interpreted[23] as arising from the $[Fe(CN)_5NO]^{3-}$ ion with nonlinear coordination of the NO group. In solution, the brown species can be converted to a blue complex best formulated as $[Fe(CN)_5NOH]^{2-}$. Subsequent studies by Harris[24] have confirmed that the charge on the blue species is indeed − 2. Irradiation of crystalline $Na_2[Fe(CN)_5NO] \cdot 2H_2O$ also produces both the brown and the blue species[25], both of which were demonstrated to have non-linear MNO groups by EPR. The non-linearity of the FeNO group of the brown complex, $[Fe(CN)_5NO]^{3-}$, and its ease of protonation suggest that the nitrosyl group is the probable site of protonation. Although the structure of the six-coordinate $Fe(CN)_5NO^{3-}$ ion is unknown, the structure and properties of another six-coordinate complex of the $\{FeNO\}^7$ group, $FeBrNO(das)_2^+$, have been reported[26]. The Fe–N–O angle is 148° in $FeBrNO(das)_2^+$, but there is a large uncertainty in this angle due to disorder problems.

The electrochemistry of $Fe(CN)_5NO^{2-}$ has been compared to the electrochemical behavior of NO^+ itself[27]. The NO^+ group exhibits three reduction waves. The first is a one-electron wave corresponding to $NO^+ + e \rightarrow NO$. The second wave results from the reduction of N_2O_2 formed by dimerization of NO prior to the electrode reaction. Finally, a wave corresponding to the three-electron reduction of NO to NH_2OH is observed at more negative potential. The $Fe(CN)_5NO^{2-}$ anion ($\{FeNO\}^6$) first undergoes reduction to $Fe(CN)_5NO^{3-}$ described in the previous paragraph. This trianion then either undergoes protonation and reduction *via* a second wave or reduction to the stable hydroxylamine complex, $Fe(CN)_5(NH_2OH)^{3-}$, in a three-electron wave at more negative potential. The similarity of the electrochemical behavior of NO^+ and $Fe(CN)_5NO^{2-}$ is completely consistent with the molecular orbital scheme of Fig. 3.

The cyano derivative of $\{CoNO\}^8$ is unstable to dimerization[28], and consequently, it has not yet been structually or chemically characterized. However, there are several other six-coordinate derivatives of the $\{CoNO\}^8$ group whose structures are well-known, including $CoNO(NH_3)_5^{2+}$ (ref. 29), $CoClNO(en)_2^+$ (ref. 30) and $Co(NCS)(NO)(das)_2^+$ (ref. 31). The bonding scheme used to describe the pentacyanonitrosyl complexes includes only information which depends upon the number of ligands attached to the metal and not upon their detailed chemical properties. Therefore, Fig. 3 may also be applicable to these

other six-coordinate derivatives of the $\{CoNO\}^8$ group. All of these complexes have Co–N–O bond angles in the 120–135° range (Table 1) with rather long Co–N bonds. A linear CoNO arrangement in these $\{CoNO\}^8$ complexes would require two electrons to reside in the totally anti-bonding $3e$ molecular orbital (Fig. 3). Consequently, the CoNO group in these complexes is strongly bent. The Co–N–O bond angles of 120–135° correspond to the localization of a pair of electrons on the N atom and further substantiate the molecular orbital scheme of Fig. 3. These facts are also consistent with treating these mononitrosyl complexes as perturbed triatomic species to which Walsh's concepts[3] are applicable.

Bending the MNO moiety will have several effects: (1) the symmetry will be reduced from C_{4v} to C_s; (2) the relative energies of the metal d orbitals and the NO π-orbitals (formerly $3e$ and $2e$) will be modified in such a way as to lower the total energy of the complex; (3) a pair of electrons will be localized in a non-bonding orbital of nitrogen; and (4) the cobalt will have what amounts to a d^6 electron configuration.

Spectroscopic studies of the six-coordinate $\{CoNO\}^8$ complexes have been made[32] The visible spectra of $CoX(NO)(en)_2^+$ and $CoX(NO)(das)_2^+$ have been assigned to d–d transitions of a $Co(d^6)$ ion in a field of tetragonal symmetry. In addition, charge transfer bands were observed which are consistent with a ligand to metal transition (LMCT). Since the symmetry is no longer C_{4v}, and the character of the $3e$ and $2e$ molecular orbitals has been radically changed, the energy level diagram in Fig. 3 no longer applies to the six-coordinate bent $\{CoNO\}^8$ complex. The information obtained from the visible–UV spectra of the cobalt complexes has been utilized to construct the r.h.s. of the correlation diagram shown in Fig. 4. This diagram is similar in many respects to those proposed by Pierpont and Eisenberg[5] and Mingos[6] for correlating linear with bent nitrosyl complexes. However, two points concerning Fig. 4 are worth emphasizing. First, the order of the energy levels on both the right-hand and left-hand sides of the correlation diagram are based upon experimental observations, not solely on the symmetry of the molecular orbitals. Second, the ultimate geometry assumed by MNO group is dependent not only on the *total number of electrons* but equally importantly upon the *nature of the highest occupied molecular orbital.*

The successful extension above of the bonding scheme for pentacyanonitrosyl complexes to a variety of six-coordinate $\{CoNO\}^8$ mononitrosyl complexes suggest that Figs. 3 and 4 should be generally useful for understanding the structures and electronic properties of six-coordinate mononitrosyl complexes. For example, the $\{FeNO\}^6$ complex $FeXNO(das)_2^{2+}$ would be expected to have spectroscopic and structural properties similar to those of $Fe(CN)_5(NO)^{2-}$. Table 1 shows that the infrared and photoelectron spectra of these complexes are indeed very similar and are consistent with a $(2e)^4$ $(1b_2)^2$ configuration and a linear FeNO grouping. The formal addition of an electron to give the $\{FeNO\}^7$ complex, $FeXNO(das)_2^+$, should place an electron in the $3e$ orbital. The Fe–N–O angle of 148° observed[26] for X = Br demonstrates that the addition of even a single electron to the $3e$ orbital leads to some bending of the FeNO moiety, just as it does when one electron is added to NO_2^+. The magnetic properties of $FeXNO(das)_2^+$ complexes have been investigated

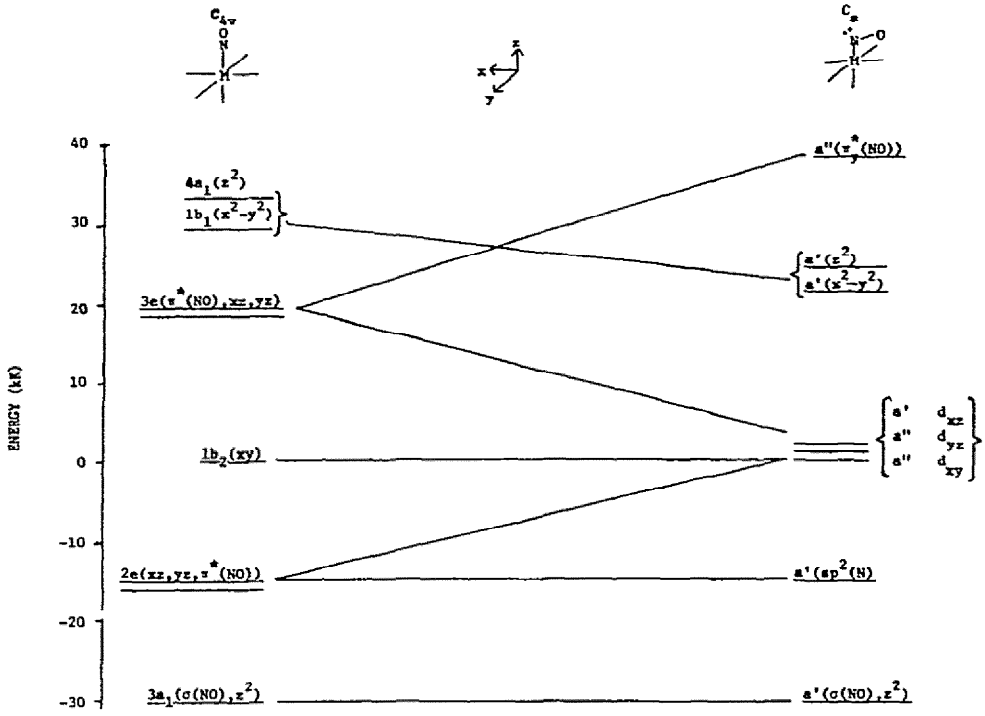

Fig. 4. The correlation diagram relating one-electron molecular orbitals of linear and bent six-coordinate MNO complexes. The energies of the molecular orbitals on the l.h.s. were estimated from the spectra of $[Fe(CN)_5NO]^{2-}$ and $[Cr(CN)_5NO]^{3-}$. The energies on the r.h.s. were estimated from the spectra of $[CoCl(NO)(en)_2]^{+}$ and $[FeCl(NO)(das)_2]^{+}$.

(ref. 33). The complexes have one unpaired electron, a rhombic g tensor, and a temperature dependent magnetic susceptibility which is consistent with a spin-paired t_{2g}^5 electron configuration in a strong rhombic field[34]. The large rhombic field is a consequence of having only a single electron in the $3e$ orbital. In terms of the correlation diagram in Fig. 4, the six-coordinate $\{FeNO\}^7$ complex lies between the r.h.s. and l.h.s. The visible spectrum of this complex was also investigated[35,36], and although there is considerable uncertainty about the detailed assignments, the excited states arise from transitions between the rhombically split t_{2g} and e_g orbitals, a', a'', and a'' (d_{xz}, d_{yz}, and d_{xy}) and a', a' ($d_{x^2-y^2}$ and d_{z^2}), respectively. Such transitions correspond to those of a spin-paired Fe^{III} complex in a rhombically distorted field.

The photoelectron spectra and IR spectra of $[FeCl(NO)(das)_2]^{2+}$ and $[FeCl(NO)(das)_2]^{+}$ provide considerable information about the FeNO group. $[FeCl(NO)(das)_2]^{2+}$ has a very high N—1s binding energy and high ν_{NO}, while $[FeCl(NO)(das)_2]^{+}$ has a low N—1s binding energy and a low value for ν_{NO}. These properties are what would be expected from the correlation diagram in Fig. 4, which indicates that the addition of an electron to the $3e$ level would both reduce and bend the NO group. The presence of two electrons in the $3e$ level will serve to further reduce and bend the nitrosyl group, which leads in turn to very low val-

ues of the N–1*s* binding energy and the low frequency for ν_{NO} observed for the $\{CoNO\}^8$ complex, $[CoCl(NO)(das)_2]^+$.

Additional justification for treating six-coordinate mononitrosyl complexes as perturbed triatomic species is provided by detailed studies of their infrared spectra. Miki[37], Quinby[38], and Tosi[39] demonstrated that six-coordinate mononitrosyl complexes possess MNO vibrational frequencies which can be closely approximated using a three-body model (i.e. the interaction between the MNO group and the other ligands is negligible). This approximation is reasonably successful even for compounds such as $Co(NO)(CO)_3$ in which mechanical coupling due to the similarity of the CoCO and CoNO frequencies, and chemical interaction due to the similarity of bonding between the cobalt and the carbonyl and nitrosyl groups might be expected to cause large departures from this simple model[37,122]. Several mononitrosyl complexes whose force constants have been evaluated using the three-body model and ^{15}NO derivatives are listed in Table 3. Miki[37] found that for ruthenium derivatives of the NO group the three-body model accounted for the observed isotopic shifts as well as a more complicated eight-body model. Tosi[39] found that substitution of ^{15}NO for ^{14}NO in $Na_2FeNO(CN)_5 \cdot 2H_2O$ produced shifts of five infrared frequencies: the three associated with the FeNO group and two associated with the axial and equatorial cyanide groups. However, the shifts of the (mainly) cyanide frequencies were small (4 cm^{-1} and 2 cm^{-1} respectively), and moreover, Paliani[40] found no shifts of these two iron-cyanide frequencies upon substitution of ^{15}N in the nitrosyl group. The success of the triatomic model for the force constants of the MNO species is consistent with the present treatment of MNO complexes as perturbed triatomic moieties.

TABLE 3
Force constants for six-coordinate $M\overset{k_1}{-}N\overset{k_2}{-}O$ complexes in C_{4v} symmetry

$[M(NO)L_5]^n$	Electron configuration	k_1^a	k_2	k_δ	Ref.
$CrNO(CN)_5^{3-}$	$\{CrNO\}^5$	5.06	10.18	1.14	*b*
$CrNO(NH_3)_5^{2+}$	$\{CrNO\}^5$	4.14	11.14	0.88	*b*
$MnNO(CN)_5^{3-}$	$\{MnNO\}^6$	6.06	10.62	1.19	*c*
$FeNO(CN)_5^{2-}$	$\{FeNO\}^6$	5.47	14.81	1.21	*d*
$RuNOCl_5^{2-}$	$\{RuNO\}^6$	5.62	14.16	0.995	*b*
$RuNOBr_5^{2-}$	$\{RuNO\}^6$	5.71	13.72	0.945	*b*
$RuNOCl(das)_2^{2+}$	$\{RuNO\}^6$	5.45	13.84	0.99	*e*
$CoNO(NH_3)_5^{2+}$	$\{CoNO\}^8$	4.57	10.00	0.990	*b*

a The units for the force constants k_1 (M–N stretch) and k_2 (N–O stretch) are mdyne/Å, and for k_δ (M–N–O bend) are mdyne/Å.

b See ref. 37.

c E. Miki, S. Kubo, K. Mizumachi, T. Ishimori and H. Okumo, *Bull. Chem. Soc. Jap.* 44 (1971) 1024.

d See ref. 39.

e See ref. 38.

It is not necessarily true that the molecular orbital scheme of Fig. 3 applies to all six-coordinate complexes, or that the order of levels remains the same as electrons are addded or removed from a given complex. It might be expected that large perturbations would be brougt about by changing from a 3*d* to a 4*d* or 5*d* transition metal. However, several studies indicate that this same molecular orbital scheme also applies to complexes of the 4*d* metals. For example, the electronic spectra of a series of six-coordinate $[RuNO]^{3+}$ complexes ($\{MNO\}^6$ cases) have recently been interpreted[41] on the basis of energy levels similar to those of Fenske and DeKock[8]. Although the spectral assignments have not been confirmed by the use of other techniques, they place the $2e$, $1b_2$, $3e$, $1b_1$ and $4a_1$ levels in the same juxtaposition as in $\{FeNO\}^6$ complexes discussed above. The major difference is that the electronic transitions of the ruthenium complex occur at somewhat higher energies than those of the corresponding iron complex, as would be expected since ligands are usually bound more strongly to the 4*d* metals than to the 3*d* metals. In addition, the $[RuNO]^{3+}$ species have ν_{NO} in the 1900 cm^{-1} range[38], and rather high values for the N_{1s} binding energies. Structural investigations[42] have shown that the RuNO moiety is linear with a rather short Ru–N bond distance. Again these data are completely consistent with those properties expected from the bonding model in Fig. 3.

The spectral data for the $\{FeNO\}^6$ and $\{RuNO\}^6$ complexes also suggest that the $3e$ level is not necessarily lower than the sigma antibonding orbitals, $4a_1$ and $1b_1$ (d_{z^2} and $d_{x^2-y^2}$). If either the $1b_1$ or $4a_1$ orbital is of lower energy than the $3e$ orbital and is populated in the complex, then the most likely occurrence would be ligand labilization or loss. One possible example of the population of $1b_1$ or $4a_1$ in a metal nitrosyl complex is encountered in the reaction[43] of $Mn(CO)_5^-$ with NO^+ to yield the five-coordinate species, $Mn(NO)(CO)_4$ (ref. 44) rather than a six-coordinate complex with a bent NO group. Similarly, $Mn(NO)(CO)_4$ undergoes both thermal[45] and photochemical[46] substitution by an associative mechanism

$$Mn(NO)(CO)_4 + L \rightarrow Mn(NO)(CO)_3L + CO \qquad (I)$$

These observations are consistent with a six-coordinate intermediate in which $3e$ is of higher energy than $1b_1$. The intermediate observed in the photochemical reaction may have had the $3e$ level partially populated by electronic excitation with commensurate bending of the MnNO group and the production of an empty or partially empty orbital with which the associating ligand L can bind:

$$Mn(NO)(CO)_4 + h\nu \rightarrow [Mn(NO)(CO)_4]^*$$

followed by

$$[Mn(NO)(CO)_4]^* + L \rightarrow [Mn(NO)(CO)_4L]^* \rightarrow Mn(NO)(CO)_3L + CO$$

In summary, the properties of six-coordinate mononitrosyl complexes, whether linear or bent, can be understood in terms of a bonding model in which the π^* orbitals of the NO

group and the metal d orbitals are of similar energy and are strongly mixed in forming the $2e$ and $3e$ molecular orbitals of the complex. Furthermore, in many of the complexes the $3e$ orbital is the anti-bonding orbital of lowest energy. Population of this $3e$ level by electrons results in the lengthening of the M–N distance, and a decrease of the M–N–O angle toward 120°.

This simple molecular orbital discussion has treated six-coordinate mononitrosyl complexes as perturbed MNO triatomic species whose geometry can be understood by the proper application of Walsh's concepts for simple triatomic species. Identical results are also obtained by applying valence bond concepts to a perturbed MNO complex. An $\{MNO\}^6$ species can be represented by the valence bond structures (a), (b) and (c) (Fig. 5). Representation (a) can be formally described as an NO^+ ligand donating a lone pair of electrons from an sp orbital to a metal with a d^6 configuration. Valence bond structures (b) and (c) represent the resonance forms in which there are, respectively, one and two π bonds between the metal and the nitrogen. All three representations require a linear MNO moiety, and are consistent with six-coordination, because each form leaves two d orbitals unoccupied and consequently available for formation of d^2sp^3 hybrid orbitals for bonding with the six ligands. For a six-coordinate $\{MNO\}^8$ species, however, the situation is quite different. In order that two d orbitals be left available for bond formation via d^2sp^3 hybrid orbitals, one pair of electrons must reside on the nitrosyl group, giving rise to a bent structure which can be represented by resonance forms (d) and (e). The bent structures (d) and (e) can be formally described as d^6 complexes of NO^- in which the nitrogen is utilizing sp^2 hybrid orbitals for bond formation with the metal. It should also be apparent from these valence bond forms (a)–(e) that it is very tenuous to infer M–N–O angles from ν_{NO}, since both geometries can give rise to formal N–O bond orders of one and two.

It has now been shown that both molecular orbital concepts and the valence bond formalism can account for linear and non-linear M–N–O geometries. In both approaches, the number of ligands attached to the metal is important in determining the structure of the MNO moiety. Although the molecular orbital description will be utilized throughout the remainder of the discussion, the equivalent valence bond structures could also have been used to describe these MNO systems.

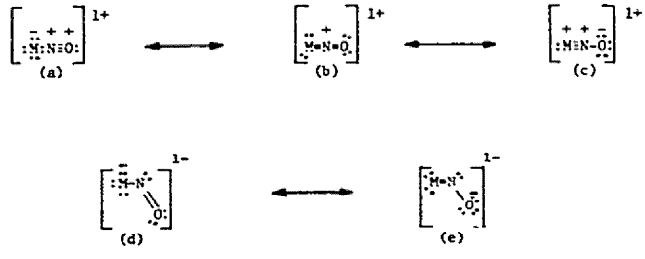

Fig. 5. (a), (b) and (c) are the possible resonance structures for a six-coordinate $\{MNO\}^6$ complex; (d) and (e) are the possible resonance structures for a six-coordinate $\{MNO\}^8$ complex.

C. Five-coordination

The above discussion has demonstrated that mononitrosyl complexes can be usefully discussed as triatomic species which are perturbed by the coordination of other ligands to the metal. The factors which are important in determining the molecular and electronic structures of the resultant complexes are: (1) the number of additional ligands and (2) the site symmetry of the metal. A description of the structure and bonding of five-coordinate metal mononitrosyls is complicated because site symmetries ranging from C_{4v} to C_1 are available to the metal. However, the bonding in five-coordinate mononitrosyls can be investigated by examining the perturbations which arise by placing the MNO group in fields of the appropriate symmetry.

The correlation diagram relating the molecular orbitals of linear MNO ($C_{\infty v}$) to the molecular orbitals of MNO in a field of four other ligands in C_{4v} symmetry is shown in Fig. 6. The molecular orbital diagram for the tetragonal pyramidal (TP) complex outlined in Fig. 6 is, of course, almost identical to that of the six-coordinate complexes previously discussed (Fig. 3). The only important difference is the lowering of $4a_1(z^2)$ in the five-coordinate complex.

The molecular orbital diagram for trigonal bipyramidal (TBP) complexes are derived

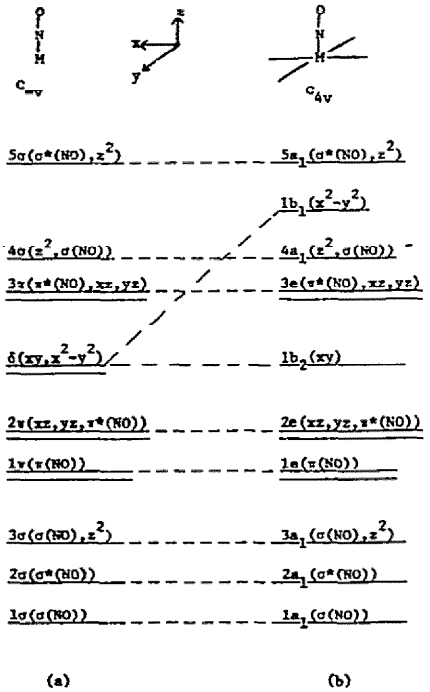

Fig. 6. The effects of a perturbing field with C_{4v} symmetry on the molecular orbitals of a linear MNO species.

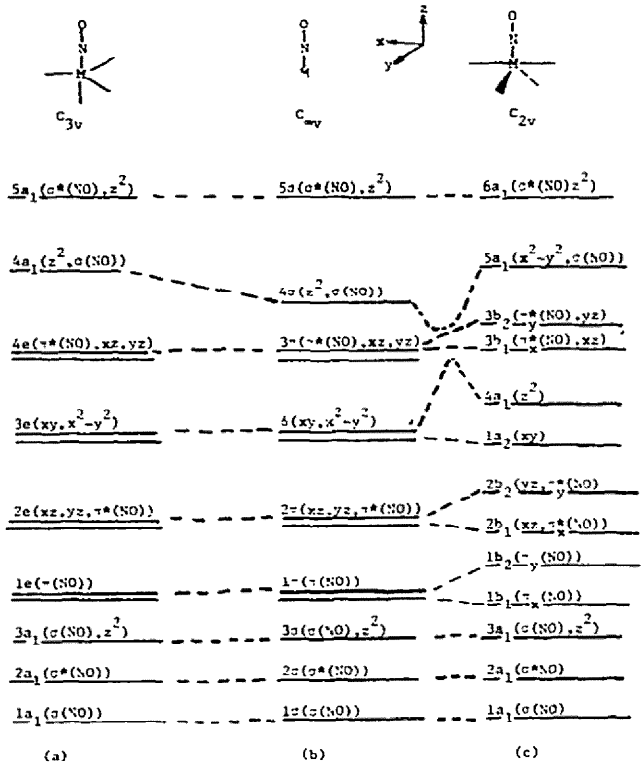

Fig. 7. The correlation diagram for a linear MNO group in fields of C_{2v}, C_{3v} and $C_{\infty v}$ symmetry.

from linear MNO in the correlation diagrams in Fig. 7. The molecules with C_{3v} symmetry correspond to TBP complexes with the nitrosyl group in the axial position, while those with C_{2v} symmetry correspond to the TBP complexes with the nitrosyl group in the equatorial position. It is important to note that the axis of quantization (z) of the TBP complexes with C_{2v} symmetry corresponds to one of the two-fold axes of the D_{3h} point group, and not to the axis of quantization in D_{3h} (ref. 47). The molecular orbital diagrams appropriate to TBP complexes in various symmetries will be individually discussed below.

1. {MNO}^{8} complexes

Examination of their structures (Table 4) reveals that both TP and TBP geometries are known. However, to date, all five-coordinate {MNO}^{8} species with strongly bent NO coordination have TP geometry and all linear {MNO}^{8} species have TBP geometry. In Section II.B the point was made that the M–N–O angle is a direct consequence of the number of electrons in the 3e orbital of a tetragonal complex, and that when the energies of the $4a_1$ and 3e orbitals are sufficiently close (Fig. 4) then the orbital occupied depends upon the nature and geometry of the other ligands around the metal. Figures 8(b) and 8(c) show two possible

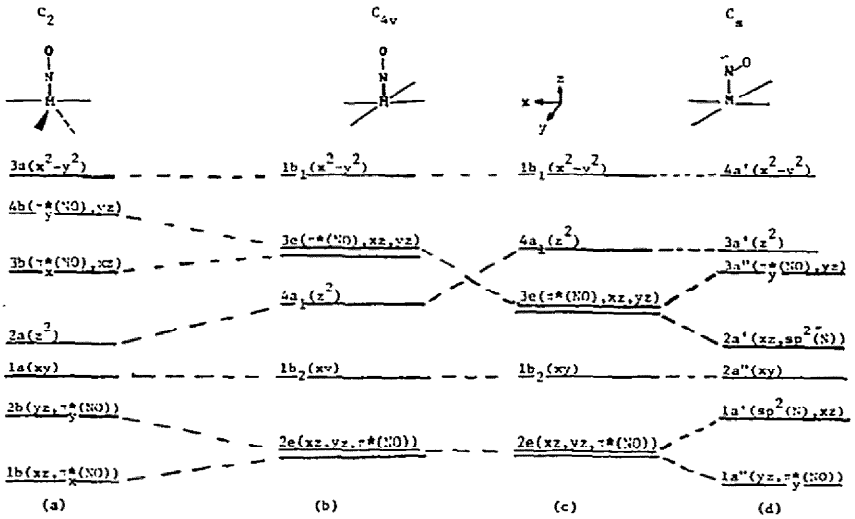

Fig. 8. A correlation diagram relating the molecular orbitals of five-coordinate MNO complexes in fields of C_2, C_{4v} and C_s symmetry. The $\{MNO\}^8$ complex on the r.h.s. is bent because $3a'$ is higher in energy than at least one of the components of $3e$.

orbital schemes for a five-coordinate complex having C_{4v} symmetry and show the correlation diagrams relating these two schemes to each other and to the observed TBP and TP geometries. When the $3e$ orbitals are lower in energy than the $4a_1$ (Fig. 8(c)), then an $\{MNO\}^8$ complex would have two electrons in the $3e$ orbitals which would lead to bending of the MNO group as discussed in Section II.B. Figure 8(d) shows the resultant ordering of the orbitals in a TP complex with a strongly bent MNO group.

When the $4a_1$ orbital (z^2) is of lower energy than the $3e$ orbital (Fig. 8(b)), the electron configuration of the five-coordinate $\{MNO\}^8$ complex would be $(2e)^4\ (1b_2)^2\ (4a_1)^2$. In this C_{4v} geometry, the $4a_1$ orbital is strongly anti-bonding. Distortion of the molecule toward TBP geometry will make $4a_1$ less anti-bonding. This distortion will also make the yz component of $3e$ anti-bonding with respect to the other two ligands in the equatorial plane of the TBP, thereby facilitating delocalization of electron density from the σ orbitals of these ligands into the π^* orbitals of the NO group. Both of these factors favor the distortion of an $\{MNO\}^8$ complex from C_{4v} to C_2 as outlined in Fig. 8(b)→8(a), while retaining a linear MNO group.

Correlation diagrams for the bending of the NO group in TP complexes have been proposed previously[5,6,47,48]. However, these diagrams indicate that the MNO group will spontaneously bend whenever two electrons occupy the $4a_1$ orbital, purportedly on the basis of Walsh's ideas for triatomic molecules. We pointed out in our discussion of six-coordinate complexes that Walsh related deviations from linearity to occupation of an orbital which was localized on the central atom and was strongly anti-bonding with respect to all three atoms. Clearly $4a_1$ is not an orbital of this type. Some bending of the MNO

TABLE 4
Five-coordinate mononitrosyl complexes [a]

Complex	ν_{NO} (cm^{-1})	N-1s (eV)	Geometrical constraint [b]	Observed geometry [b]	M–N (Å)	M–N–O (deg)	X_{eq}–M–X_{eq} (deg)
$Mn(NO)(CO)_4$	1763 [c]	–	None	TBP, NO_{eq} [d]	1.80(1)	180(0)	118.9(5)
$Mn(NO)(CO)_3P(C_6H_5)_3$	1712 [c]	–	None	TBP, NO_{eq} [e]	1.78(1) [f]	178(1) [f]	120(1) [f]
$Mn(NO)(CO)_2[P(C_6H_5)_3]_2$	1662 [c]	–	*trans*-PR_3	TBP, NO_{eq} [g]	1.73(1)	178(1)	120.0(7)
$Os(NO)(CO)_2[P(C_6H_5)_3]_2^+$	1750 [h]	–	*trans*-PR_3	TBP, NO_{eq} [h]	1.89(1)	177(1)	124.5(5)
$Co(NO)Cl_2[PCH_3(C_6H_5)_2]_2$	1735	401.7					108.4(3) [l]
	1630 [i]	399.6 [i, j]	*trans*-PR_3	Intermediate [i,k]	1.70(1)	165(1)	168(1) [m]
$Ir(NO)(CO)Cl[P(C_6H_5)_3]_2^+$	1680 [n]	–	*trans*-PR_3	TP, NO_{ax} [n]	1.97(1)	124(1)	175.7(1) [m]
							161.3(3)
$Ir(NO)(CO)I[P(C_6H_5)_3]_2^+$	1720 [o]	–	*trans*-PR_3	TP, NO_{ax} [o]	1.89(3)	125(3)	168.2(3) [m]
							158(1)
$Ir(NO)(CH_3)I[P(C_6H_5)_3]_2$	1525 [p]	–	*trans*-PR_3	TP, NO_{ax} [q]	1.91(2)	120(2)	169.2(2) [m]
							151(1)
$Ir(NO)Cl_2[P(C_6H_5)_3]_2$	1560 [r]	–	*trans*-PR_3	TP, NO_{ax} [s]	1.94(2)	123(2)	157.4(1) [l]
							170.2(1) [m]
$Co(NO)(das)_2^{2+}$	1852 [t]	402.3 [j]	TBP, NO_{eq}	TBP, NO_{eq} [u]	1.68(2)	179(2)	99.3(2)
$Ru(NO)(diphos)_2^+$	1673 [v]	–	TBP, NO_{eq}	TBP, NO_{eq} [v]	180(1)	176(1)	99.3(2)
$Ru(NO)H[P(C_6H_5)_3]_3$	1640 [w]	–	TBP, NO_{ax}	TBP, NO_{ax} [w]	1.79(1)	176(1)	–
$Ir(NO)H[P(C_6H_5)_3]_3^+$	1715 [p]	–	TBP, NO_{ax}	TBP, NO_{ax} [x]	1.68(3)	175(3)	–
Co(NO)(TPP)	–	–	TP, NO_{ax}	TP, NO_{ax} [y]	1.83(5)	135(1)	–
Co(NO)(acacen)	1654 [z, aa]	–	TP, NO_{ax}	TP, NO_{ax} [bb]	1.89(1)	122.4(5)	–
Co(NO)(benacen)	1635 [aa]	–	TP, NO_{ax}	TP, NO_{ax} [bb]	1.88(1)	122.9(8)	–
$Co(NO)[S_2CN(CH_3)_2]_2$	1630 [cc]	–	TP, NO_{ax}	TP, NO_{ax} [cc]	1.75(1)	135(1)	153.5(5)
			TBP, NO_{eq}				

group can occur when the $4a_1$ orbital is singly occupied (see Section II.C.2) or when the $4a_1$ and $3e$ orbitals are degenerate (see Section II.G).

Figure 8 implies that the energy differences among five-coordinate nitrosyls are sufficiently subtle so that fixing the geometry of a five-coordinate complex determines the electron configurations (and hence the M–N–O angle). By the same token, a given electron configuration implies a specific geometry for the complex. Several examples of this are listed in Table 4. The complexes $Co(das)_2NO^{2+}$ (ref. 31) and $Ru(diphos)_2(NO)^+$ (refs. 47, 49) have TBP coordination geometry with the NO group in the equatorial plane. Space-filling models show that the steric interactions between the bulky chelating ligands are much less in the observed structures than in a TP complex with L–M–N bond angles of $\sim 100°$. Therefore, these are complexes of C_2 symmetry with the coordination geometry constrained to be TBP, and the molecular orbitals through $2a(z^2)$ will be filled (Fig. 8(a)).

Other complexes constrained to TBP geometry include $Ir(NO)H[P(C_6H_5)_3]_3^+$ (ref. 4) and $Ru(NO)H[P(C_6H_5)_3]_3$ (refs. 48, 49). In these species the steric requirements of the three bulky phosphine groups are minimized in TBP geometry with the NO group in the axial position (C_{3v}). The appropriate molecular diagram is shown in Fig. 7(a) and in ref. 48.

TABLE 4 (references continued)

a $\{MNO\}^8$ complexes.
b TBP = trigonal bipyramid, TP = tetragonal pyramid, ax = axial, eq = equatorial.
c See ref. 45.
d See ref. 44.
e J.H. Enemark and J.A. Ibers, *Inorg. Chem.*, 7 (1968) 2339.
f Average of one NO group and two CO groups disordered in the equatorial plane.
g See ref. 54.
h See ref. 55.
i See ref. 62.
j See ref. 21.
k See Fig. 9.
l Cl–M–Cl
m P–M–P
n See ref. 57.
o See ref. 56.
p C.A. Reed and W.R. Roper, *Chem. Commun.*, (1969) 155.
q See ref. 58.
r M. Angoletta, *Gazz. Chim. Ital.*, 93 (1963) 1591.
s See ref. 59.
t See ref. 32.
u See ref. 31
v See ref. 49.
w See ref. 48.
x See ref. 4.
y See ref. 51.
z M. Tamaki, I. Masuda and K. Shimra, *Bull. Chem. Soc. Jap.*, 42 (1969) 2858.
aa F. Calderazzo, C. Floriani, R. Henzi and F.L'Epplatenier, *J. Chem. Soc. A*, (1969) 1378.
bb See ref. 50.
cc See ref. 63.

From this diagram it is clear that an $\{MNO\}^8$ complex will have the electron configuration $(2e)^4$ $(3e)^4$ and consequently have a linear MNO group as is observed. Finally, structures have been determined for three compounds in which the ligand constrains the MNO group to TP geometry: *N,N'*-ethylenebis(acetylacetoneiminato)nitrosylcobalt[50], *N,N'*-ethylenebis(benzoylacetoneiminato)nitrosylcobalt[50], and tetraphenylporphinatonitrosylcobalt[51]. In these compounds the Co–N–O angles are 122°, 123°, and 136°, respectively.

Removal of some of these severe steric restraints allows the structure adopted by the MNO group to be determined by other and perhaps even more subtle factors. Three limiting structures must be considered for sterically unconstrained $M(NO)L_4$ complexes: (1) TBP with a linear nitrosyl group in the axial position (C_{3v}); (2) TBP with a linear nitrosyl group in the equatorial position (C_{2v}); (3) TP with a bent nitrosyl group in the axial position (C_s or C_1). The molecular orbitals appropriate to these complexes are summarized in Figs. 7 and 8.

In a TBP complex with an axial nitrosyl group, the 4*e* orbitals interact only with the 1*e* and 2*e* orbitals which have no contribution from the σ orbitals of any of the ligands (Fig. 7(a)). In the equatorial position of a TBP, the $3b_1$ and $3b_2$ orbitals interact with the $1b_1$, $2b_1$ and $1b_2$, $2b_2$ orbitals. The $2b_2$ orbital is comprised of the d_{yz} orbital of the metal and of the σ orbitals of the ligands in the equatorial plane. Thus, the σ-bonds between the equatorial ligands and the metal can be strengthened by the presence of good π-accepting ligands in the equatorial plane. This synergistic effect leads to the recent postulate that d^8 TBP complexes adopt structures which place the best π-accepting ligands in the equatorial plane[52]. Recent detailed infrared studies[38] support the commonly accepted idea[53] that NO is the best π-accepting ligand. Consequently only two structures are expected for sterically unconstrained $M(NO)L_4$ complexes: TBP geometry with a linear nitrosyl group in an equatorial position and TP geometry with a strongly bent nitrosyl group in the axial position. Which of these structures is adopted by a particular complex depends upon the relative energies of the $4a_1$ and 3*e* orbitals as shown in Figs. 8(b) and 8(c).

In a TBP complex with an equatorial nitrosyl group, the $4a_1(z^2)$ orbital (Fig. 7(c)) interacts with both the σ and π orbitals of the equatorial ligands, and hence the presence of several π-accepting ligands favors TBP geometry with a linear nitrosyl group in the equatorial plane as is observed for $Mn(NO)(CO)_4$ (ref. 44). Substitution of two of the carbonyl ligands of $Mn(NO)(CO)_4$ by triphenylphosphine results in a *trans* arrangement of the bulky phosphines and retention of TBP geometry[54]. This structure leaves the best π-accepting ligands in the equatorial plane and the MnNO group remains linear.

The energy of the $4a_1(z^2)$ orbital relative to $3b_1$ (Fig. 7(c)) can also be increased by changing from a metal of the first transition series (3*d*) to a metal of the third transition series (5*d*). This change is not sufficient to increase the energy of $4a_1$ above that of $3b_1$ if at least two π-accepting ligands are attached to the metal as evidenced by the osmium complex, $Os(NO)(CO)_2[P(C_6H_5)_3]_2^+$. This osmium complex has TBP geometry with *trans* phosphine ligands and a linear OsNO group[55]. On the other hand, if one of the two remaining carbonyl groups is replaced by halide, hydride or methyl substituents, then the energy of $4a_1$ is raised sufficiently so that TP geometry with *trans* phosphines and a strong-

ly bent nitrosyl group in the axial position results (Fig. 8(d)). The structures of several such complexes including $IrI(NO)(CO)[P(C_6H_5)_3]_2^+$ (ref. 57), $IrCl(NO)(CO)[P(C_6H_5)_3]_2^+$ (ref. 56), and $IrI(NO)(CH_3)[P(C_6H_5)_3]_2$ (ref. 58) have been determined.

Replacement of the remaining carbonyl ligand of an $M(NO)(CO)X(PR_3)_2$ complex by halide will further increase the energy of the orbital which is primarily d_{z^2} of the metal ($2a$ in C_2, $4a_1$ in C_{4v}, $3a'$ in C_s). This replacement is of no consequence for metals of the third transition series, because the d_{z^2} orbital is already higher in energy than the $3e$ orbital of the mononitrosyl complexes. Thus, $Ir(NO)Cl_2[P(C_6H_5)_3]_2$ has TP geometry and a strongly bent IrNO array[59]. For metals of the first transition series, however, especially interesting behavior is observed for these $M(NO)X_2(PR_3)_2$ complexes.

The series of complexes $Co(NO)Cl_2(PR_3)_2$, first prepared by Booth and Chatt[60], exhibit two infrared stretching frequencies in the NO region separated by 60–100 cm^{-1}. More recently these complexes have been extensively studied by Collman et al. [61], who demonstrated that the relative intensities of the NO frequencies are dependent upon the nature of the phosphine. In addition, for a given phosphine the relative intensities of the two bands are temperature dependent. This behavior suggests the presence of the two conformers for these complexes, and it was proposed[61] that these complexes exist as "hybridization isomers", i.e. a TBP molecule with a linear MNO group and a TP molecule with a strongly bent MNO group. The structure of one form of $Co(NO)Cl_2[P(CH_3)(C_6H_5)_2]_2$ has been determined by single-crystal X-ray diffraction[62]. The authors describe the molecule as possessing trigonal bipyramidal geometry with a linear nitrosyl group. Figure 9 shows a view of the molecule normal to the equatorial plane of the proposed trigonal bipyramid. The five atoms (Co, N, O, Cl(1) and Cl(2)) are essentially coplanar, but the N–Co–Cl angles are grossly dissimilar (117° and 134°), and the Co–N–O angle of 164.5(6)° is very significantly different from 180°. Clearly the molecule posseses an irregular coordination geometry and has an intermediate Co–N–O angle. From the available data it

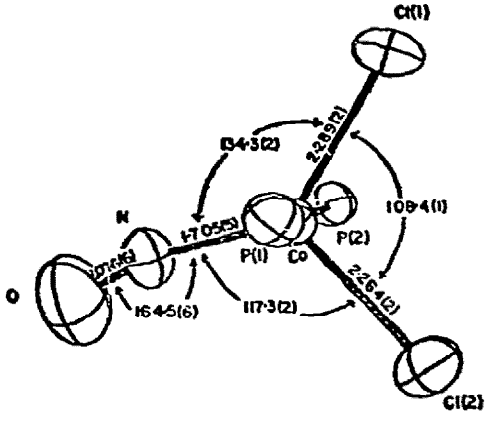

Fig. 9. The inner coordination sphere of $CoL_2(NO)[P(CH_3)(C_6H_5)_2]_2$ viewed perpendicular to the $CoCl_2(NO)$ plane. (Reproduced from ref. 62.)

is not possible to unambiguously determine which of the two nitrosyl stretching frequencies is characteristic of this distorted molecule. Nothing is known about the structure of the other isomer of this complex, although it has been proposed[62] that the other form will have essentially the same molecular structure as the iridium complex, $Ir(NO)Cl_2[P(C_6H_5)_3]_2$ (ref. 59).

The properties of the $Co(NO)Cl_2(PR_3)_2$ complexes suggest that these molecules are near the crossing point of the $4a_1$ and $3e$ molecular orbitals (Figs. 8(b) and 8(c)). The implications of such a crossing for these levels are considered in more detail in Fig. 10. The maximum symmetry which the $Co(NO)Cl_2(PR_3)_2$ complexes can have in either TBP or TP coordination geometry is C_{2v}. In C_{2v} symmetry e splits into b_1 and b_2, and a_1 is unchanged. Figure 10(b) shows a $Co(NO)Cl_2(PR_3)_2$ molecule with true C_{2v} symmetry and gives the orbital compositions of the a_1, b_1 and b_2 molecular orbitals. The three molecular orbitals have been made degenerate since the behavior of the system at the crosssing point is of interest. Bending vibrations of the nitrosyl group in the xz (or yz) plane lower the symmetry of the molecule from C_{2v} to C_s, and result in $a_1 \rightarrow a'$, $b_1 \rightarrow a'$ (or a''), and $b_2 \rightarrow a''$(or a'). Since orbitals of the same symmetry can mix but not cross, it is clear that bending of the nitrosyl group away from linearity in the case of accidental degeneracy will couple and strongly mix the two a' orbitals. The strong mixing of the a' orbitals induced by the bending vibrations of the molecule means that the Born–Oppenheimer ap-

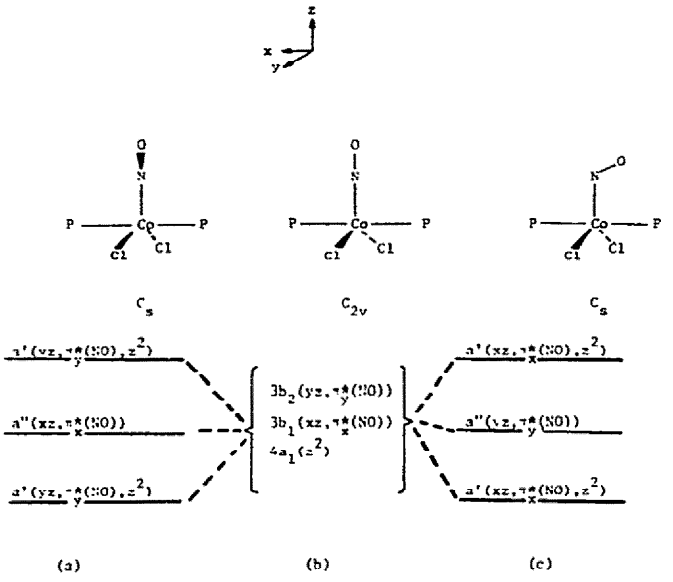

Fig. 10. Proposed molecular orbital scheme for the $CoCl_2(NO)(PR_3)_2$ complexes. (a) shows the composition of the molecular orbitals when the nitrosyl group bends in the $CoCl_2$ plane, (c) shows the composition of the orbitals when the nitrosyl group bends in the CoP_2 plane, and (b) depicts the situation for C_{2v} symmetry (see Fig. 7(c)) where all three orbitals are nearly degenerate. In the $CoCl_2(NO)(PR_3)_2$ complexes these three orbitals are occupied by a single pair of electrons.

proximation is not valid for the $Co(NO)Cl_2(PR_3)_2$ complexes. The consequences of strong vibronic coupling is considered in more detail in Section II.G.

Figure 10(a) shows bending of the nitrosyl ligand in the plane of the chlorine atoms (*yz* plane). Concomitant movements of the chlorine atoms in this plane will lead to the distorted geometry observed for one form of $Co(NO)Cl_2[P(CH_3)(C_6H_5)_2]_2$ (ref. 62). Figure 10(c) illustrates bending of the nitrosyl ligand in the plane of the phosphorus atoms (*xz* plane.) This bending of the nitrosyl group can also be accompanied by changes in the Cl–Co–Cl angle, but it is unlikely that the P–Co–P angle will change substantially because of the bulky nature of the phosphine ligands. Figures 10(a) and 10(c) suggest that the two nitrosyl stretching frequencies observed for $Co(NO)Cl_2[P(CH_3)(C_6H_5)_2]_2$ can also be attributed to the two distinct conformers of a non-linear nitrosyl group rather than to TBP and TP complexes. The conformers with the nitrosyl group bent in the Cl–Co–Cl plane and in the P–Co–P plane need not have, and indeed would not be expected to have, idential Co–N–O angles. However, if the two conformers are of similar energy, then changes of solvent, temperature, crystal lattice, or pressure would alter the relative abundances of the two forms.

The molecule $Co(NO)[S_2CN(CH_3)_2]_2$ is an example of a complex that contains good σ-donors and poor π-acceptors and which is free to adopt either TP or TBP geometry. The complex exhibits TP geometry and a strongly bent CoNO group (135°) (ref. 63) as shown in Fig. 11(a).

2. $\{MNO\}^7$ *complexes*

Several five-coordinate $\{FeNO\}^7$ complexes of chelating sulfur ligands have been prepared and three have been structurally characterized[64–69]. Common to all three structures is TP geometry and a poorly defined FeNO group. For example, the X-ray data from $Fe(NO)[S_2CN(C_2H_5)_2]_2$ have been interpreted on the basis of an Fe–N–O angle of 174(4)° with large thermal motion of the O atom[64]. Two different investigators[65,66] have examined the structure of $Fe(NO)[S_2CN(CH_3)_2]_2$ at room temperature and interpreted the data on the basis of an Fe–N–O angle of ~ 160° and two-fold disorder of the bent nitrosyl group. Subsequently, the structure was reinvestigated at − 80° and the data at 20 ° reinterpreted[67]. At 20° the structure was assigned an Fe–N–O angle of 173(2)° with very anisotropic vibration of the O atom and a maximum r.m.s. amplitude of 0.55 Å. At − 80° the Fe–N–O angle is 170.4(6)°, but the thermal motion is still very anisotropic with a maximum r.m.s. amplitude of 0.43 Å. The Fe–N vector makes angles of 5° and 10° with the plane of the four S atoms at 20° and − 80°, respectively. A view of the molecule normal to the plane of the four S atoms is shown in Fig. 11(b). It is clear that the non-linearity of the FeNO group results in the O atom being over one of the chelate rings but preferentially directed toward one of the S atoms (S_1) and leads to overall C_1 symmetry for the molecule. The angle between the molecular *x*-axis and the projection of the Fe–N (or Fe–O) vector onto the *xy* plane is ~ 20°. The position of the O atom relative to the rest of the complex is very similar to that of the O atom in the isomorphous

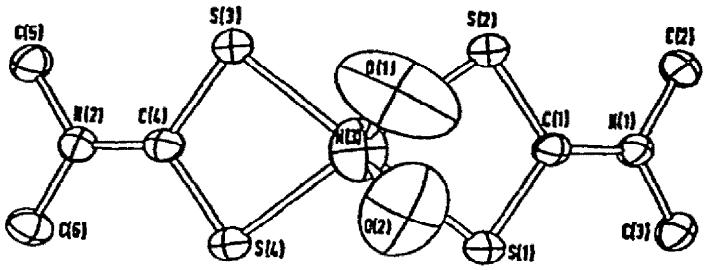

Fig. 11(a). Projection of the structure of $Co(NO)[S_2CN(CH_3)_2]_2$ normal to the plane of the four S atoms. Both of the half-oxygen atoms of the disordered NO group are shown. The thermal ellipsoids are drawn to enclose 30% of the probability distribution. (Reproduced from ref. 63.)

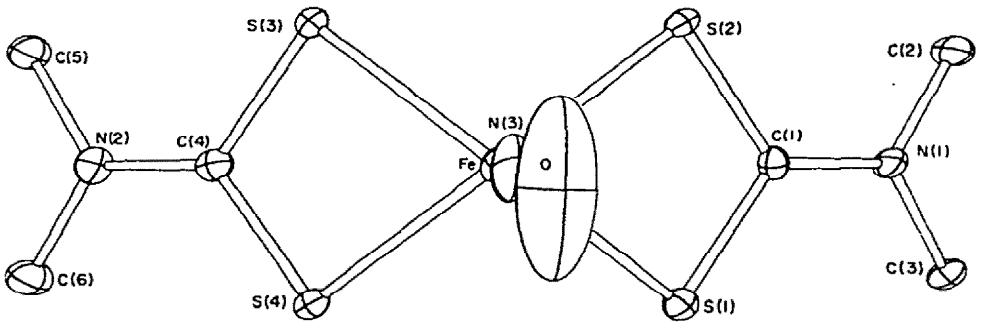

Fig. 11(b). Projection of the structure of $Fe(NO)[S_2CN(CH_3)_2]_2$ at $-80°$ normal to the plane of the four S atoms. The thermal ellipsoids are drawn to enclose 30% of the probability distribution.

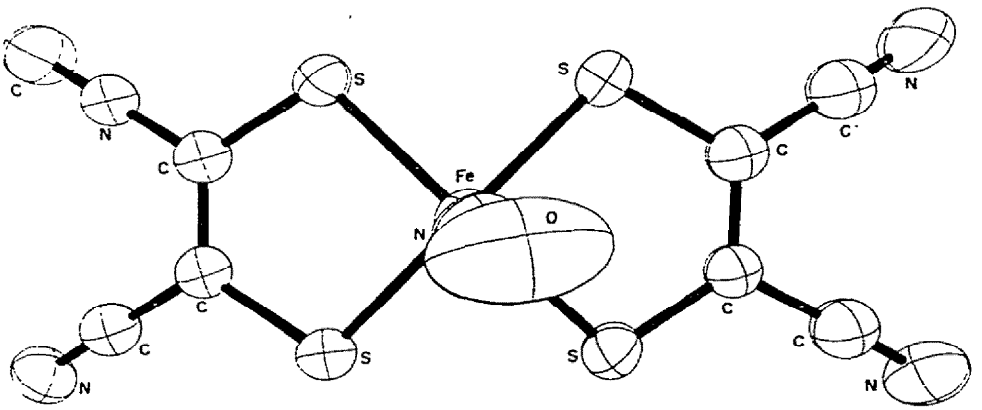

Fig. 11(c). Projection of the structure of the $[Fe(NO)(mnt)_2]^{2-}$ anion normal to the plane of the four S atoms. The thermal ellipsoids are drawn to enclose 30% of the probability distribution.

diamagnetic complex, $Co(NO)[S_2CN(CH_3)]_2$ (Fig. 11(a)[63]. However, the Co–N–O angle is only 135°, the Co–N vector is perpendicular to the plane of the four sulfur atoms, and the direction of maximum thermal motion is different. Nevertheless it is important to note the close similarity of the two structures before discussing the EPR results for $Fe(NO)[S_2CN(CH_3)_2]_2$ diluted in $Co(NO)[S_2CN(CH_3)_2]_2$.

The EPR spectrum of $Fe(NO)[S_2CN(CH_3)_2]_2$ has been studied in solid $Fe(NO)[S_2CN(CH_3)_2]_2$ (ref. 70), in styrofoam (ref. 71) and in single crystals of the diamagnetic host, $Co(NO)[S_2CN(CH_3)_2]_2$ (ref. 72). $Fe(NO)[S_2CN(C_2H_5)_2]_2$ has been extensively studied in solution and in an EPA glass[73]. In the diamagnetic host[72] $Fe(NO)[S_2CN(CH_3)_2]_2$ exhibits a three-line spectrum due to the hyperfine splitting by the nitrogen of the nitrosyl group with $g_z = 2.028$, $g_x = 2.048$, $g_y = 2.039$, and $A_z = 14.9$, $A_x = 12.6$, $A_y = 12.2$ gauss. The g and A_N tensors have the same principal directions, but they are not collinear. The angle between them is 5°. The A_N tensor is composed of an isotropic component of 13.2 gauss (obtained from $CHCl_3$ solution) and an anisotropic tensor which can be decomposed into two components each having cylindrical symmetry. One of the anisotropic components is axially symmetric about the z-axis and accounts for about 75% of the anisotropic A_N tensor. The second anisotropic component is axially symmetric about the x-axis and accounts for the remaining 25% of the anisotropic A_N tensor. This result requires unequal contributions of the p_x and p_y orbitals of the N atom of the nitrosyl group to the electronic wave function. In addition, the g-values are larger than the free-electron value of 2.0023. The differences in the g-values from the free-electron values will be inversely proportional to the energy separation between the $5a_1$ (z^2) orbital and the filled $2b_1$ (xz) and $2b_2$ (yz) orbitals. Therefore, it has been deduced[73] from the g-values that $2b_1$ is closer in energy to $5a_1$ than is $2b_2$, as shown in the one-electron molecular orbital scheme of Fig. 12.

The EPR results obtained for $Fe(NO)[S_2CN(C_2H_5)_2]_2$ in EPA glass by Goodman *et al.*[73] are also consistent with the results described above and with the molecular orbital scheme of Fig. 12. One conclusion which could be drawn from all the EPR results is that only a single FeNO species is present on the EPR time scale and that its average FeNO geometry is non-linear. Alternatively, if the FeNO group is linear, then it *cannot* be normal to the plane of the four S atoms. Thus, the unpaired electron resides in the $5a_1$ molecular orbital (Fig. 12) which is *unequally* perturbed by spin–orbit coupling with the filled $2b_1$ and $2b_2$ orbitals. For Fe, λ ($\sim 400\ cm^{-1}$) (ref. 74) is comparable to FeNO bending frequencies and may lead to the small bending of the FeNO group between the x and y axes of the molecule, as shown in Fig. 11(b). Moreover, the g-values can be affected by excitation of the low-energy bending modes of the FeNO group, as evidenced by the temperature dependence of the g-values in solution[73].

The anionic $\{FeNO\}^7$ complex of maleonitriledithiolate, $Fe(NO)[S_2C_2(CN)_2]_2^{2-}$, has been prepared and its structure determined. Like the dithiocarbamate complexes described above, this anion exhibits TP coordination geometry and a poorly defined FeNO group. The initial structure determination[68] of this complex gave an Fe–N–O angle of 168(6)° and showed large thermal motions for the O atom of the nitrosyl group. The structure has recently been redetermined[69], and it has been shown that at least two models for the

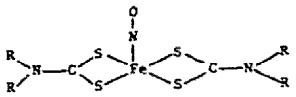

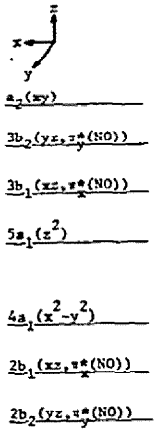

Fig. 12. The molecular orbital diagram for the TP dithiocarbamate derivatives of $FeNO^{2+}$.

FeNO group are equally compatible with the X-ray data. The Fe–N–O angles in these models range from 152° to 168°. A view of the complex normal to the plane of the four S atoms is shown in Fig. 11(c). The EPR spectrum of this compound in solution exhibits nitrogen hyperfine splitting and g-values consistent with the electron configuration $(5a_1)^1$ and a $^2A_1$ ground state[75]. Single-crystal EPR data for this complex have not as yet been reported so that its electronic properties cannot be discussed in further detail.

All of the five-coordinate $\{FeNO\}^7$ complexes discussed above can have only a single electron in either the $5a_1$ or $3b_1$ and $3b_2$ orbitals (Fig. 12). In each case, the EPR results indicate that the orbital occupied is primarily $5a_1$ (z^2). There are no known examples of five-coordinate $\{MNO\}^7$ complexes with a $(3b_1, 3b_2)^1$ electron configuration. However, this electron configuration does presumably occur in the six-coordinate species, $[Fe(NO)(das)_2X]^+$ (refs. 33, 34) and $Fe(CN)_5NO^{3-}$ (refs. 24, 25) (see Section II.B).

3. $\{MNO\}^6$ complexes

There is only one example[69] of an $\{MNO\}^6$ complex which is pentacoordinate, $Fe(NO)[S_2C_2(CN)_2]_2^-$. From Fig. 12 the highest filled orbital should be $a_2(x^2-y^2)$. Unless the energy of the $3b_1$ and $3b_2$ orbitals can be markedly lowered, or the energy of the $a_2(x^2-y^2)$ orbital can be greatly increased, the $3b_1$ (or $3b_2$) orbitals will not be populated, and the FeNO group will remain linear. Therefore, it is reasonable that a linear FeNO grouping is

found[69] for the above mentioned complex, even though its coordination geometry is TP. There appear to be no structually characterized examples of pentacoordinate mononitrosyl complexes with fewer than six electrons, although the paramagnetic complex, $Fe(NO)[S_2C_2(C_6H_5)_2]_2$, has been prepared[75] and its EPR spectrum reported. The g-values were found to be anisotropic and there was no observable nitrogen hyperfine splitting. This is consistent with the molecular orbital diagram in Fig. 12 which places the unpaired electron in the $a_2(x^2 - y^2)$ orbital, giving rise to a $^2A_2$ ground state. Since the a_2 orbital is orthogonal to the π^* orbitals of the NO group no nitrogen hyperfine splitting would be expected in the absence of configuration interaction or spin polarization.

D. Four-coordination

Relatively few structures of four-coordinate mononitrosyl complexes have been determined. Table 5 shows that all of the known structures are $\{MNO\}^{10}$ complexes. By analogy with the five-coordinate $\{MNO\}^8$ compounds which were just discussed, two limiting coordination geometries and M–N–O angles should also be available to $\{MNO\}^{10}$ complexes: (1) tetrahedral complexes with linear MNO groups (C_{3v}), and (2) square planar

TABLE 5
Four-coordinate pseudotetrahedral mononitrosyl complexes[a]

Complex	ν_{NO} (cm^{-1})	N–1s (eV)	M–N(Å)	M–N–O (deg)
$Co(NO)(CO)_2[P(C_6H_5)_3]$	1756[b]	–	1.74(1)[c,d]	178.5(6)
			1.76(1)	178.3(8)
			1.72(1)	177.9(6)
$Co(NO)(CO)[P(C_6H_5)_3]_2$	1714[b]	–	1.72(1)[c,d]	177.4(7)
$Ir(NO)[P(C_6H_5]_3$	1615[e]	–	1.67(2)[f]	180(0)
$Ir(NO)(CO)[P(C_6H_5)_3]_2$	1645[e]	399.6[g]	1.79(1)[h]	174(1)
$Ni(NO)(tep)^+$	1760[i]	–	1.63[j]	180(0)
$Ni(NO)(N_3)[P(C_6H_5)_3]_2$	1710[k]	399.6[g]	1.69(1)[k]	153(1)

a $\{MNO\}^{10}$ complexes.
b W. Hieber and J. Ellermann, *Chem. Ber.*, 96 (1963) 1643.
c V.G. Albano, P.L. Bellon and G. Ciani, *J. Organometal. Chem.*, 38 (1972) 155.
d The NO and CO groups are disordered in this structure.
e M. Angoletta, *Gazz. Chim. Ital.*, 93 (1963) 1591.
f V.G. Albano, P.L. Bellon and M. Sansoni, *J. Chem. Soc. A*, (1971) 2420.
g See ref. 21.
h C.P. Brock and J.A. Ibers, *Inorg. Chem.*, 11 (1972) 2812.
i D. Berglund and D.W. Meek, *Inorg. Chem.*, 11 (1972) 1493.
j See ref. 76.
k See ref. 77.

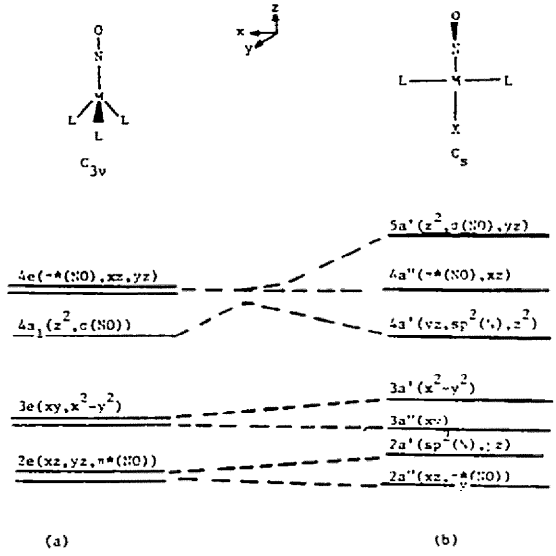

Fig. 13. The correlation diagram relating the molecular orbitals of pseudotetrahedral four-coordinate $\{MNO\}^{10}$ complex of C_{3v} symmetry to those of a planar $\{MNO\}^{10}$ complex with C_s symmetry and a non-linear MNO group.

complexes with strongly bent MNO groups (C_s). Figure 13 gives the correlation diagram for these two classes of four-coordinate mononitrosyl complexes quantized along the M–N bond.

All of the $\{MNO\}^{10}$ compounds whose structures have been determined have pseudo-tetrahedral geometry with relatively short M–N distances (Table 5). Of particular interest are the $\{NiNO\}^{10}$ complexes, $Ni(NO)(N_3)[P(C_6H_5)_3]_2$ and $Ni(NO)(tep)^+$ (where tep is $CH_3C[CH_2P(C_2H_5)_2]_3$). The tep complex has C_{3v} symmetry imposed on the nickel by the tep ligand, and has a linear NiNO group, with a short Ni–N distance[76]. The symmetry of the closely related molecule, $Ni(NO)(N_3)[P(C_6H_5)_3]_2$, can be no higher than C_s. The structure[77] of this azide derivative (Fig. 14) exhibits an ordered well-resolved nitrosyl ligand with an Ni–N–O angle of 153°, an Ni–N distance somewhat longer than Ni(NO)-(tep)$^+$ (ref. 76), and overall C_1 symmetry. The N–Ni–N angle of 121° and the P–Ni–P angle of 129° also show that the coordination sphere in this complex is severely flattened from that of a regular tetrahedron. It has been proposed that the Ni–N–O bond angle results from the low-symmetry of the complex which lifts the degeneracy of the Ni–N π-interaction and removes the three-fold symmetry of the overall electron density distribution about the metal[77]. The effect which lowering the symmetry from C_{3v} to C_s has on the molecular orbitals of the $\{NiNO\}^{10}$ group can clearly be seen in Figs. 13(a) and 13(b). Since the $\{NiNO\}^{10}$ group is linear in C_{3v} symmetry, the $4a_1$ orbital must lie below the $4e$ orbital giving the electron configuration $(2e)^4\ (3e)^4\ (4a_1)^2$.

Lowering the symmetry from C_{3v} to C_s results in $e \rightarrow a' + a''$ and $a_1 \rightarrow a'$. In a pseudo-

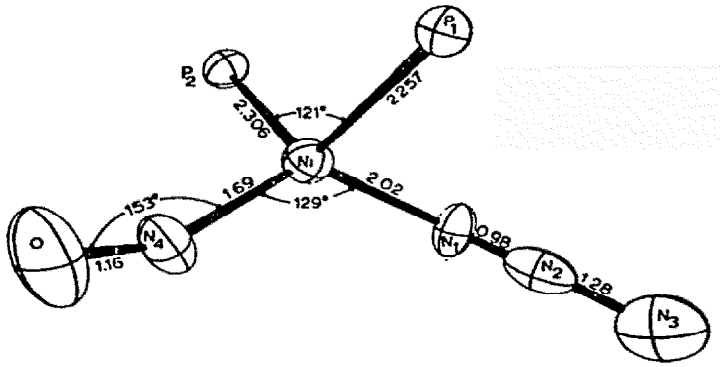

Fig. 14. Perpective view of the inner coordination sphere of $Ni(N_3)(NO)(P(C_6H_5)_3)_2$. The ellipseids are drawn to enclose 30% of the probability distribution. (Reproduced from ref. 77.)

tetrahedral complex the $4e$ orbital interacts with both the σ and π orbitals of the ligands. Thus, the order and magnitude of the splitting of the $4e$ orbital in C_s symmetry in $Ni(NO)X[P(C_6H_5)_3]_2$ will be related to the relative σ-donating abilities of the azide ion and triphenylphosphine. If the splitting of the $4e$ orbitals is similar to the separation of the $4a_1$ and $4e$ orbitals in C_{3v} symmetry then in C_s symmetry (Fig. 13(b)) the $4a'$ and $4a''$ orbitals will be accidentally degenerate. This degeneracy can be lifted by distortions leading to overall C_1 symmetry for the complex. Thus, the intermediate coordination geometry, the intermediate M–N–O angle, the orientation of the N_3^- ligand, the significantly different Ni–P distances (Fig. 14), and the overall C_1 symmetry of $Ni(NO)(N_3)[P(C_6H_5)_3]_2$ may arise from vibronic coupling of the $4a'$ and $4a''$ levels, with the final structure determined by the relative contributions of the appropriate atomic orbitals to the $4a'$ molecular orbital. The inequality of Ni–P distances has also been rationalized on the basis of nonbonded intramolecular interactions[77].

The exact interpretation of the structure of $Ni(NO)(N_3)[P(C_6H_5)_3]_2$ is not completely unambiguous, however. Careful inspection of the thermal motion of the atoms shows that the r.m.s. amplitudes of vibration of the oxygen atom of the nitrosyl ligand are 0.4 Å. These amplitudes are comparable to those often observed in metal nitrosyl and metal carbonyl complexes, but describe an angular range of 135–170°. This angular range nearly encompasses both the linear and strongly bent MNO geometries, and therefore it is conceivable that the observed structure results from two species with distinctly different Ni–N–O angles which are in thermal equilibrium at room temperature. The infrared spectrum shows only a single band in the nitrosyl region, but it would still be desirable to investigate the structure of this compound at low temperature. In any event, the observed intermediate geometry for this four-coordinate mononitrosyl complex indicates that pseudo-tetrahedral mononitrosyl complexes with a linear MNO group and square planar complexes with a bent MNO group are of similar energy. No discrete square planar complexes with a strongly bent MNO group are presently known, and the design of a complex which imposes this

geometry upon the MNO group remains a challenge to the synthetic chemistry.

Finally, Fig. 13(b) suggests that a diamagnetic $\{MNO\}^8$ complex such as $Ru(NO)Cl[P(C_6H_5)_3]_2$ (ref. 78) should be square planar with a linear MNO group.

E. Other coordination numbers

The compound $Mo(NO)[S_2CN(C_4H_9)_2]_3$ has been shown to be seven-coordinate. The structure is described as a pentagonal bipyramid with the nitrosyl group in one of the apical positions. The Mo–N–O angle for this $\{MoNO\}^4$ complex is 173° (ref. 79), consistent with the fact that a pentagonal bipyramidal $\{MNO\}^4$ complex with an apical NO group would have no anti-bonding orbitals occupied. Cotton and co-workers[80,81] have investigated the crystal structures and the temperature dependent proton magnetic resonance spectra of $(C_5H_5)_3Mo(NO)$ and $(C_5H_5)_2(CH_3)Mo(NO)$. The structure of $(C_5H_5)_3Mo(NO)$ shows one *monohapto* cyclopentadienyl group and two equivalent *polyhapto* cyclopentadienyl groups. In $(C_5H_5)_2(CH_3)Mo(NO)$ there are also two equivalent *polyhapto* cyclopentadienyl rings. In both compounds there are three kinds of Mo–C distances for the equivalent *polyhapto* rings. The M–N–O angles are 179.2(2)° (ref. 80) and 178(2)° (ref. 81).

F. Summary

The structures and physical properties of mononitrosyl complexes are best understood by considering the $\{MNO\}^n$ group as an "inorganic functional group" which is perturbed by the field imposed by the other ligands attached to the metal. Unlike organic functional groups the $\{MNO\}^n$ group has several possible ground states, each possessing its own characteristic structure and physical properties. In nearly all complexes, however, the $\{MNO\}^n$ group adopts one of two limiting ground states (linear or strongly bent), dictated by four factors: (1) the coordination number; (2) the coordination geometry; (3) the number of electrons (n); and (4) the nature of the occupied one-electron molecular orbitals.

The dependence of the M–N–O angle upon each of these factors has been discussed in the previous sections and is readily summarized. The $\{MNO\}^n$ group is linear unless the π-type orbital which is anti-bonding with respect to M, N, and O is occupied (3π in Fig. 2; $3e$ in Figs. 3, 4, 6(b), 8(b), 8(c); $4e$ in Figs. 7(a), 13(a)). Therefore, all six-coordinate $\{MNO\}^n$ groups are linear when $n \leqslant 6$, and bent when $n \geqslant 7$. Similarly, all five-coordinate $\{MNO\}^n$ groups are linear when $n \leqslant 6$. The $\{MNO\}^8$ group will be linear in a five-coordinate complex with TBP geometry and bent in a complex with TP geometry. There are no known examples of five-coordinate complexes with $n > 8$, but they are predicted to be bent in either TBP or TP geometry. Complexes with $n = 7$ are discussed in more detail in Section II.G. Four-coordinate complexes with $n = 10$ are linear in tetrahedral geometry and are predicted to be bent in square planar geometry.

Those few complexes whose ground state properties are not adequately described as

either linear or strongly bent are discussed in more detail in Section II.G. The chemical implications and chemical properties of the $\{MNO\}^n$ functional group are discussed in Section II.H.

G. Other effects

Jahn–Teller effects have been previously invoked[82] to explain *all* deviations of MNO groups from linearity. It is clear from the above discussion that the structures and spectroscopic properties of most MNO groups can easily be explained by simple one-electron molecular orbital diagrams without resort to other interactions. Two additional factors which can be important in MNO complexes are spin–orbit coupling and vibronic coupling (Jahn–Teller effects). These two factors and their possible effects on individual complexes are discussed separately below.

1. Spin-orbit coupling

The five-coordinate complexes of $\{FeNO\}^7$ (Section II.C.2) appear to be examples of complexes in which spin–orbit coupling may cause minor distortion of the FeNO moiety from linearity. The structural[64–67] and magnetic[70–73] studies of $Fe(NO)(dtc)_2$ complexes show that the complexes have TP geometry with a $5a_1$ electron configuration (Fig. 12). The dtc ligands restrict the symmetry about the $\{FeNO\}^7$ group to C_{2v} (or lower) and lift the degeneracy of the filled d_{xz}, d_{yz} orbitals to give $2b_1(xz)$ and $2b_2(yz)$. Spin–orbit coupling mixes the $2b_1$ and $2b_2$ orbitals unequally with $5a_1$ as evidenced by the values of g_x and g_y (refs. 72, 73). Consequently, the spin-orbital derived from $4a_1$ has a greater contribution from d_{xz} than from d_{yz}. This larger contribution of $2b_1$ to the $5a_1$ spin-orbital should lead to a small displacement of the nitrogen atom along the x axis. The structural data for $Fe(NO)[S_2CN(CH_3)_2]_2$ at $-80°$ do show that the Fe–N bond is not perpendicular to the plane of the four S atoms and that the N atom is displaced along the x direction of the molecule (Fig. 11(b)). The FeNO group is also bent more along x than along y because in the non-linear arrangement the $2b_1$ orbital, which is comprised of both d_{xz} and $\pi_x^*(NO)$, mixes more strongly with the $5a_1$ orbital than does $2b_2$.

If these small distortions of the FeNO group were found only for $Fe(NO)[S_2CN(CH_3)_2]_2$ then they could be reasonably attributed to solid state effects. However, a similar distortion is observed[69] in the crystallographically unrelated $\{FeNO\}^7$ complex, $Fe(NO)[S_2C_2(CN)_2]_2^{2-}$ (Fig. 11(c)). Although the bite angle of the S atoms in $Fe(NO)[S_2C_2(CN)_2]_2^{2-}$ does not impose C_{2v} symmetry on the FeNO group, the dithiolate chelate rings have significantly different π-interactions with the d_{xz} and d_{yz} orbitals. Unfortunately, the principal directions and values of the g tensor in this complex have not yet been determined. However, the average values (ref. 75) of g and A_N are very similar to those of the dtc complexes and indicative of a $5a_1$ electron configuration (Fig. 12). A careful examination of the g and A tensors of $Fe(NO)[S_2C_2(CN)_2]_2^{2-}$ would be an important test of the possible effects of spin–orbit coupling on the structures of $\{MNO\}^7$ complexes. Another test of the importance of spin–

orbit coupling in $\{MNO\}^7$ complexes would be to prepare the analogous Ru or Os compounds in which the spin–orbit coupling constant (λ) will be much larger.

2. Vibronic coupling

Throughout this review we have emphasized that strongly bent nitrosyl groups occur whenever the π-type molecular orbital which as anti-bonding with respect to M, N, and O is occupied. We will now examine in more detail the quantum mechanical basis for this correlation between the electronic structure of the complex and the molecular structure of the complex, using the extensively studied five-coordinate $\{MNO\}^8$ series as an example.

The maximum possible symmetry for a five-coordinate $M(NO)L_4$ complex is C_{4v}. Reference to Figs. 8(b) and 8(c) shows that for an $\{MNO\}^8$ complex the highest occupied molecular orbital is either $4a_1$ or $3e$, and that the electron configuration for these complexes can therefore range from $(4a_1)^2$ to $(3e)^2$. The $3e$ orbital is two-fold degenerate and will be half-filled in a $(3e)^2$ electron configuration. Moreover, somewhere between Fig. 8(b) and Fig. 8(c) the $4a_1$ and $3e$ orbitals cross and thereby become accidentally degenerate. At this crossing point there are three degenerate molecular orbitals to be occupied by a single pair of electrons.

Degeneracy (accidental or imposed) is a common occurrence in the application of molecular orbital theory to chemical bonding. However, special consideration is required for systems having partially filled degenerate molecular orbitals. In order to properly discuss such systems it is necessary to: (1) obtain the manifold of electronic states which result from the occupation of the degenerate orbitals; (2) examine the possible mixing of the states by configuration interaction; (3) evaluate the effects of spin–orbital coupling; and (4) consider mixing of the states by vibronic coupling (Jahn–Teller and Rennner–Teller effects).

The problem of obtaining and ordering the electronic states of an $\{MNO\}^8$ complex at or near the crossing point of the $4a_1$ and $3e$ molecular orbitals is analogous to the problem of obtaining and ordering the electronic states of a free ion in a medium crystal field[83]. Consequently, the behavior of the electronic states of the $\{MNO\}^8$ group in a field of C_{4v} symmetry can qualitatively be analyzed by drawing the state correlation diagram between the limiting situations, $4a_1 \ll 3e$ and $3e \ll 4a_1$. The relative energies of all of the possible electronic states which can arise from $(4a_1, 3e)^2$ electron configurations in C_{4v} symmetry have been calculated assuming that $4a_1$ and $3e$ are pure d orbitals. (The details of the calculation appear in the Appendix.) In Fig. 15 are plotted the relative energies of these states (in units of B, the interelectronic repulsion parameter) versus the energy difference (in units of B) between the $4a_1$ and $3e$ orbitals ($E_{4a_1} - E_{3e}$). Although Fig. 15 cannot be quantitatively correct because $4a_1$ and $3e$ are not pure d orbitals, it does show the important qualitive features of the behavior of the electronic states of an $\{MNO\}^8$ species upon crossing the $4a_1$ and $3e$ orbitals in C_{4v} symmetry.

It is apparent from Fig. 15 that the ground state is ${}^1A_1(4a_1)^2$ whenever the $4a_1$ orbital is much lower in energy than the $3e$ orbital. If $4a_1$ is much higher in energy that $3e$ then

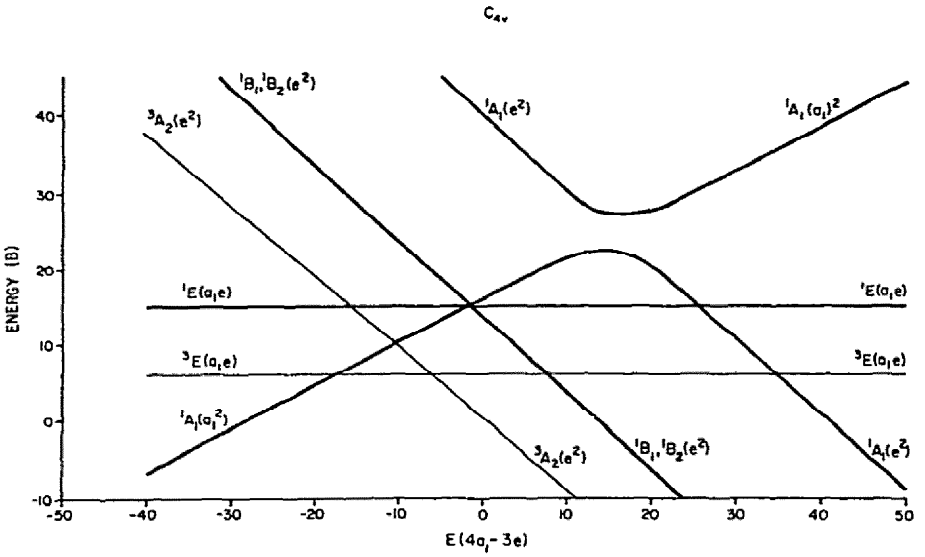

Fig. 15. The electrostatic energies of the states arising from $(4a_1, 3e)^2$ configurations as a function of the energy separation between $4a_1$ and $3e$ orbitals in a field of C_{4v} symmetry.

the electronic ground state is predicted to be $^3A_2(3e)^2$ *for a linear* $\{MNO\}^8$ *group.* However, since Walsh's rules for triatomic species[3] apply to mononitrosyl complexes a bent MNO group with a singlet ground state would be expected to be more stable than the linear $^3A_2(3e)^2$ state. Indeed, all of the $\{MNO\}^8$ species which have been isolated and characterized to date are diamagnetic. Therefore, the subsequent discussion will consider only the manifold of singlet states arising from the $(4a_1, 3e)^2$ electron configurations.

Five singlet states arise from the $(4a_1, 3e)^2$ electron configurations. One of these, $^1A_1(3e)^2$, can never be the ground state in C_{4v} symmetry. The remaining four electronic states, $^1A_1(4a_1)^2$, $^1B_1(3e)^2$, $^1B_2(3e)^2$, and $^1E(4a_1)^1(3e)^1$ are nearly degenerate when the $4a_1$ and $3e$ orbitals are degenerate. Factors which may affect the degeneracy of these states are considered next.

Configuration interaction occurs only between the two $^1A_1$ states and would not necessarily remove the degeneracy of all of the states of the singlet manifold. Spin–orbit coupling would introduce a varying amount of temperature independent paramagnetism (TIP) into the singlet states ($\sim\lambda/\Delta$, where Δ is the singlet–triplet separation), but this factor is even less important than configuration interaction. Vibronic coupling among the electronic states can be important, however. Renner[84] has considered vibronic coupling in linear molecules in detail, and has shown that a linear molecule with a degenerate ground state spontaneously distorts to non-linear geometry if the degeneracy of the ground state is sufficiently split by one of the vibrational modes of the molecule. Several discussions of the Renner–Teller effect are available[85,86]. In order to investigate the applicability of the

Renner–Teller effect to the MNO group of mononitrosyl complexes it is necessary to: obtain the normal modes of vibration for our example, an $M(NO)L_4$ species with C_{4v} symmetry; tabulate the coupling of the electronic states by the vibrational modes; ascertain whether the appropriate modes are of sufficiently low energy to be effective in lifting the degeneracy of the ground electronic states.

The seven atoms of a five-coordinate $M(NO)L_4$ complex possessing C_{4v} symmetry give rise to 15 normal modes of vibration, namely $4A_1$, $2B_1$, $1B_2$, and $4E$ modes (Fig. A.1 of the Appendix). Focusing our attention on the applicability of the Renner–Teller effect to the MNO group, however, eliminates the A_1, B_1, and B_2 vibrations from consideration because the MNO group remains linear during these vibrations. The most important of the four E modes is the E(M–N–O) mode, which is primarily the degenerate bending motion δ(M–N–O). The effects of this vibration upon the singlet states of the $M(NO)L_4$ complex in C_{4v} symmetry (Fig. 15) will now be considered.

We will first re-examine the case in which the $4a_1$ orbital is much lower in energy than the $3e$ orbital, and the ground electronic state is $^1A_1(4a_1)^2$. The E(M–N–O) mode can couple this non-degenerate state to the $^1E(4a_1)^1(3e)^1$ state, but the coupling will not be effective unless the separation between these states is small ($\sim kT$). Therefore, it can be concluded that the MNO group will remain linear whenever the $4a_1$ orbital is much lower in energy than the $3e$ orbital and that the $^1A_1(4a_1)^2$ ground electronic state is described by the potential surface shown in Fig. 16(a).

Next we consider the case where the $3e$ orbital is much lower in energy than the $4a_1$ orbital. Figure 15 shows that in this situation the only singlet states which need to be considered are $^1B_1(3e)^2$ and $^1B_2(3e)^2$. These two states are accidentally degenerate in C_{4v} symmetry and are interconverted by the A_2 rotation of the molecule about its four-fold axis. Since the molecule retains full C_{4v} symmetry during such a rotation the two states

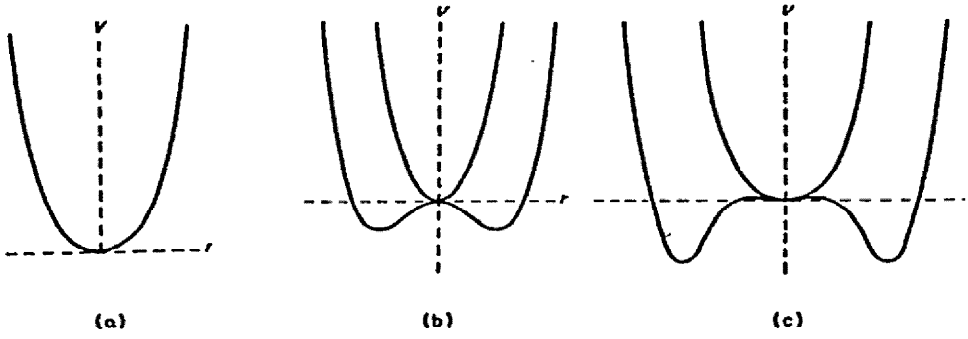

Fig. 16. Potential functions for the vibronic interaction of the bending vibration of a triatomic molecule with the electronic states. The abscissa is the bending coordinate. (a) non-degenerate state; (b) degenerate state with intermediate vibronic interaction; (c) degenerate state with large vibronic interaction. From G. Herzberg, *Molecular Spectra and Molecular Structure*, Vol. III: *Electronic Spectra and Electronic Structure of Polyatomic Molecules*. © 1966, reprinted by permission of Van Nostrand Reinhold Company.

must remain degenerate at all times. Therefore, it is convenient to refer the $^1B_1(3e)^2$ and $^1B_2(3e)^2$ states back to the $^1\Delta$ state in $C_{\infty v}$ symmetry from which they arise. It has already been demonstrated that a $^1\Delta$ state can be strongly split by a large vibronic interaction with the degenerate bending mode of a triatomic species[84–86]. Thus, for an $M(NO)L_4$ complex the degeneracy of the $^1B_1(3e)^2$ and $^1B_2(3e)^2$ electronic states can be lifted by bending the MNO group to give a potential surface similar to that shown in Fig. 16(c).

Finally, we examine the case where the $4a_1$ and $3e$ orbitals are accidentally degenerate. Figure 15 shows that near the crossing point of the $4a_1$ and $3e$ orbitals four singlet electronic states, $^1A_1(4a_1)^2$, $^1E(4a_1)^1(3e)^1$, $^1B_1(3e)^2$, and $^1B_2(3e)^2$ become degenerate. The effect of the E(M–N–O) vibration upon three of these states has already been explored. Only $^1E(4a_1)^1(3e)^1$ remains to be examined, but it has already been shown[84–86] that the degeneracy of such a state can be lifted by vibronic coupling with the degenerate bending vibration of the triatomic species. Since the $^1E(4a_1)^1(3e)^1$ state arises from an electron configuration intermediate between $(4a_1)^2$ and $(3e)^2$ it is not unreasonable to assume that the bending of the MNO group introduced by vibronic coupling of this state with the E(M–N–O) vibration will be less than that for the $^1B_1(3e)^2$ and $^1B_2(3e)^2$ degenerate pair. The appropriate potential surface for the $^1E(4a_1)^1(3e)^1$ state is shown in Fig. 16(b).

To complete this discussion of the E(M–N–O) vibrational mode it is important to examine any other couplings that this mode can effect among the degenerate singlet states. We have already pointed out that E(M–N–O) couples $^1A_1(4a_1)^2$ with $^1E(4a_1)^1(3e)^1$. This mode also couples $^1E(4a_1)^1(3e)^1$ with $^1B(3e)^2$ and with $^1B_2(3e)^2$. The vibration does not, however, couple the two B states with one another or with the $^1A_1(4a_1)^2$ state.

We have shown that the geometry of the MNO group of five-coordinate $\{MNO\}^8$ complexes is adequately explained by splitting of the degeneracy of the singlet electronic states of the linear $\{MNO\}^8$ moiety by the E(M–N–O) vibration (Renner–Teller effect). Now we can proceed to examine any additional effects which can arise from the coupling of other vibrational modes of the $M(NO)L_4$ complex with the degenerate singlet states of the complex (Jahn-Teller effect). Only the remaining B and E modes (Fig. A.1) need be considered because the A_1 modes preserve C_{4v} symmetry and can couple only A_1 electronic states.

The $B_1(T_{2u})$ mode (Fig. A.1) is particularly attractive for vibronic coupling because during this mode the L - - - L distances are always greater than or equal to the equilibrium L - - - L distances in C_{4v} symmetry, whereas the other B and E modes involve either stretching of the M–L bonds or involve L - - - L distances which are less than the equilibrium distances in C_{4v} symmetry. Moreover, the normal coordinates of the $B_1(T_{2u})$ mode are those which take a TP complex with C_{4v} symmetry into a TBP complex with C_{2v} symmetry and a linearly coordinated nitrosyl group in the equatorial position. The mode also lifts the degeneracy of the $^1E(4a_1)^1(3e)^1$ state and of the $^1B_1(3e)^2$ and $^1B_2(3e)^2$ states, and can couple the $^1A_1(4a_1)^2$ and $^1B_1(3e)^2$ states.

We have now demonstrated two low-energy bending vibrations for our present model, five-coordinate $M(NO)L_4$ complexes of C_{4v} symmetry containing the $\{MNO\}^8$ group, which can lift the degeneracy of the singlet electronic states which arise from a $(4a_1, 3e)^2$ electron configuration. The limiting geometry for vibronic interaction with the E(M–N–O) mode is a TP complex with a strongly bent nitrosyl group and C_s symmetry, whereas the limiting geometry for vibronic interaction with the $B_1(T_{2u})$ mode is a TBP complex with a linear nitrosyl group and C_{2v} symmetry. Figure 17 shows the correlation diagram relating the singlet states for the two limiting geometries. On the left-hand side are the states for the C_{2v} molecule and on the right-hand side are the states for the C_s molecule with a non-linear MNO group. The center of the diagram shows the ordering of the singlet states in true C_{4v} symmetry near the crossing point of the $4a_1$ and $3e$ orbitals where there can be as much as a five-fold degeneracy of the singlet states.

The state diagram (Fig. 15) supports our previous analysis of the structures of five-coordinate $\{MNO\}^8$ complexes, which was based solely on the relative energies of the $4a_1$ and $3e$ molecular orbitals (Section II.C.1). The far l.h.s. of Fig. 15 gives the relative energies of the states derived from $(4a_1, 3e)^2$ when the energy of $4a_1 \ll 3e$, and corresponds to the molecular orbital diagram in Fig. 8(a). The far r.h.s. has the energy of $3e \ll 4a_1$ corresponds to the molecular orbital diagram in Fig. 8(d). The center of Fig. 15 represents the point at which the $4a_1$ and $3e$ orbitals become degenerate. The fact that four singlet states become degenerate when $4a_1$ and $3e$ are degenerate suggests that these are the circumstances in which five-coordinate $\{MNO\}^8$ complexes may have intermediate coordination geometries and/or intermediate M–N–O bond angles. The properties of the other ligands and of the metal atom will determine which of these states of the singlet manifold is actually the ground state, and will also determine whether any of the manifold of singlet states are degenerate in C_{4v} symmetry. Consequently, the choice among TBP coordination geometry with a linear MNO group, TP coordination geometry with a strongly bent MNO group, or intermediate coordination geometry with an intermediate M–N–O angle can be controlled by the symmetry and design of specific ligands and by the particular metal atom bound to the NO group.

The correlation between molecular and electronic structure of mononitrosyl complexes has already been pursued in considerable detail. We will now explore those $\{MNO\}^8$ complexes which may have $4a_1$ and $3e$ nearly degenerate with respect to the state correlation diagram of Fig. 17. When four identical ligands are attached to a bent $\{MNO\}^8$ group, the overall symmetry of the complex is C_s. If the symmetry of the ML_4 group is C_{4v}, then all four orientations of the bent MNO group will be of equal energy and have identical M–N–O angles. The energy barrier for the interconversion from one of these four rotameric forms to the other is the energy separation between the $^1A'(a')^2$ and $^1A''(a')^1(a'')^1$ states on the r.h.s. of Fig. 17. For ML_4 moieties of symmetry lower than C_{4v}, the energies of the four orientations of the bent nitrosyl group may differ, and the M–N–O angles in the four orientations need not be identical.

The maximum symmetry for the substituted complexes $M(NO)L_2X_2$ and $M(NO)L'_2$ (where L' is a bidentate ligand) is C_{2v}. If the ground state(s) of these C_{2v} complexes (with linear MNO groups) is still accidentally degenerate, then the molecule will distort along

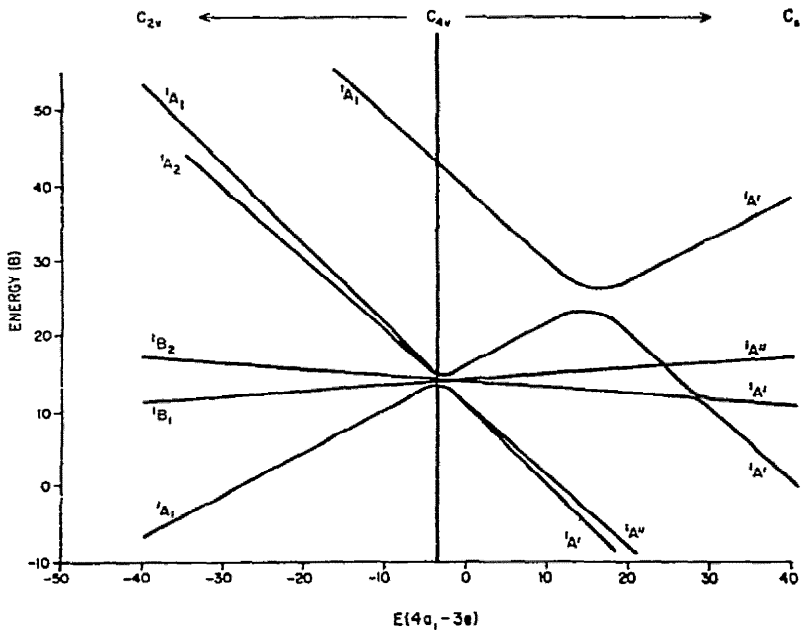

Fig. 17. The correlation diagram for the singlet states of $(4a_1, 3e)^2$ configurations in the fields of C_{2v}, C_{4v} and C_s symmetries.

another vibrational coordinate and thereby lower the symmetry to C_2 or C_s. Similarly, any degeneracy remaining in C_2 or C_s symmetry will finally be removed by distorting the molecule to C_1 symmetry. In C_1 symmetry, all the electronic states and normal modes of vibration are of A symmetry and the ground state will be non-degenerate.

The $Co(NO)Cl_2(PR_3)_2$ complexes[60–62] were discussed in Section II.C.1. The structure of one form of $Co(NO)Cl_2[P(CH_3)(C_6H_5)_2]_2$ is shown in Fig. 9. The highest possible symmetry of the coordination sphere of this complex is C_{2v}. We propose that in C_{2v} symmetry, the ground state of this molecule would be accidentally degenerate and that this degeneracy has been lifted by lowering the symmetry to C_s. The observed structure is consistent with a distortion along a composite normal coordinate comprised of the appropriate components of the $E(T_{2g})$ and E(M–N–O) vibrations shown in Fig. A.1. Distortion along the other components of these two E vibrations is also possible, and would result in a complex with the nitrosyl group bent in the MP_2 plane (Fig. 10(c)). If these two vibronic states are of similar energy then the existence of two different forms of the $Co(NO)Cl_2(PR_3)_2$ complexes can easily be understood. The two vibronic states correspond to bending the nitrosyl group in the MCl_2 plane and in the MP_2 plane, and would be thermally accessible by rotation of the NO group. These facts place the $Co(NO)Cl_2(PR_3)_2$ molecules only slightly to the C_s side of the correlation diagram (Fig. 17). To our knowledge, this series of complexes is the *only* class of five-coordinate mononitrosyl complexes whose properties require recourse

to vibronic coupling between degenerate or nearly degenerate states in order to be adequately explained. The properties of all other five-coordinate nitrosyls are adequately accounted for by the one-electron molecular orbital diagrams of Fig. 8.

It is also necessary to invoke vibronic coupling between singlet states which are accidentally degenerate to explain the intermediate structure of the four-coordinate $\{MNO\}^{10}$ complex, $Ni(NO)(N_3)[P(C_6H_5)_3]_2$. However, the nature and composition of the electronic states are very similar to those for five-coordinate $\{MNO\}^8$ complexes (see Appendix). Thus, Figs. 15 and 17 are generally applicable to understanding the structure and bonding of mononitrosyl complexes.

In summary, this analysis of the electronic states and the vibronic couplings of the singlet states of five-coordinate $\{MNO\}^8$ complexes accounts for the structures and physical properties of all of the mononitrosyl complexes in this category, including complexes with intermediate geometry. This analysis provides a more detailed quantum mechanical basis for discussing these complexes than does the one-electron molecular orbital model developed in this review, and simultaneously demonstrates the general validity of the conclusions drawn from the one-electron model.

H. Reactions of coordinated nitrosyl groups

The equilibrium geometries of metal nitrosyl complexes exhibit M–N–O angles ranging from 120° to 180°, and consequently the simplest reaction which a coordinated nitrosyl group can undergo is the transformation from one limiting geometry to another. It has already been shown above that the M–N–O angle in five-coordinate $\{MNO\}^8$ mononitrosyl complexes is determined by the coordination geometry, and Fig. 17 demonstrates the inherent electronic barrier to the interconversion of a TBP complex with a linear MNO group and a TP complex with a strongly bent MNO group. There is no definitive example of such a reaction occurring, although it was originally proposed[61] that the $CoCl_2(NO)(PR_3)_2$ complexes have two NO stretching frequencies in solution and in the solid state because both the TBP and TP species are present in dynamic equilibrium. However, the structure determination for one of the forms of $CoCl_2(NO)[PCH_3(C_6H_5)_2]_2$ shows a distorted coordination geometry[62], and we have suggested that the compound exists as two conformers differing primarily in the rotational orientation of the non-linear CoNO group (Sections II.C.1 and II.G.2).

To our knowledge there is only one well-documented example of the conversion of a coordinated nitrosyl group from one limiting geometry to the other by a simple change in stereochemistry. Reaction II occurs readily upon mixing the reagents at room temperature (ref. 32).

$$[Co(NO)(das)_2]^{2+} + X^- \rightarrow [Co(NO)X(das)_2]^+ \qquad \text{(II)}$$

Table 6 summarizes the marked differences in the physical properties of the two complexes, and Fig. 18 shows the coordination environment of each. It is clear that the change in stereo-

TABLE 6
Physical properties of $[Co(NO)(das)_2]^{2+}$ and $[Co(NO)(das)_2X]^{+}$

	ν_{NO} (cm^{-1})	N–1s (eV)	Co–NO (A)	Co–N–O (deg)
$[Co(NO)(das)_2][ClO_4]_2$	1852 [a]	402.3 [b]	1.68(2) [c]	179(2)
$[Co(NO)(das)_2(NCS)]NCS$	1587 [a, d] 1561	–	1.87(2) [c, e]	134(2)
$[Co(NO)(das)_2Cl]Cl$	1562 [a, d] 1548	400.5 [b]	–	–

a See ref. 32.
b See ref. 21.
c See ref. 31.
d The two frequencies presumably result from *cis* and *trans* isomers (see ref. 32).
e *Trans* isomer.

chemistry from five- to six-coordination has resulted in a change in the geometry of the $[CoNO]^{2+}$ moiety, an $\{MNO\}^8$ system, from linear to strongly bent. This reaction is readily interpreted upon examination of Fig. 8. $[Co(NO)(das)_2]^{2+}$ is a TBP cation and should have d_{z^2} as the highest occupied orbital (Fig. 8(a)). Increasing the coordination number from five to six changes d_{z^2} from a non-bonding or weakly anti-bonding orbital into a sigma anti-bonding orbital ($4a_1$) of higher energy than $3e$ (Fig. 8(c)). As a result the $3e$ orbital now contains a pair of electrons, and the $\{CoNO\}^8$ triatomic exhibits a strongly bent geometry

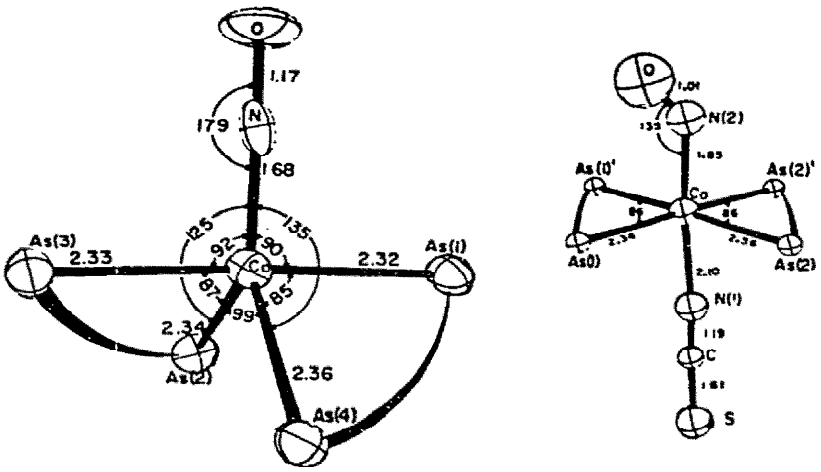

(a) (b)

Fig. 18. (a) Perspective view of the inner coordination sphere of $[Co(NO)(das)_2]^{2+}$; (b) perspective view of the inner coordination sphere of $[Co(NO)(das)_2(NCS)]^{+}$. (Reproduced from ref. 31.)

represented by orbital scheme 8(d). The crossing of the $3e$ and $4a_1$ levels in Fig. 8 upon going from five-coordinate TBP geometry to six-coordination results in the transfer of a pair of electrons from a predominantly metal orbital (d_{z^2}) to an orbital with a large amount of NO character ($3e$). Therefore, the overall reaction which is initiated by an increase in coordination number from five to six can be formally described as a two-electron reduction of the coordinated NO^+ group with the concomitant oxidation of the metal from Co(I) to Co(III) (ref. 31).

Reaction III (ref. 87) represents another probable example of the conversion of a coordinated nitrosyl group from one valence form to another

$$[Fe(NO)X(das)_2]^+ \rightarrow [Fe(NO)X(das)_2]^{2+} + 1e^- \qquad \text{(III)}$$

This reaction involves oxidation of the $\{FeNO\}^7$ triatomic to the $\{FeNO\}^6$ triatomic but no change in coordination geometry or coordination number. Table 7 summarizes some pertinent physical data for the two complexes. It is important to note that this oxidation reaction results in an *increase* in the formal positive charge on the nitrosyl group and a *decrease* in the formal positive charge on the Fe atom. Figure 4 presents the correlation diagram for this reaction which can be described as a two-electron *oxidation* of a coordinated NO^- ligand to a coordinated NO^+ group with concomitant *reduction* of the metal from Fe(III) to Fe(II). The transformation is initiated by an overall one-electron oxidation of the complex. Unfortunately, definitive structure determinations are not available for these two compounds. However, a preliminary report[26] of the structure of the reduced complex has shown an Fe–N–O angle of 148°, and the oxidized form of the complex almost certainly has a linear FeNO array (Section II.F).

It has not yet been possible to carry out the reverse of reaction III, the one-electron reduction of the $\{FeNO\}^6$ species to the $\{FeNO\}^7$ complex. However, this reduction is well-known[22–24] for the formally isoelectronic nitroprusside anion (reaction IV).

$$Fe(NO)(CN)_5^{2-} + 1e^- \rightarrow Fe(NO)(CN)_5^{3-} \qquad \text{(IV)}$$

TABLE 7
Properties of $[Fe(NO)(das)_2Cl]^+$ and $[Fe(NO)(das)_2Cl]^{2+}$

	ν_{NO} (cm^{-1})	N–1s (eV)	Fe–$2p_{\frac{3}{2}}$ (eV)
$[Fe(NO)(das)_2Cl][ClO_4]$	1620 [a]	400.0 [b]	711.5 [c]
$[Fe(NO)(das)_2Cl][ClO_4]_2$	1865 [d]	402.9 [b]	709.5 [c]

a See ref. 87.
b See ref. 21.
c R.D. Feltham, unpublished results.
d W. Silverthorn and R.D. Feltham, *Inorg. Chem.*, 6 (1967) 1662.

In addition to the transformations of coordinated nitrosyl groups from one valence form to another there are several other chemical reactions of the coordinated nitrosyl group. For example, the nitroprusside ion reacts with hydroxide ion to form the pentacyanonitro complex via reaction V (ref. 2f)

$$Fe(CN)_5(NO)^{2-} + 2OH^- \rightarrow Fe(CN)_5(NO_2)^{4-} + H_2O \qquad (V)$$

Reaction V also occurs[87] with $Fe(NO)X(das)_2^{2+}$ and $RuCl(NO)(das)_2^{2+}$ (ref. 88). Other nucleophiles including SH^- and ketones react with the coordinated nitrosyl group of $Fe(CN)_5(NO)^{2-}$ (ref. 2f), and hydrazines react with $RuClNO(das)_2^+$ according to eqns. VI and VII (ref. 88).

$$RuCl(NO)(das)_2^{2+} + 3N_2H_4 \rightarrow RuN_3Cl(das)_2 + 2N_2H_5Cl + H_2O \qquad (VI)$$

$$RuCl(NO)(das)_2^{2+} + 3H_2N{-}NHR \rightarrow RuCl(NONNHR)(das)_2 + 2NH_3NHR^+ \qquad (VII)$$

Reactions V–VII demonstrate the electrophilic character[2f] of a linearly coordinated nitrosyl group with a high NO stretching frequency ($\nu_{NO} > 1850\ cm^{-1}$) and a high N–1s binding energy ($E_{N-1s} \geqslant 402$ eV), i.e. a coordinated NO^+ group. Linearly coordinated nitrosyl groups with low NO stretching frequencies and low N–1s binding energies do not exhibit electrophilic character. In fact, $Mn(CN)_5(NO)^{3-}$ ($\nu_{NO} = 1725\ cm^{-1}$) and $Cr(CN)_5(NO)^{4-}$ ($\nu_{NO} = 1515\ cm^{-1}$) are completely stable in alkaline solution[2h]. The latter compound readily decomposes in acidic solution by a series of complex hydrolysis and reduction reactions to ultimately yield Cr^{2+}, CN^-, NH_3, and H_2O. Hydrolysis of $Cr(CN)_5(NO)^{3-}$ ($\nu_{NO} = 1645\ cm^{-1}$) also occurs in acidic solution; VIII is the initial hydrolysis reaction[89]

$$H_3O^+ + Cr(CN)_5(NO)^{3-} \rightarrow Cr(CN)_4(H_2O)(NO)^{2-} + CN^- \qquad (VIII)$$

The electrochemical reactions of several mononitrosyl complexes have been reviewed (ref. 2h) and the results generally support the conclusion[90] that the MNO group functions as an electrochemical unit.

There are several reactions which appear to be characteristic of a coordinated NO^- group. The $Fe(CN)_5(NO)^{3-}$ ion reacts with protons[23] to give a complex formulated as $Fe(CN)_5(NOH)^{2-}$. Protonation reactions are also observed for $Co(NO)X(das)_2^+$ (ref. 91), and $Os(NO)(CO)[P(C_6H_5)_3]_2Cl$ (ref. 92). Reactions with molecular oxygen to give a coordinated nitro group have been investigated[93] (reaction IX).

$$\textit{trans}\text{-}\ Co(NO)(en)_2X^{2+} + O_2 \rightarrow Co(NO_2)(en)_2X^+ \qquad (IX)$$

A coordinated nitro group also results from the reaction with excess NO (ref. 94), as shown in eqn. X

$$\textit{trans}\text{-}\ [Co(NO)(en)_2Cl]Cl + 2NO \rightarrow \textit{cis}\text{-}[CoNO_2(en)_2Cl]Cl + N_2O \qquad (X)$$

The black complex $Co(NH_3)_5(NO)^{2+}$ (ref. 29) dimerizes upon standing to give a red complex containing a bridging hyponitrite anion ($N_2O_2^{2-}$) (ref. 95).

The exchange reactions of the nitrosyl group of mononitrosyl complexes have been little studied. The ^{15}NO exchange of $Co(NO)(CO)_3$ in the gas phase occurs by an associative process and is much slower than CO exchange in the same compound. Nitrosyl exchange does not occur for $(C_5H_5)NiNO$ after 30 days at 45° (ref. 96).

Scission of an M–N bond does occur in the reactions of $Ru(bipy)_2(NO)Cl^{2+}$ (ref. 97) and $RuCl(NO)(das)_2^{2+}$ (ref. 98) with azide ion. Isotopic labeling[98] with ^{15}NO suggests that these reactions proceed by mechanism XI and involve the unstable cyclic N_4O intermediate which readily decomposes to give N_2 and N_2O

$$[Ru - {}^{15}NO]^{3+} + N_3^- \rightarrow Ru-{}^{15}N(O){}^{14}N({}^{14}N)-{}^{14}N \rightarrow \quad \text{(XI)}$$

$$\rightarrow {}^{14}N{}^{15}N + ({}^{14}N)_2 + {}^{14}N{}^{15}NO + ({}^{14}N)_2O$$

Irradiation of $(h^5\text{-}C_5H_5)Mo(CO)_2(NO)$ with ultraviolet light in the presence of $(C_6H_5)_3P$ results in the formation of $(h^5\text{-}C_5H_5)Mo(NCO)(CO)_2[P(C_6H_5)_3]$ and $(C_6H_5)_3PO$. It has been proposed[99] that this reaction involves abstraction of an O atom from the coordinated NO group by $(C_6H_5)_3P$ to generate an organometallic nitrene which then captures carbon monoxide to give the coordinated NCO ligand.

The chemical behavior of mononitrosyl complexes outlined above shows that the M–N bond is very robust for both linear and non-linear MNO groups. Indeed, a recent extensive review[2k] shows that substitution reactions of the other ligands attached to the metal are the most common reactions for metal nitrosyl complexes. The inertness of the MNO group to cleavage of the M–N or N–O bonds provides additional chemical justification for our treatment of mononitrosyl complexes as $\{MNO\}^n$ species perturbed by the coordination of other ligands to the metal.

III. POLYNITROSYL COMPLEXES

The previous sections of this review have been concerned exclusively with mononitrosyl complexes, and it was shown that the structures, bonding and reactivity of that class of compounds can be understood as simple MNO triatomic species perturbed by the coordination of other ligands to the metal. It would be logical to extend this model to polynitrosyl complexes by considering them as perturbed $M(NO)_x$ species. Several factors, however, complicate such an analysis of polynitrosyl complexes. Consider for example, the penta-atomic species $M(NO)_2$: (1) there are many ways of making the O–N–M–N–O group non-linear, whereas M–N–O has only one variable bond angle; (2) there are no simple bases for predicting the geometries of penta-atomic molecules of the non-transition

elements, whereas Walsh treated triatomic molecules in detail many years ago[3]; (3) the metal atom is necessarily the central atom of $M(NO)_2$, whereas the metal atom is the terminal atom of MNO; (4) there are few structural data and almost no spectroscopic or chemical data on polynitrosyl complexes, whereas considerable data are available for mononitrosyl complexes.

In spite of these complications, a surprising amount of insight into the structure, bonding, and reactivity of polynitrosyl complexes can be obtained from the model developed for mononitrosyl complexes with the aid of one new assumption. For polynitrosyl complexes it is assumed that changes in the N–M–N angles are more important than changes in the M–N–O angles and that the observed deviations of the MNO groups

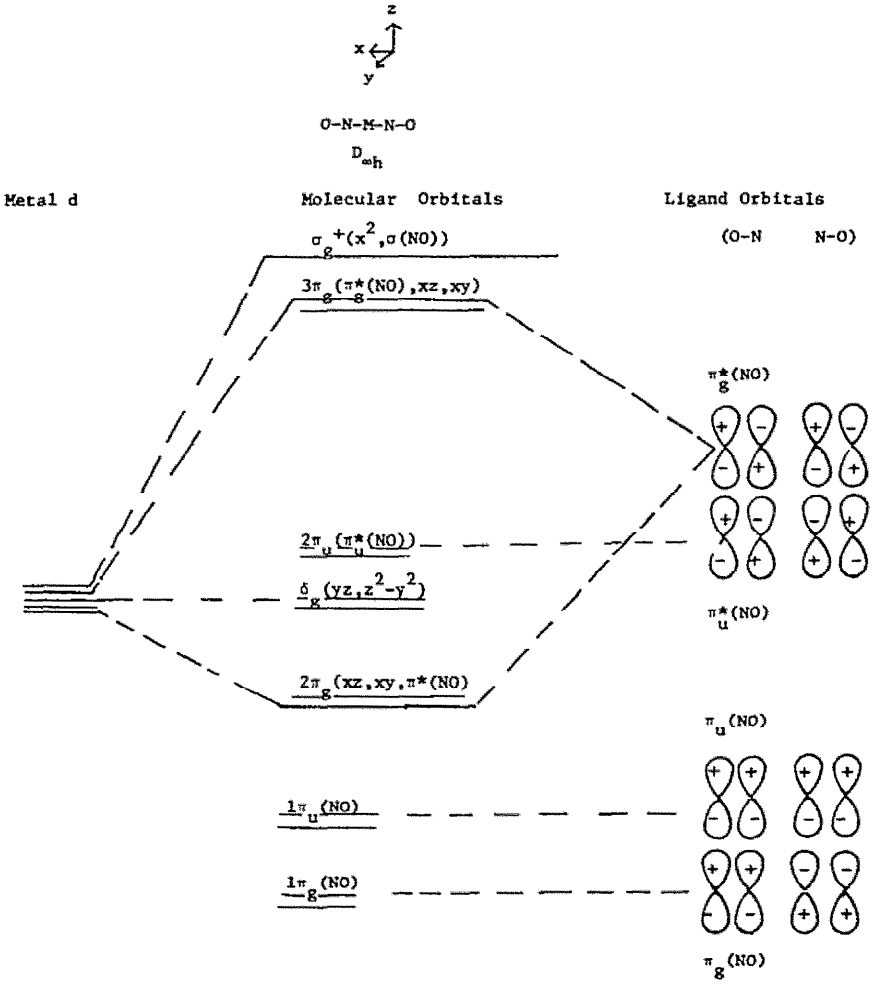

Fig. 19. Proposed molecular orbital scheme for the linear $M(NO)_2$ group. In this figure and in all subsequent figures z is defined as the bisector of the N–M–N angle. The metal d orbitals were obtained from the conventional d orbitals by the transformation $x \rightarrow z$, $y \rightarrow y$, $z \rightarrow x$.

from linearity can be understood as perturbations of an $M(NO)_x$ species with equilibrium N–M–N angles.

A. $M(NO)_2$ complexes

The simplest polynitrosyl is the hypothetical penta-atomic species $M(NO)_2$. The highest symmetry possible for this species is $D_{\infty h}$, and the one-electron molecular orbital diagram for the linear O–N–M–N–O penta-atomic is shown in Fig. 19, which considers the interactions among the metal *d* orbitals and the π(NO) and π^*(NO) orbitals of the nitrosyl ligands. The bisector of the N–M–N angle has been defined as *z* in order to simplify subsequent discussions. Upon comparison with Fig. 2 it can be seen that the presence of two nitrosyl ligands results in a ligand localized molecular orbital, $2\pi_u(\pi_u^*(NO))$, which has a node at the metal atom. In this approximation the energy of the $2\pi_u$ orbital would be similar to that of the free nitrosyl ligands, and hence similar to the energy of the metal *d* orbitals as well.

The simple penta-atomic, $M(NO)_2$, has no other ligands whose effects need to be considered, and thus possible changes in the N–M–N angle and M–N–O angles can be investigated for various electron configurations. Any change in the N–M–N angle leads to a molecule of C_{2v} symmetry and the correlation diagram relating $D_{\infty h}$ and C_{2v} is shown in Fig. 20. Figure 21 shows diagrammatically the ligand orbitals referred to in C_{2v} symmetry. One important difference between $M(NO)_2$ in $D_{\infty h}$ and in C_{2v} symmetry (N–M–N = 90°) is that there are three molecular orbitals which are bonding with respect to M and N in

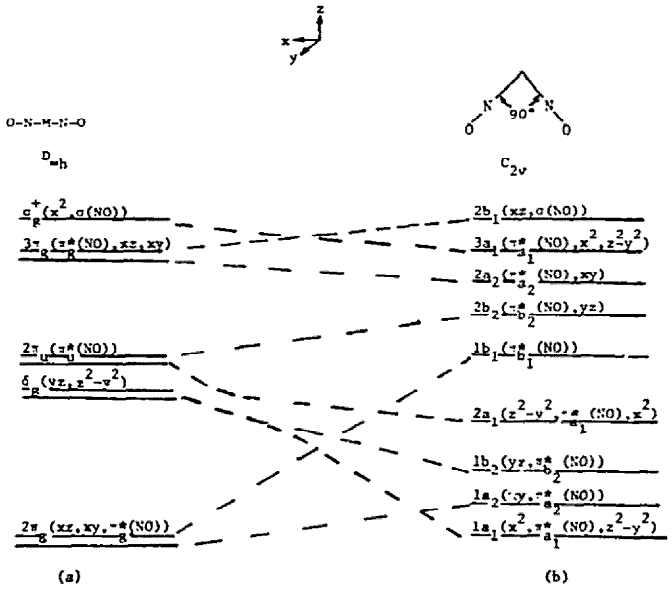

Fig. 20. Correlation diagram relating the molecular orbitals for a linear $M(NO)_2$ group with $D_{\infty h}$ symmetry (a) to those for C_{2v} symmetry (b). The metal *d* orbitals are those of Fig. 19.

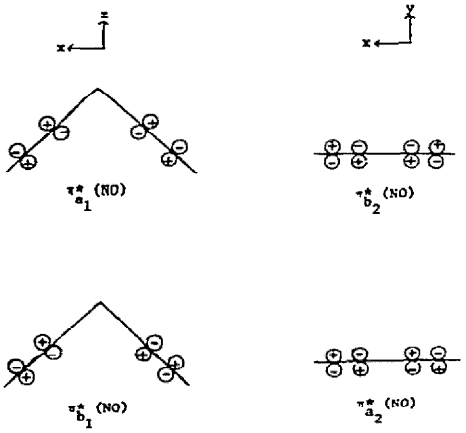

Fig. 21. The ligand localized molecular orbitals in C_{2v} symmetry derived from the π^*(NO) orbitals of two NO ligands.

C_{2v}, whereas only two bonding interactions are possible in $D_{\infty h}$. It has also been pointed out[100] that in C_{2v} there is no rotational symmetry along the M–N bonds, and that therefore the MNO angles may deviate somewhat from linearity in this symmetry. Inspection of the ligand localized orbitals (Fig. 21) which are involved in the three bonding interactions shows that the $\pi^*_{a_1}$(NO) and the $\pi^*_{b_2}$(NO) orbitals are bonding with respect to the two N atoms and with respect to the two O atoms. Thus, the $1a_1$ and the $1b_2$ orbitals (Fig. 20(b)) can be further stabilized in C_{2v} symmetry by small changes in the M–N–O angles (in the xz plane) so as to move the O atoms closer together. Such changes will destabilize the $1a_2$ and $1b_1$ orbitals.

The implications of the one-electron molecular orbital scheme of Fig. 20 can now be examined. Clearly an $\{M(NO)_2\}^4$ species would have two bonding interactions between the M and N atoms in either linear ($D_{\infty h}$) or bent (C_{2v}) geometry, but linear geometry ($D_{\infty h}$) minimizes repulsions between the two NO groups. Additional electrons will occupy the δ_g orbital in $D_{\infty h}$ symmetry. The δ_g orbital is non-bonding with respect to M and N, and therefore, the additional electrons lead to no new bonding interactions in this geometry. In a bent species with C_{2v} symmetry, however, there are three orbitals which are bonding with respect to M and N: $1a_1$, $1a_2$, and $1b_2$. Thus, an $\{M(NO)_2\}^6$ species should adopt a bent structure with C_{2v} symmetry. There may also be slight deviations of the MNO groups from linearity because of the nature of the $1a_1$ and $1b_2$ orbitals.

The molecular orbital scheme of Fig. 20 also predicts C_{2v} symmetry for an $\{M(NO)_2\}^8$ species. However, an $\{M(NO)_2\}^8$ entity could exhibit $D_{\infty h}$ symmetry if the $2\pi_u$ orbital were much higher in energy than δ_g. In the latter case decreasing the N–M–N angle from 180° would not result in sufficient interaction between the $2\pi_u$ and δ_g orbitals to compensate for the non-bonded repulsions of the two nitrosyl groups.

Finally we consider the $\{M(NO)_2\}^{10}$ penta-atomic species. In C_{2v} symmetry this

species will have the electron configuration $(1a_2)^2\,(1a_1)^2\,(1b_2)^2\,(2a_1)^2(1b_1)^2$. At an N–M–N angle of 90° the $1b_1$ orbital is entirely localized on the NO groups and is non-bonding with respect to M and N. It is anti-bonding with respect to the two N atoms and anti-bonding with respect to the two O atoms (Fig. 21). Thus, population of this orbital would be expected to cause the N–M–N angle to increase and could also lead to changes in the M–N–O angles so as to move the O atoms farther apart.

This completes our examination of the expected behavior for the hypothetical $\{M(NO)_2\}^n$ complexes for various values of n, and we can now turn our attention to known complexes containing the $M(NO)_2$ molecular fragment. These complexes will be classified by coordination number as was done for mononitrosyl complexes.

1. Four-coordination

The coordination of two additional ligands to the penta-atomic $M(NO)_2$ moiety can give rise to *trans*-square planar (D_{2h}), *cis*-square planar (C_{2v}), and pseudo-tetrahedral (C_{2v}) geometries (Fig. 22).

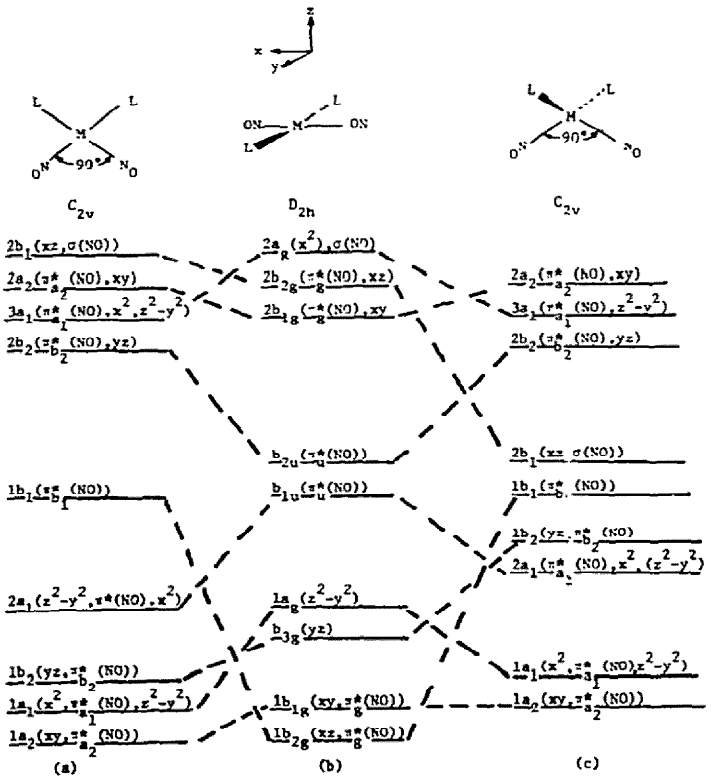

Fig. 22. Correlation diagram relating the molecular orbital scheme for *cis*-square planar (a), *trans*-square planar (b), and pseudo-tetrahedral (c) four-coordinate dinitrosyl complexes. An N–M–N angle of 90° has been used to construct (c) so that the $1b_1(\pi^*_{b_1}(NO))$ and $2b_1(xz, \sigma(NO))$ orbitals will be orthogonal to one another. The *d* orbitals are defined in Fig. 19.

Although no structures of four-coordinate $\{M(NO)_2\}^8$ complexes have been reported, Fig. 22 as well as the preceding discussion of the $M(NO)_2$ penta-atomic species predict that *cis*-square planar geometry (C_{2v}) with nearly linear MNO groups will be more stable. There may be some bending of the MNO groups in the plane of the complex so as to move the two O atoms closer to one another. It is also interesting to note that Figs. 22(a) and (b) demonstrate the inherent electronic barrier to unimolecular *cis–trans* isomerization of diamagnetic square planar d^8 complexes.

Figure 22 can also be used to analyze the structure and bonding of $\{M(NO)_2\}^{10}$ complexes. It is clear that the stability of the highest filled molecular orbital is greatest at geometries intermediate from the three limiting diagrams shown. Moreover, by examining the nature of the $\pi^*_{b_1}$(NO) ligand orbital (Fig. 21) and the b_{1u} orbital (π^*_u in $D_{\infty h}$, Fig. 19), the changes in the N–M–N angle and in the M–N–O angles which would stabilize the highest filled orbital in each symmetry can be predicted. In *cis*-square planar geometry (Fig. 22(a)) the highest filled orbital is the ligand orbital $\pi^*_{b_1}$(NO), which is anti-bonding with respect to the two N atoms and anti-bonding with respect to the two O atoms. Thus, population of this orbital should increase the N–M–N angle and change the M–N–O angles so as to move the O atoms farther from one another. Expansion of the N–M–N angle is difficult in *cis*-square planar geometry because of the proximity of the other two ligands in the plane.

In D_{2h} symmetry (Fig. 22(b)) the $b_{1u}(\pi^*_u(NO))$ orbital will be the highest occupied molecular orbital. This orbital has no metal d character and is bonding with respect to the two N atoms and bonding with respect to the two O atoms. This orbital will be stabilized by decreasing the N–M–N angle and by changing the M–N–O angles so as to move the O atoms closer to one another. Any change in the N–M–N angle lowers the symmetry to C_{2v} and results in $b_{1u} \rightarrow a_1$.

Decreasing the N–M–N angle to 90° along with a concomitant decrease of the L–M–L angles leads to the limiting pseudo-tetrahedral geometry of Fig. 22(c). It is important to note that in pseudo-tetrahedral geometry an $M(NO)_2L_2$ molecule has two molecular orbitals of b_1 symmetry which can potentially be of very similar energy ($1b_1$ and $2b_1$). For N–M–N = 90° these two orbitals are orthogonal to one another. However, any change in the N–M–N angle will mix these two levels as is evident from Fig. 22(c). In tetrahedral geometry all five metal d orbitals can interact with both the σ and π orbitals of the ligands. Therefore, the composition of the $1b_1$ orbital in the ground state geometry of the molecule will depend upon the σ-donating and π-accepting character of the other ligands coordinated to the metal as well as upon the nature of the metal atom.

Insight into the possible ground state geometries is provided by Fig. 23, which considers only the two b_1 orbitals in question. In Fig. 23(b), the $\pi^*_{b_1}$(NO) orbital is considered to be much lower in energy than d_{xz}. From the diagram of the $\pi^*_{b_1}$(NO) orbital in Fig. 21 it is clear that population of this orbital will favor the structural changes shown by Fig. 23(b) → 23(a). On the other hand, if the metal d_{xz} orbital is much lower in energy than $\pi^*_{b_1}$(NO) then nearly tetrahedral geometry will be expected with perhaps some slight

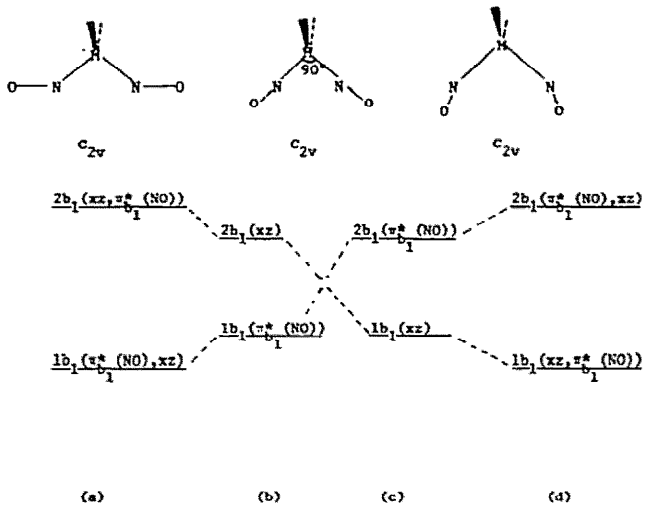

Fig. 23. Correlation diagram showing the proposed behavior of the $1b_1$ and $1b_2$ molecular orbitals in four-coordinate $\{M(NO)_2\}^{10}$ complexes with a $(1b_1)^2$ electron configuration. Scheme (b) means that $\pi^*_{b_1}$(NO) is lower in energy than d_{xz} and leads to structure (a). Scheme (c) means that d_{xz} is lower than $\pi^*_{b_1}$(NO) and leads to (d). The complete bonding scheme and the choice of coordinate system are shown in Fig. 22.

bending of the M–N–O groups so as to move the two O atoms closer together because of the respective contributions of $\pi^*_{a_1}$(NO) and $\pi^*_{b_2}$(NO) to the $1a_1$ and $1b_2$ molecular orbitals. Structure 23(a) will be favored by metals of the third transition series (5*d*) and ligands which are poor π-acceptors; structure 23(d) will be favored by metals of the first transition series (3*d*) and ligands which are good π-acceptors.

Table 8 summarizes the properties of several four-coordinate $\{M(NO)_2\}^{10}$ complexes whose structures have been determined. Included in this table are two iron complexes containing metal–metal bonds, but for which at least one $\{M(NO)_2\}^{10}$ valence structure can be written. All the compounds in Table 8 can be analyzed by utilizing Figs. 22(c) and 23. Of particular interest are the three complexes: $Fe(NO)_2[P(C_6H_5)_3]_2$ (ref. 101), $Ru(NO)_2[P(C_6H_5)_3]_2$ (ref. 102) and $Ir(NO)_2[P(C_6H_5)_3]_2^+$ (ref. 103). The increase in the N–M–N angle from 124° to 154° and the increase in the O–M–O angle to 167.5° in going from the Fe compound to the Ir compound are consistent with a gradual increase in the contribution of $\pi^*_{b_1}$(NO) (Fig. 21) to the $1b_1$ molecular orbital. The N–M–N and O–M–O angles also indicate that the Ru (ref. 102) and Ir (ref. 103) complexes are best described by the bonding scheme in Fig. 23a. All of the other compounds of Table 8 for which sufficient information is available are best described by the bonding scheme of Fig. 23d, in which the $1b_1$ molecular orbital is primarily composed of d_{xz} of the metal.

It is important to note that the $1b_1$ molecular orbital will be non-bonding only when

TABLE 8
Four-coordinate dinitrosyl complexes

Complex	ν_{NO} (cm^{-1})	M–N (A)	N–M–N (deg)	O–M–O (deg)	M–N–O (deg)	L–M–L (deg)
$[Fe(NO)_2I]_2$	1818, 1771 [a]	1.67(4) [a, b]	116(2)	98(3)	161(3) [b]	107.4(6)
$[Fe(NO)_2SC_2H_5]_2$	1773, 1748 [c]	1.67(1) [b, d]	117.4(2)	106.6(2)	167(4) [b]	106.0(1)
$Fe(NO)_2(f_6fos)$	1746, 1702 [e]	1.65(1) [b, f]	125.4(4)	123	177(1) [b]	86.8(1)
$Fe(NO)_2(CO)_2$	1810, 1766 [g]	1.77(2) [h]	–	–	180 [i]	–
$Fe(NO)_2[P(C_6H_5)_3]_2$	1714, 1674 [j]	1.650(7) [k]	123.8(4)	–	178.2(7)	111.9(1)
$Ru(NO)_2[P(C_6H_5)_3]_2$	1655, 1605 [l]	1.762(6) [l]	139.2(3)	142.7(2)	177.7(6) 170.6(5)	103.85(6)
$[Co(NO)_2Cl]_2$	1859, 1790 [m]	1.73(3) [n]	110(2)	99	166(3)	88(1)
$[Co(NO)_2I]_x$	1846, 1792 [a]	1.61(4) [a]	118(2)	110(1)	171(4)	96.2(1)
$[Co(NO)_2(NO_2)]_x$	1878, 1783 [o]	1.67 [o]	112	102	166	–
$Co_4(NO)_6(NO_2)_2N_2O_2$	1850, 1796 [p]	1.65(1) [p]	113(1)	–	164(1)	84.5 86.7
$\{Ir(NO)_2[P(C_6H_5)_3]_2\}^+$	1760, 1715 [q]	1.77(1) [q]	154(1)	167.5(5)	164(1)	116.3(2)

a L.F. Dahl, E.R. deGil and R.D Feltham, *J. Amer. Chem. Soc.*, 91 (1969) 1653.
b Average of chemically equivalent groups.
c A. Jahn, *Z. Anorg. Allgem. Chem.*, 301 (1959) 301.
d J.T. Thomas, J.H. Robertson and E.G. Cox, *Acta Cryst.*, 11 (1958) 599.
e J.P. Crow, W.R. Cullen, F.G. Herring, J.R. Sams and R.L. Tapping, *Inorg. Chem.*, 10 (1971) 1616.
f W. Harrison and J. Trotter, *J. Chem. Soc. A.*, (1971) 1542.
g See Table 3 of ref. 2e.
h Electron diffraction study, L.O. Brockway and J.S. Anderson, *Trans Faraday Soc.*, 33 (1937) 1233.
i Assumed.
j D.E. Morris and F. Basolo, *J. Amer. Chem. Soc.*, 90 (1968) 2531.
k See ref. 101.
l See ref. 102.
m See Table 6 of ref. 2e.
n S. Jagner and N.G. Vannerberg, *Acta Chem. Scand.*, 21 (1967) 1183.
o C.E. Strouse and B.I. Swanson, *Chem. Commun.*, (1971) 55.
p R. Bau, I.H. Saberwhal and A.B. Burg, *J. Amer. Chem. Soc.*, 93 (1971) 4926.
q See ref. 103.

the N–M–N angle is 90°. At other N–M–N angles the d_{xz} and $\pi^*_{b_1}$(NO) orbitals will not be orthogonal and hence can be strongly mixed. The exact geometry adopted by the $\{M(NO)_2\}^{10}$ group in the complex depends upon the relative contributions of d_{xz} and $\pi^*_{b_1}$(NO) to the $1b_1$ molecular orbital, as we have pointed out above.

2. Five-coordination

The properties of the two five-coordinate dinitrosyl complexes that have been structurally characterized are summarized in Table 9. Both are $\{M(NO)_2\}^8$ complexes of ele-

TABLE 9
Five-coordinate dinitrosyl complexes

	ν_{NO} (cm^{-1})	N–1s (eV)	M–N (A)	(M–N–O) (deg)
$RuCl(NO)_2[P(C_6H_5)_3]_2^+$	1845, 1687 [a]	402.6, 400.2 [b]	1.74(2) [a] 1.85(2)	178(2) 138(2)
$Os(OH)(NO)_2[P(C_6H_5)_3]_2$	1860 [c]		1.71(4) [d] 1.98(5)	~ 180 128(2)

a See ref. 104.
b See ref. 21.
c M. Angoletta and G. Caglio, *Gazz. Chim. Ital.*, 93 (1963) 188.
d K.R. Grundy, C.A. Reed and W.R. Roper, *Chem. Commun.*, (1970) 1501.

ments of the third transition series (5*d*), and in both the two nitrosyl groups are dramatically inequivalent as evidenced by the data in Table 9 and Fig. 24, a perspective view of $\{Ru(NO)_2Cl[P(C_6H_5)_3]_2\}^+$ (ref. 104).

The highest symmetry possible for an $M(NO)_2L_2X$ complex is C_{2v}, thus it should be possible to adapt the bonding schemes in Fig. 22 to these five-coordinate complexes. Figure 25 shows the possible $M(NO)_2L_2X$ structures having C_{2v} symmetry. It has already been pointed out (Section III.A) that an $\{M(NO)_2\}^8$ complex favors *cis* geometry for the two nitrosyl groups. This requirement is satisfied by a TBP molecule with the two NO groups in the equatorial plane (Fig. 25(b)), a coordination geometry which places the bulky phosphine ligands the maximum distance apart. If the *z* axis of the molecule is again

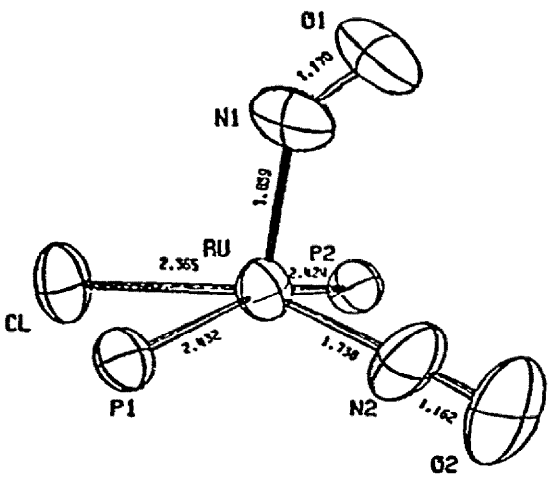

Fig. 24. A perspective drawing of the inner coordination geometry of $[RuCl(NO)_2(P(C_6H_5)_3)_2]^+$. (Reproduced from ref. 104.)

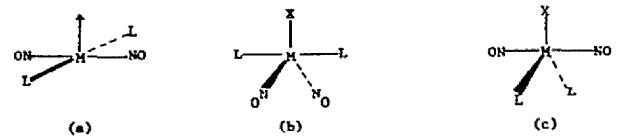

Fig. 25. The possible structures for an $M(NO)_2L_2X$ complex possesing C_{2v} symmetry.

defined as the bisector of the N–M–N angle then the bonding in the complex can be analyzed by using Fig. 22(c) with only slight modifications. The $M(NO)_2X$ fragment defines the xz plane and the y axis is the pseudo-three-fold axis of the TBP. This means that the $2a_1$ orbital will be strongly sigma anti-bonding, and therefore only the molecular orbitals $1a_2$, $1a_1$, $1b_2$, $1b_1$, and $2b_1$ need be considered. There are only eight electrons to be placed in these five orbitals, and the nature and interaction of the two b_1 molecular orbitals are of primary importance for understanding the five-coordinate $\{M(NO)_2\}^8$ complexes, as was the case for the four-coordinate $\{M(NO)_2\}^{10}$ complexes.

Figure 26 considers the two b_1 molecular orbitals in more detail and examines the consequences of the two limiting descriptions of the $1b_1$ molecular orbital. When the N–M–N angle is 90° the d_{xz} and $\pi^*_{b_1}$ (NO) orbitals will be orthogonal to one another. Figure 26(b) considers the case where the $\pi^*_{b_1}$ (NO) is of lower energy than d_{xz}. In this

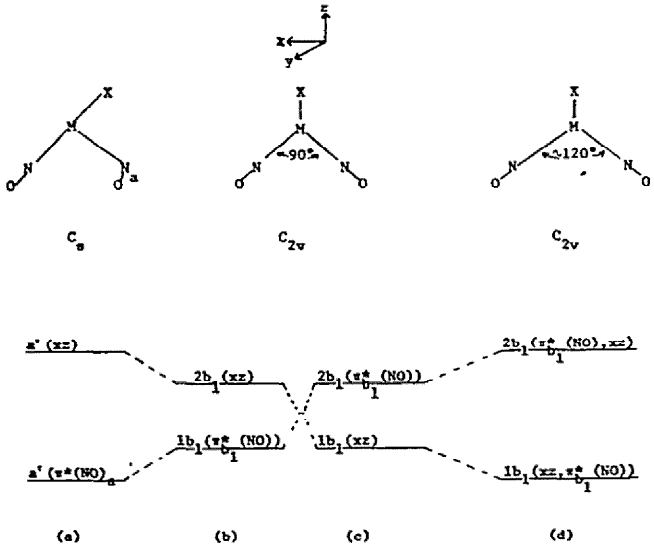

Fig. 26. Correlation diagram showing the proposed behavior of the $1b_1$ and $2b_1$ molecular orbitals in five-coordinate $\{M(NO)_2\}^8$ complexes with a $(1b_1)^2$ electron configuration. Scheme (b) has $\pi^*_{b_1}$(NO) lower in energy than d_{xz} and leads to structure (a). Scheme (c) has d_{xz} lower in energy than $\pi^*_{b_1}$(NO) and leads to (d).

situation the $1a_2$, $1a_1$ and $1b_2$ orbitals are also filled and consequently in C_{2v} symmetry the X^- ligand points directly at one of the lobes of the filled $1a_1$ (x^2,$\pi^*_{a_1}$,(NO), z^2-y^2) orbital. However, the $b_1(xz)$ orbital is empty and a motion of the X^- ligand in the xz plane to form a TP complex will direct X^- at the empty d_{xz} orbital and stabilize the complex (Fig. 26(b) → 26(a)). Such a motion of the X^- ligand lowers the symmetry of the complex to C_s and therby removes the equivalence of the two nitrosyl groups. As a consequence the $a'(\pi^*(NO))$ orbital is primarily localized on one of the two nitrosyl groups to give one strongly bent and one nearly linear nitrosyl group.

Figure 26(c) considers the case where d_{xz} is much lower energy than the $\pi^*_{b_1}$(NO) orbital. Here there are no vacant metal d orbitals in the xz plane. Expansion of N–M–N toward 120° (Fig. 26(c) → 26(d)) gives a TBP molecule of C_{2v} symmetry and allows mixing of the d_{xz} and $\pi^*_{b_1}$(NO) orbitals. In structure 26(d) there can be slight changes in the M–N–O angles so as to move the O atoms closer to one another because of the contribution of the $\pi^*_{a_1}$(NO) and $\pi^*_{b_2}$(NO) ligand orbitals (Fig. 21) to the $1a_1$ and $1b_2$ molecular orbitals (Fig. 22(c)). Presently there are no well-characterized examples of five-coordinate $\{M(NO)_2\}^8$ complexes having structure 26(d). This structure would be favored by the presence of good π-accepting ligands and by first-row ($3d$) transition metals.

3. Six-coordination

Relatively few six-coordinate $M(NO)_2$ complexes are known, and all are $\{M(NO)_2\}^6$ species. Table 10 presents the data for the three complexes that have been structurally characterized. For the purposes of this discussion the *pentahapto* cyclopentadiene ring is considered to occupy three coordination sites of the metal. The cyclopentadienyl rings impose *cis* geometry upon the two nitrosyl ligands in the two Cr compounds (refs. 105, 106). *Cis* nitrosyl groups are also observed[107] in $Mo(NO)_2Cl_2[P(C_6H_5)_3]_2$.

TABLE 10
Six-coordinate dinitrosyl complexes

	ν_{NO} (cm^{-1})	M–N (Å)	M–N–O (deg)
$(h^5-C_5H_5)Cr(NO)_2Cl$	1818, 1711 [a]	1.72(1) [b] 1.70(1)	171(1) 166(1)
$(h^5-C_5H_5)Cr(NO)_2(NCO)$	1824, 1722 [a]	1.716(3) [c, d]	171.0(2)
$Mo(NO)_2Cl_2[P(C_6H_5)_3]_2$	1790, 1670 [e]	1.826(7) [f] 1.98(1)	180(0) 167(1)

a T.S. Piper and G. Wilkinson, *J. Inorg. Nucl. Chem.*, 2 (1956) 38.
b See ref. 105.
c See ref. 106.
d C_s symmetry imposed by space group.
e F.A. Cotton and B.F.G. Johnson, *Inorg. Chem.*, 3 (1964) 1609.
f See ref. 107b and Fig. 27.

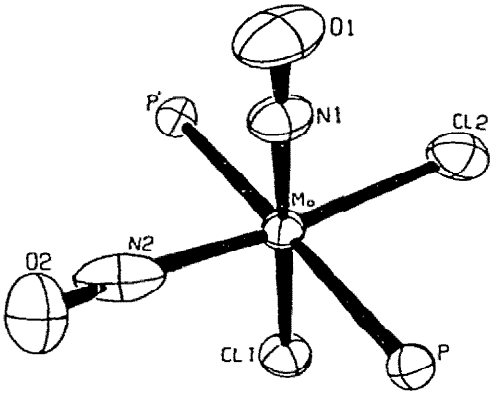

Fig. 27. The inner coordination sphere of $MoCl_2(NO)_2[P(C_6H_5)_3]_2$, showing the C_1 symmetry of the molecule; Mo–N_1 = 1.826(7) Å, Mo–N_2 = 1.98(1) Å, Mo–N_1–O_1 = 180(0)°, Mo–N_2–O_2 = 167(1)°. The molecule is disordered in the solid with a crystallographically imposed two-fold axis passing through Cl_1, Mo, N_1, and O_1. (Reproduced from ref. 107b.)

The bonding in these compounds can be investigated by reference to Fig. 22(a). However, because a six-coordinate complex has two ligands along the y-axis, the $2a_1$ orbital will be strongly anti-bonding. Thus, in C_{2v} symmetry six-coordinate $\{M(NO)_2\}^6$ should have *cis* geometry of the nitrosyl groups and the electron configuration $(1a_2)^2(1a_1)^2)(1b_2)^2$. The nitrosyl groups should be nearly linear with perhaps some bending in the xz plane so as to decrease the distance between the two O atoms. In C_s symmetry $a_2 \rightarrow a''$, $a_1 \rightarrow a'$, and $b_2 \rightarrow a'$, but the discussion is unchanged. The two Cr complexes[105,106] in Table 10 have effective C_s symmetry, and the geometry of each $Cr(NO)_2$ moiety is consistent with the above bonding description. The structure of $Mo(NO)_2Cl_2[P(C_6H_5)_3]_2$ is complicated by crystallographically imposed disorder between one of the nitrosyl ligands and one of the chloride ligands. Even so it is apparent that the effective point group of the $Mo(NO)_2$ moiety is only C_1 (Fig. 27). The earlier refinement of this molecule in an acentric space group also led to an $Mo(NO)_2$ moiety of C_1 symmetry[107a]. One possible rationalization for the low symmetry of the Mo complex is that the unfilled $1b_1(\pi^*_{b_1}(NO))$ orbital is sufficiently close in energy to the filled $1b_2$, $1a_1$, and $1a_2$ molecular orbitals so that one or one or more of the excited singlet states $^1B_1$, $^1B_2$, and $^1A_2$ are relatively close in energy to the $^1A_1$ state expected for a $(1a_2)^2(1a_2)^2(1b_2)^2$ electron configuration. This could lead to a vibronically distorted molecule of C_1 symmetry. We have already discussed vibronic distortion to C_1 symmetry in Section II.G.2.

B. $M(NO)_3$ complexes

There are no structural data available for $M(NO)_3$ complexes. Detailed molecular orbital calculations have recently been carried out for a series of $\{M(NO)_x\}^{10}$ molecules by Fenske and Rabitz[108], assuming pseudo-tetrahedral geometries and linear MNO arrays. A com-

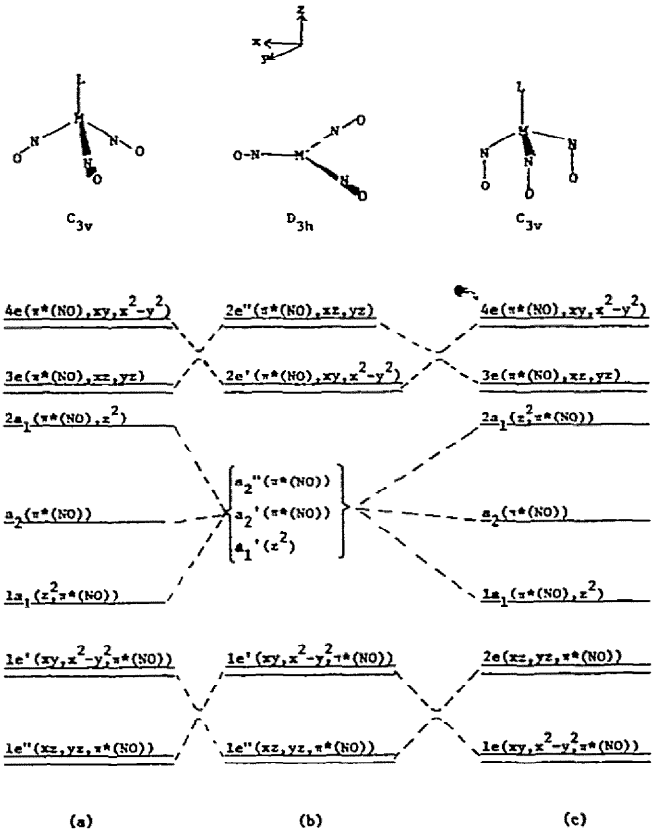

Fig. 28. Proposed molecular orbital schemes for the $M(NO)_3$ group in D_{3h} (b) and C_{3v} (*a*, *c*) symmetry. A four-coordinate $\{M(NO)_3\}^{10}$ complex with the $1a_1$ orbital comprised primarily of $\pi^*(NO)$ is predicted to have structure (c). A four-coordinate $\{M(NO)_3\}^{10}$ complex with the $1a_1$ orbital comprised primarily of d_{z^2} is predicted to have structure (a).

parison of $(\nu_{NO})^2$ with the electron population of the N–O bond gave a linear relationship for the entire series *with the exception of Mn(NO)$_3$CO.* Fenske[109] has predicted that there is something unusual about $Mn(NO)_3CO$, but has not suggested what the unusual feature might be.

The highest possible symmetry for an $M(NO)_3$ moiety is D_{3h}, and the one-electron molecular orbital scheme for such a moiety is shown in Fig. 28(b). Of particular interest are the molecular orbitals $a_1'(z^2)$, $a_2'(\pi^*(NO))$, and $a_2''(\pi^*(NO))$. In this geometry $a_1'(z^2)$ is non-bonding or weakly anti-bonding, and a_2' and a_2'' are orbitals which are localized entirely on the nitrosyl ligands because there are no *d* orbitals of a_2' or a_2'' symmetry. These three orbitals would be of similar energy and are shown as essentially degenerate in Fig. 28(b). Coordination of a fourth ligand along the *z* axis of the molecule leads to a complex of C_{3v} symmetry and results in $a_2'' \rightarrow a_1$, $a_1' \rightarrow a_1$, and $a_2' \rightarrow a_2$. The two a_1 orbitals

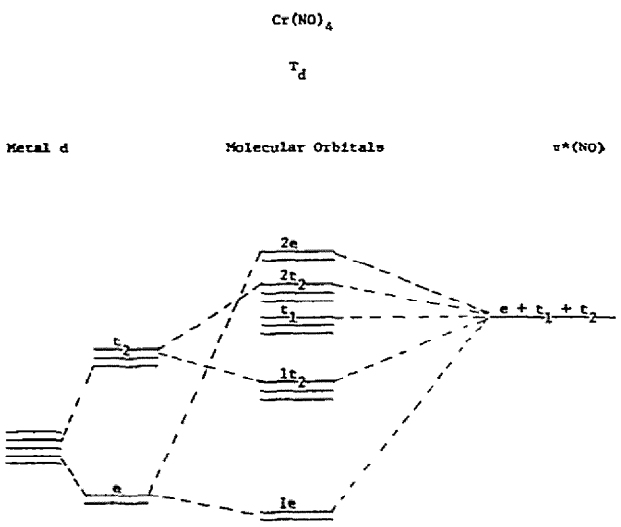

Fig. 29. Proposed molecular orbital scheme for $Cr(NO)_4$.

can strongly mix as shown in Fig. 28(b) → 28(c) and in Fig. 28(b) → 28(a). Figure 28(c) depicts the situation when the $1a_1$ molecular orbital is primarily $\pi^*_{a_1}$(NO). This orbital is bonding with respect to the three N atoms and bonding with respect to the three O atoms and can be stabilized by structure 28(c). However, if the $1a_1$ orbital is primarily d_{z^2} of the metal (Fig. 28(a)) then a pseudotetrahedral molecule with essentially linear MNO groups should result. We predict that the unusual feature of $Mn(NO)_3CO$ is a tripod structure with distinctly non-linear MNO groups as shown in Fig. 28(c).

C. $M(NO)_4$ complexes

The only known complex in this category is the $\{M(NO)_4\}^{10}$ species $Cr(NO)_4$, which has only recently been prepared[110]. On the basis of its infrared and Raman spectra the molecule has been assigned T_d symmetry. Figure 29 shows the one-electron molecular orbital diagram for the $Cr(NO)_4$ molecule. In T_d symmetry the metal d orbitals transform as e and t_2, and the π^*(NO) orbitals of the four nitrosyl groups transform as e, t_1 and t_2. Ten electrons will fill the orbitals through $1t_2$ and no deviations from true T_d symmetry are expected if the separation between $1t_2$ and t_1 is greater than the spin pairing energy.

D. Reactions of polynitrosyl complexes

The reactions and transformations of coordinated nitrosyl ligands in polynitrosyl complexes have been little studied. The striking inequivalence of the two nitrosyl groups in

$Ru(NO)_2Cl[P(C_6H_5)_3]_2^+$ (ref. 104) raises the question as to whether the two groups readily interconvert. Collman et al.[61] carried out reaction XII and showed that the product

$$Ru(^{15}NO)Cl[P(C_6H_5)_3]_2 + NO^+ \rightarrow Ru(^{15}NO)(NO)Cl[P(C_6H_5)_3]_2^+ \qquad \text{(XII)}$$

exhibits four NO stretching frequencies as would be expected if ^{15}NO can occur in either coordination position of the TP species. Mechanism XIII has been proposed[104b] to explain these results.

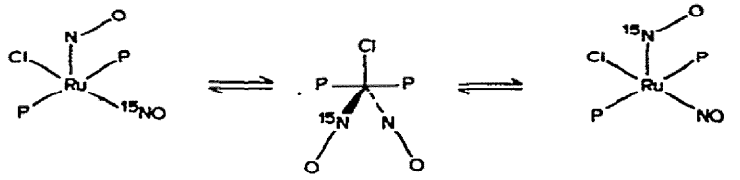

(XIII)

It has not been generally recognized. however, that the ^{15}NO experiment does *not* prove that rapid interconversion of axial and equatorial NO groups occurs in the TP complex. The data are equally compatible with XIV, a mechanism involving a symmetric TBP transition state that collapses to either of the two TP complexes which themselves have a large barrier to interconversion

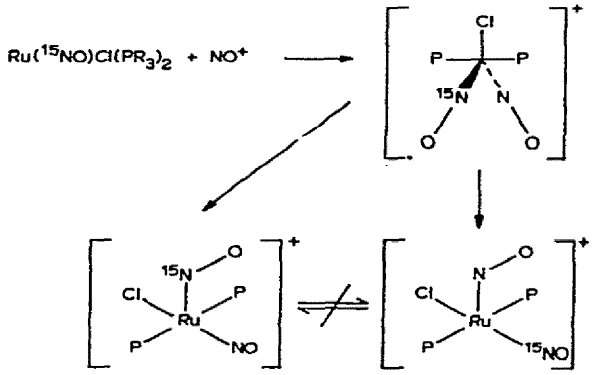

(XIV)

Recently it has been shown[121] that for $\{Ir(NO)_2[P(C_6H_5)_3]_2\}^+$ coupling of the two NO ligands to give nitrous oxide can be induced by reaction with donor ligands (reaction XV)

$$\{Ir(NO)_2[P(C_6H_5)_3]_2\}PF_6 + 4\,CO \rightarrow \{Ir(CO)_3[P(C_6H_5)_3]_2\}PF_6 + CO_2 + N_2O \qquad \text{(XV)}$$

IV. CONCLUSIONS

A. Inorganic functional groups

A recent review of the structural chemistry of transition metal complexes[2j] concludes that "the existing literature remains a challenge to the chemist to develop a sound and all-encompassing theory of chemical bonding to account for the diverse structural properties of five-coordinate transition metal complexes and transition metal nitrosyl complexes." In this review, we have shown that the structure, bonding and reactivity of mononitrosyl complexes are adequately accounted for by a simple bonding model which treats the $\{MNO\}^n$ moiety as an "inorganic functional group" perturbed by the field of the other ligands coordinated to the metal. Simple electrostatic energy calculations (see Appendix) support this model and have led to an energy level diagram (Fig. 15), which accounts for the chemical and physical properties of mononitrosyl complexes. In addition, qualitative one-electron molecular orbital diagrams for polynitrosyl complexes have shown that the unusual chemical and physical properties of these complexes are clarified by treating them as derivatives of the appropriate inorganic functional group, i.e. $\{M(NO)_2\}^n$, $\{M(NO)_3\}^n$ or $\{M(NO)_4\}^n$. Thus, we conclude that the functional group approach is a generally valid one for understanding the complex behavior of metal nitrosyl compounds.

B. Stereochemical control of valence

1. Metal nitrosyls

The physical and chemical properties of the $\{M(NO)_x\}^n$ functional groups are dictated by (1) n, the total number of electrons associated with the metal d and $\pi^*(NO)$ orbitals; (2) the coordination number of the metal; (3) the coordination symmetry about the metal; (4) the nature of the occupied one-electron molecular orbitals. For a given class of complexes additional perturbations can be introduced by changing the metal and/or the donor atoms of the ligands. We have chosen to collectively call these determining factors "stereochemical control of valence"[31] because the formal oxidation states of the atoms, the geometry of the $M(NO)_x$ moiety, and the chemical reactivity of the $M(NO)_x$ group are dictated by the overall stereochemistry of the complex ion.

It is important to emphasize that stereochemical control of valence (SCV) determines *both* structure *and* chemical reactivity of the coordinated NO ligand(s). A graphic example of control of chemical reactivity is provided by the complexes $Co(NO)(das)_2^{2+}$ and $Co(NO)(das)_2X^+$ (ref. 91). The nitrosyl group of the six-coordinate complex does not react with strong bases, but is readily protonated to give an HNO complex. On the other hand, the nitrosyl group of the five-coordinate complex does not react with protons, but is readily attacked by good nucleophiles. Thus, a metal nitrosyl complex can, in effect, function as its own "protecting group" in certain chemical reactions.

2. Other ligands

Extensive consideration of the general applicability of the concept of stereochemical control of valence to other inorganic functional groups is not appropriate to this review of structure, bonding, and reactivity of metal nitrosyl complexes. However, the procedures employed for metal nitrosyl complexes should be capable of extension to a variety of other ligands including: CO, N_2, O_2, olefins, acetylenes, nitriles, and isocyanides. For many of these ligands there is less structural, spectroscopic, and theoretical information available than for metal nitrosyl complexes.

3. Dinitrogen complexes

One obvious extension of the concept of stereochemical control of valence is to the reduction of coordinated dinitrogen[31] because the N_2 molecule is isoelectronic with the NO^+ ion. A number of transition metal dinitrogen compounds have been prepared in recent years[112], but relatively few reactions of coordinated dinitrogen have been demonstrated. Of particular interest is reaction XVI, recently reported by Chatt et al.[111], in which a coordinated N_2 group is reduced to a diimide species with concomitant oxidation of the metal to which the ligand is coordinated.

$$W^0(N_2)_2\,(dmpe)_2 + HX \rightarrow W^{II}(N_2H_2)\,(dmpe)_2X_2 + N_2 \qquad \text{(XVI)}$$

The metal must be the reducing agent in this reaction because no hydrogen is evolved and the metal itself is oxidized. Another important feature of this reaction is that the yields of the reduced products depend upon the nature of X^-. Although no mechanistic studies have as yet been carried out this dependency upon X^- suggests that the anion participates in the crucial reductive step which transfers a pair of electrons from the ligand to the metal, and is reminiscent of reaction II in which a coordinated NO^+ group is reduced to a coordinated NO^- group upon increase in coordination number by attack of an X^- ion. It is also interesting to note that reaction XVI involves reduction of coordinated N_2 in a bis-dinitrogen complex. It was pointed out in Section III that in a complex in which two ligands with identical π-systems are coordinated to the metal there can be ligand-localized π^* orbitals which do not interact with the metal *d*-orbitals. For bis-dinitrogen complexes such ligand localized π^* orbitals should be lower in energy than the π-type orbitals which are totally anti-bonding with respect to all atoms of the $M(N_2)_2$ moiety. The availability of ligand-localized π^* orbitals in a bis-dinitrogen complex and the accessibility of coordination number seven for low-valent tungsten may both be important factors in the facile reduction of coordinated N_2 according to reaction XVI.

Borodko et al.[113] have recently isolated the dinitrogen complex, $[(C_5H_5)_2Ti]_2N_2$, which undergoes reaction with acid to form a coordinated diimide species. The nature of the products is dependent upon the basicity of the solvent, again suggesting the participation of a base during the crucial reduction step.

Increase of coordination number and bis-dinitrogen complexes may also be an important feature in the biological reduction of dinitrogen by the metalloenzyme nitrogenase.

It has been proposed[114,123] that an important step in this reduction is an increase in the coordination number of an enzyme–dinitrogen complex by attack by a second molecule of dinitrogen.

4. General utility[31]

The structural principles set forth for metal nitrosyl complexes ought also to apply to the equilibrium geometries of metal complexes of other ligands with π systems whenever the energies (in the complex) of the metal d orbitals and of the π^* orbitals of the ligand are similar. By the same token, *stereochemical control of valence should be a generally useful pathway for converting the mechanical and chemical energy of a structural and/or electronic change of a transition metal catalyst into a chemical change of a coordinated molecule* provided that the metal d orbitals and the appropriate orbitals of the coordinated molecules have similar energies in the activated complex. Stereochemical control of valence may not lead to a single unique mechanism for a particular metal-catalyzed reaction; however, it can eliminate some mechanisms from consideration and does provide a small set of operating principles which form a unified framework for planning and executing additional synthetic, kinetic, spectroscopic, structural, and theoretical studies.

V. APPENDIX

A. Calculation of electrostatic energies for the MNO groups

Nearly all metal nitrosyl complexes are low-spin and consequently are examples of "strong field complexes". The molecular structures and electron configurations of most of the metal nitrosyls discussed in this review are adequately described by one-electron molecular orbital schemes in which the energy separation between the orbitals is greater than spin-pairing energies. In those few cases in which partially filled degenerate molecular orbitals have been encountered, the strong field d wave functions have been used to elicit information regarding the energies and nature of the electronic states arising from all the possible electron configurations.

In C_{nv} symmetry ($n \geqslant 3$), the d_{z^2} orbital transforms as a_1 and d_{xz}, d_{yz} transform as e. The presence of a single electron in these orbitals gives rise to $^2A_1$ and ^2E electronic states. When these states become degenerate, they can be analyzed as if they comprised a $^2T_1$ state. If there are two electrons in the a_1 and e orbitals, then the situation is somewhat more complicated and is treated in detail below. Cases in which three, four, five, or six electrons are present in these orbitals have not been encountered and are not considered.

1. C_{3v} symmetry

Figure 13 shows that in four-coordinate mononitrosyl complexes with C_{3v} symmetry, the $4a_1$ and $4e$ orbitals of an $\{MNO\}^{10}$ complex may be nearly degenerate. These one-electron molecular orbitals are not pure metal d orbitals, but the d functions can be used

to calculate the ordering of the electronic states arising from the $(4a_1, 4e)^2$ electron configurations. Covalency decreases the electron–electron repulsion[115], and therefore, these calculations give the maximum separations between the electronic states of the $(4a_1, 4e)^2$ electron configurations.

The six electronic states which arise from the $(4a_1, 4e)^2$ configurations are $(4a_1)^2$: $^1A_1$; $(4a_1)^1\,(4e)^1$: ^1E, ^3E; and $(4e)^2$: $^1A_1$, ^1E, and $^3A_2$. The strong field wave functions and electrostatic energies for these states have been obtained by using the tables and methods outlined by Griffith[116], and are set out below. Since there are two $^1A_1$ states and two ^1E states, the effects of configuration interaction (C.I.) have also been calculated. There is no C.I. between the two ^1E states. The effect of C.I. on the two $^1A_1$ states is small ($\sim 5B$), but prevents them from becoming degenerate.

The wave functions are listed below. In the ket $|^3E, b_1, 1\rangle$, ^3E represents the state in C_{3v} symmetry; b_1 refers to the orbital component of the ^3E state in C_{2v} symmetry; and the number refers to the value of M_s. In C_{2v} symmetry, d_{z^2} ($e\theta$ in Griffith's[116] notation) transforms as a_1, d_{xz} ($t_2\eta$) as b_1, and d_{yz} ($t_2\xi$) as b_2.

$(e)^2$ electron configuration

$$|^3A_2, 1\rangle = \frac{1}{\sqrt{2}}\,[b_1(1)b_2(2) - b_2(1)b_1(2)]\,\alpha(1)\alpha(2)$$

$$|^3A_2, 0\rangle = \tfrac{1}{2}\,[b_1(1)b_2(2) - b_2(1)b_1(2)]\,[\alpha(1)\beta(2) + \beta(1)\alpha(2)]$$

$$|^3A_2, -1\rangle = \frac{1}{\sqrt{2}}\,[b_1(1)b_2(2) - b_2(1)b_1(2)]\,\beta(1)\beta(2)$$

$$|^1E, a_2, 0\rangle = \tfrac{1}{2}[b_1(1)b_2(2) + b_2(1)b_1(2)]\,[\alpha(1)\beta(2) - \beta(1)\alpha(2)]$$

$$|^1E, a_1, 0\rangle = \tfrac{1}{2}[b_1(1)b_1(2) - b_2(1)b_2(2)]\,[\alpha(1)\beta(2) - \beta(1)\alpha(2)]$$

$$|^1A_1, 0\rangle = \tfrac{1}{2}[b_1(1)b_1(2) + b_2(1)b_2(2)]\,[\alpha(1)\beta(2) - \beta(1)\alpha(2)]$$

$(a_1)^2$ electron configuration

$$|^1A_1, 0\rangle = \frac{1}{\sqrt{2}}\,[a_1(1)a_1(2)]\,[\alpha(1)\beta(2) - \beta(1)\alpha(2)]$$

$(a_1)^1(e)^1$ electron configuration

$$|^1E, b_1, 0\rangle = \tfrac{1}{2}\,[a_1(1)b_1(2) + b_1(1)a_1(2)]\,[\alpha(1)\beta(2) - \beta(1)\alpha(2)]$$

$$|^1E, b^2, 0\rangle = \tfrac{1}{2}\,[a_1(1)b_2(2) + b_2(1)a_1(2)]\,[\alpha(1)\beta(2) - \beta(1)\alpha(2)]$$

$$|^3E, b_1, 1\rangle = \frac{1}{\sqrt{2}}[a_1(1)b_1(2) - b_1(1)a_1(2)]\alpha(1)\alpha(2)$$

$$|^3E, b_1, 0\rangle = \tfrac{1}{2}[a_1(1)b_1(2) - b_1(1)a_1(2)][\alpha(1)\beta(2) + \beta(1)\alpha(2)]$$

$$|^3E, b_1, -1\rangle = \frac{1}{\sqrt{2}}[a_1(1)b_1(2) - b_1(1)a_1(2)]\beta(1)\beta(2)$$

$$|^3E, b_2, 1\rangle = \frac{1}{\sqrt{2}}[a_1(1)b_2(2) - b_2(1)a_1(2)]\alpha(1)\alpha(2)$$

$$|^3E, b_2, 0\rangle = \tfrac{1}{2}[a_1(1)b_2(2) - b_2(2)a_1(1)][\alpha(1)\beta(2) + \beta(1)\alpha(2)]$$

$$|^3E, b_2, -1\rangle = \frac{1}{\sqrt{2}}[a_1(1)b_2(2) - b_2(2)a_1(1)]\beta(1)\beta(2)$$

The calculated electrostatic energies are

$(e)^2$ electron configuration

$$^3A_2 : A - 5B \approx 5B^*$$

$$^1E : A + B + 2C \approx 9B$$

$$^1A : A + 10B + 5C \approx 30B + 5B^{**} \approx 35B$$

$(a_1)^2$ electron configuration

$$^1A_1 : A + 4B + 3C \approx 16B - 5B^{**} \approx 11B$$

$(a_1)^1\,(e)^1$ electron configuration

$$^1E : A + 3B + 2C \approx 11B$$

$$^3E : A + B \approx B$$

2. C_{4v} symmetry

In five-coordinate $\{MNO\}^8$ complexes with C_{4v} symmetry, the $4a_1$ and $3e$ molecular orbitals may be degenerate (Figs. 8(b), 8(c)). The electronic states arising from the $(4a_1, 3e)^2$ configurations are $(4a_1)^2 : {}^1A_1$; $(4a_1)^1\,(3e)^1 : {}^1E, {}^3E$; and $(3e)^2 : {}^1A_1, {}^1B_1, {}^1B_2$, and ${}^3A_2$.

---

* Subtracting A and letting $C \approx 4B$.

** C.I. energy.

Thus, the only differences between the electronic states arising from $(a, e)^2$ configurations in C_{3v} and C_{4v} symmetry are the singlet states of the $(e)^2$ configuration. In C_{3v} symmetry $(4e)^2$ gives rise to $^1A_1$ and $^1E_1$ states whereas $(3e)^2$ in C_{4v} gives rise to $^1A_1$, $^1B_1$ and $^1B_2$. However, in this approximation using pure d wave functions the $^1B_1$ and $^1B_2$ states are accidentally degenerate. Consequently, the wave functions and state energies obtained above for a four-coordinate $\{MNO\}^{10}$ complex in C_{3v} symmetry are identical with those obtained for a five-coordinate $\{MNO\}^8$ complex in C_{4v} symmetry. The results of the C_{4v} calculations are plotted in Fig. 15 and discussed in Section II.G.2.

B. Vibrational modes of M(NO)L$_4$

The symmetry and approximate displacement of the atoms for the vibrations of an M(NO)L$_4$ complex are shown in Fig. A.1. The fifteen normal modes are identified by their irreducible representations in C_{4v} symmetry and by their origins in O_h symmetry (listed in the parentheses)[117].

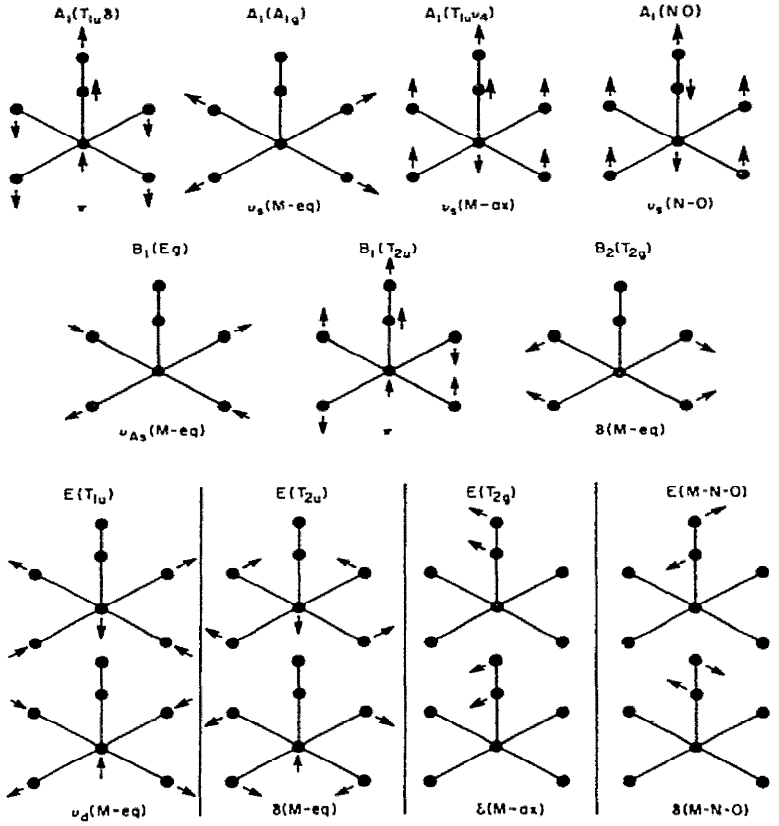

Fig. A.1. The normal vibrations of five-coordinate TP complexes of linear MNO groups. The indicated displacements are only qualitative, and the E vibrations of the MNO group will be mixed with the other vibrations of E symmetry.

NOTE ADDED IN PROOF

Several recent papers have provided additional experimental evidence regarding MNO groups. The M–N–O angles[124] for six-coordinate $\{MNO\}^6$ and $\{MNO\}^7$ complexes with TPP are described by Figs. 3 and 4. The EPR spectra[125] of both the five- and six-coordinate TPP derivatives of $\{FeNO\}^7$ correspond to the molecular orbital schemes of Figs. 4 and 8. The Mössbauer spectrum of the dtc derivatives of $\{FeNO\}^7$ group, $FeNO[S_2CN(C_2H_5)_2]_2$, is consistent with an electron configuration in which the unpaired spin is located in the $5a_1(z^2)$ orbital (Fig. 12). Finally, further studies of the infrared spectra by Miki et al. show that both linear and *bent* MNO groups can be treated as triatomic species[126].

ACKNOWLEDGEMENTS

We are indebted to Professor J.A. Ibers and Dr. B.A. Frenz for a preprint of ref. 2j prior to publication, and we thank Professors K.G. Caulton, R. Eisenberg, and J.A. Ibers for providing data prior to publication. We also thank Dr. M. Quinby Hunt for preparing Table 3. It is a pleasure to acknowledge stimulating discussions with Professors T.M. Dunn, R.F. Fenske, and K.N. Raymond. Finally, we thank the National Science Foundation of the USA for financial support.

REFERENCES

1 N.V. Sidgwick and R.W. Bailey, *Proc. Roy. Soc., London,* A144 (1934) 521.
2a T. Moeller, *J. Chem. Educ.*, 23 (1946) 441, 542.
b C.C. Addison and J. Lewis, *Quart. Rev. Chem. Soc.*, 9 (1955) 115.
c J. Lewis, R.J. Irving and G. Wilkinson, *J. Inorg. Nucl. Chem.*, 7 (1958) 32.
d W.P. Griffith, J. Lewis and G.Wilkinson, *J. Inorg. Nucl. Chem.*, 7 (1958) 38.
e B.F.G. Johnson and J.A. McCleverty, *Prog. Inorg. Chem.*, 7 (1966) 277.
f J.H. Swinehart, *Coord. Chem. Rev.*, 2 (1967) 385.
g W.P. Griffith, *Advan. Organometal. Chem.*, 7 (1968) 211.
h J. Mašek, *Inorg. Chim. Acta Rev.*, 3 (1969) 99.
i J.A. McGinnety, *M.T.P. Int. Rev. Sci., Inorg. Chem., Ser. One,* 5 (1972) 229.
j B.A. Frenz and J.A. Ibers, *M.T.P. Int. Rev. Sci., Phys. Chem., Ser. One,* 11 (1972) 33.
k N.G. Connelly, *Inorg. Chim. Acta Rev.*, 6 (1972) 48.
3 A.D. Walsh, *J. Chem. Soc.*, (1953) 2266.
4 D.M.P. Mingos and J.A. Ibers, *Inorg. Chem.*, 10 (1971) 1479.
5 C.G. Pierpont and R. Eisenberg, *J. Amer. Chem. Soc.*, 93 (1971) 4905.
6 D.M.P. Mingos, *Inorg. Chem.*, 12 (1973) 1209.
7 G. Herzberg, *Electronic Spectra and Electronic Structure of Polyatomic Molecules,* Van Nostrand Reinhold, New York, 1965, pp. 319.
8 R.F. Fenske and R.L. DeKock, *Inorg. Chem.*, 11 (1972) 437.
9 P.T. Manoharan and H.B. Gray, *Inorg. Chem.*, 5 (1966) 823.
10 J.H. Enemark, M.S. Quinby, L.L. Reed, M.S. Steuck and K.K. Walthers, *Inorg. Chem.*, 9 (1970) 2397.
11 A. Tullberg and N.G. Vannerberg, *Acta Chem. Scand.*, 21 (1967) 1462.
12 P.T. Manoharan and W.C. Hamilton, *Inorg. Chem.*, 2 (1963) 1043.

13 D.A.C. McNeil, J.B. Raynor and M.C.R. Symons, *Proc. Chem. Soc., London*, (1964) 364.
14 D.A.C. McNeil, J.B. Raynor and M.C.R. Symons, *J. Chem. Soc.*, (1965) 410.
15 J.J. Fortman and R.G. Hayes, *J. Chem. Phys.*, 43 (1965) 15.
16 H.A. Kuska and M.T. Rogers, *J. Chem. Phys.*, 42 (1965) 3034.
17 B.A. Goodman, J.B. Raynor and M.C.R. Symons, *J. Chem. Soc. A*, (1966) 994.
18 I. Bernal, S.D. Robinson, L.S. Meriwether and G. Wilkinson, *Chem. Commun.*, (1965) 571.
19 B.R. McGarvey and J. Pearlman, *J. Chem. Phys.*, 46 (1967) 4992.
20 P.T. Manoharan and H.B. Gray, *Chem. Commun.*, (1965) 324.
21 P. Finn and W.L. Jolly, *Inorg. Chem.*, 11 (1972) 893.
22 R. Nast and J. Schmidt, *Angew. Chem. Internat. Edit.*, 8 (1969) 383.
23 J.D.W. van Voorst and P. Hemmerich, *J. Chem. Phys.*, 45 (1966) 3914.
24 A.H. Harris, *M.S. Thesis*, Univ. of Arizona, 1970.
25 M.D.B. Bloom, J.B. Raynor and M.C.R. Symons, *J. Chem. Soc. A*, (1971) 3843.
26 R.W. Perry, *Ph.D. Thesis*, Univ. of Wisconsin, 1968.
27 J. Mašek and R. Pribil, Jr., *Inorg. Chim. Acta*, 5 (1971) 499.
28 B. Jezowska-Trzebiatowska, J. Hanuza and M. Ostern, *Inorg. Chim. Acta*, 6 (1972) 141.
29 C.S. Pratt, B.A. Coyle and J.A. Ibers, *J. Chem. Soc. A*, (1971) 2146.
30 D.A. Snyder and D.L. Weaver, *Chem. Commun.*, (1969) 1425.
D.A. Snyder and D.L. Weaver, *Inorg. Chem.*, 9 (1970) 2760.
31 J.H. Enemark and R.D. Feltham, *Proc. Nat. Acad. Sci. USA*, 69 (1972) 3534.
32 R.D. Feltham and R.S. Nyholm, *Inorg. Chem.*, 4 (1965) 1334.
33 R.D. Feltham, W. Silverthorn, H. Wickman and W. Wesolowski, *Inorg. Chem.*, 11 (1972) 676.
34 W. Wesolowski, *Ph.D. Thesis*, Univ. of Arizona, 1971.
35 R.D. Feltham and W. Silverthorn, *Proc. Int. Conf. Coord. Chem.*, 9 (1966) 77.
36 W. Silverthorn, *Ph.D. Thesis*, Univ. of Arizona, 1967.
37 E. Miki, Bull. Chem. Soc. Jap., 41 (1968) 1835.
38 M.S. Quinby and R.D. Feltham, *Inorg. Chem.*, 11 (1972) 2468.
39 L. Tosi, *Spectrochim. Acta*, 29A (1973) 353.
40 G. Paliani, A. Poletti and A. Santucci, *J. Mol. Struct.*, 8 (1971) 63.
41 A.F. Schreiner, S.W. Lin, P.J. Hauser, E.A. Hopcus, D.J. Hamm and J.D. Gunter, *Inorg. Chem.*, 11 (1972) 880.
42 J.T. Veal and D.J. Hodgson, *Inorg. Chem.*, 11 (1972) 1420.
43 R.B. King, *Organometallic Syntheses*, Vol. 1, Academic Press, New York, 1965, p. 164.
44 B.A. Frenz, J.H. Enemark and J.A. Ibers, *Inorg. Chem.*, 8 (1969) 1288.
45 H. Wawersik and F. Basolo, *J. Amer. Chem. Soc.*, 89 (1967) 4626.
46 D.P. Keeton and F. Basolo, *Inorg. Chim. Acta*, 6 (1972) 33.
47 C.G. Pierpont and R. Eisenberg, *Inorg. Chem.*, 12 (1973) 199.
48 C.G. Pierpont and R. Eisenberg, *Inorg. Chem.*, 11 (1972) 1094.
49 C.G. Pierpont, A. Pucci and R. Eisenberg, *J. Amer. Chem. Soc.*, 93 (1971) 3051.
50 R. Wiest and R. Weiss, *J. Organometal. Chem.*, 30 (1971) C33.
51a J.L. Hoard, *Science*, 174 (1971) 1295.
b W.R. Scheidt and J.L. Hoard, *J. Amer. Chem. Soc.*, 95 (1973) 8281.
52 S.A. Goldfield and K.N. Raymond, *Inorg. Chem.*, 13 (1974) 770.
53 F. Basolo and R.G. Pearson, *Mechanisms of Inorganic Reactions*, 2nd edn., Wiley, New York, 1967, p.538.
54 J.H. Enemark and J.A. Ibers, *Inorg. Chem.*, 6 (1967) 1575.
55 G.R. Clark, K.R. Grundy, W.R. Roper, J.M. Waters and K.R. Whittle, *Chem. Commun.*, (1972) 119.
56 D.J. Hodgson, N.C. Payne, J.A. McGinnety, R.G. Pearson and J.A. Ibers, *J. Amer. Chem. Soc.*, 90 (1968) 4486.
D.J. Hodgson and J.A. Ibers, *Inorg. Chem.*, 7 (1968) 2345.
57 D.J. Hodgson and J.A. Ibers, *Inorg. Chem.*, 8 (1969) 1282.
58 D.M.P. Mingos, W.T. Robinson and J.A. Ibers, *Inorg. Chem.*, 10 (1971) 1043.
59 D.M.P. Mingos and J.A. Ibers, *Inorg. Chem.*, 10 (1971) 1035.
60 G. Booth and J. Chatt, *J. Chem. Soc.*, (1962) 2099.

61 J.P. Collman, P. Farnham and G. Dolcetti, *J. Amer. Chem. Soc.*, 93 (1971) 1788.
62 C.P. Brock, J.P. Collman, G. Dolcetti, P.H. Farnham, J.A. Ibers, J.E. Lester and C.A. Reed, *Inorg. Chem.*, 12 (1973) 1304.
63 J.H. Enemark and R.D. Feltham, *J. Chem. Soc. Dalton*, (1972) 718.
64 M. Colapietro, A. Domenicano, L. Scaramuzza, A. Vaciago and L. Zambonelli, *Chem. Commun.*, (1967) 583.
65 G.R. Davies, R.H.B. Mais and P.G. Owston, *Chem. Commun.*, (1968) 81.
66 R.P. White, J.A. McCleverty and L.F. Dahl, quoted in ref. *a* of Table 8.
67 G.R. Davies, J.A.J. Jarvis, B.T. Kilbourn, R.H.B. Mais and P.G. Owston, *J. Chem. Soc. A*, (1970) 1275.
68 A.I.M. Rae, *Chem. Commun.*, (1967) 1245.
69 D.G. van Derveer, A.P. Gaughan, Jr., S.L. Soled and R. Eisenberg, *Abstracts Amer. Cryst. Assoc.*, 1 (1973) 190.
70 J. Gibson, *Nature*, 196 (1962) 64.
71 H.B. Gray, I. Bernal and E. Billig, *J. Amer.Chem. Soc.*, 84 (1962) 3404.
72 H. Crain, *Ph.D. Thesis*, University of Arizona, 1973.
73 B.A. Goodman, J.B. Raynor and M.C.R. Symons, *J. Chem. Soc. A*, (1969) 2572.
74 B.N. Figgis, *Introduction to Ligand Fields*, Interscience, New York, 1966, p. 60.
75 J.A. Mc Cleverty, N.M. Atherton, J. Locke, E.J. Wharton and C.J. Winscom, *J. Amer. Chem. Soc.*, 89 (1967) 6082.
76 P.G. Eller and P.W.R. Corfield, *American Crystallographic Association Summer Meeting, Ottawa, Canada, Aug. 1970, Abstracts*, p. 85.
77 J.H. Enemark, *Inorg. Chem.*, 10 (1971) 1952.
78 M.H.B. Stiddard and R.E. Townsend, *Chem. Commun.*, (1969) 1372.
79 T.F. Brennan and I. Bernal, *Chem. Commun.*, (1970) 138; *Inorg. Chim. Acta*, 7 (1973) 283.
80 J.L. Calderon, F.A. Cotton and P. Legzdins, *J. Amer. Chem. Soc.*, 91 (1969) 2528.
81 F.A. Cotton and G.A. Rusholme, *J. Amer. Chem. Soc.*, 94 (1972) 402.
82 D.M.P. Mingos, *Nature Physical Science*, 229 (1971) 193.
83 B.N. Figgis, *Introduction to Ligand Fields*, Interscience, New York, 1966, p. 145.
84 R. Renner, *Z. Phys.*, 92 (1934) 172.
85 G. Herzberg, *Electronic Spectra and Electronic Structure of Polyatomic Molecules*, Van Nostrand Reinhold, New York, 1966, p. 26.
86 R. Englman, *The Jahn–Teller Effect in Molecules and Crystals*, Wiley-Interscience, New York, 1972, p. 108.
87 A.E. Kruse and R.D. Feltham, unpublished results.
88 P.G. Douglas, R.D. Feltham and H.G. Metzger, *J. Amer. Chem. Soc.*, 93 (1971) 84.
89 D.I. Bustin, J.E. Earley and A.A. Vlček, *Inorg. Chem.*, 8 (1969) 2062.
90 D.I. Bustin and A.A. Vlček, *Collect. Czech. Chem. Comm.*, 32 (1967) 1665.
91 J. Riker-Nappier, R.D. Feltham and J.H. Enemark, to be published.
92 K.R. Grundy, C.A. Reed and W.R. Roper, *Chem. Commun.*, (1970) 1501.
93 S.G. Clarkson and F. Basolo, *Inorg. Chem.*, 12 (1973) 1528.
94 D. Gwost and K.G. Caulton, *166th National Meeting of the American Chemical Society, Chicago, Ill., Aug. 1973, Abstracts*, NOR-102.
95 B.F. Hoskins, F.D. Whillans, D.H. Dale and D.C. Hodgkin, *Chem. Commun.*, (1969) 69.
96 F.A. Palocsay and J.V. Rund, *Inorg. Chem.*, 8 (1969) 696.
97 F.J. Miller and T.J. Meyer, *J. Amer. Chem. Soc.*, 93 (1971) 1294.
98 P.G. Douglas and R.D. Feltham, *J. Amer. Chem. Soc.*, 94 (1972) 5254.
99 A.T. McPhail, G.R. Knox, C.G. Robertson and G.A. Sim, *J. Chem. Soc. A*. (1971) 205.
100 S.F.A. Kettle, *Inorg. Chem.*, 4 (1965) 1661.
101 P.L. Bellon, private communication to J.A. Ibers, quoted in ref. 102.
102 A.P. Gaughan, Jr., B.J. Corden, R. Eisenberg and J.A. Ibers, *Inorg. Chem.*, 13 (1974) 786.
103 D.M.P. Mingos and J.A. Ibers, *Inorg. Chem.*, 9 (1970) 1105.
104a C.G. Pierpont, D.G. van Derveer, W. Durland and R. Eisenberg, *J. Amer. Chem. Soc.*, 92 (1970) 4760.
b C.G. Pierpont and R. Eisenberg, *Inorg. Chem.*, 11 (1972) 1088.

105 O.L. Carter, A.T. McPhail and G.A. Sim, *J. Chem. Soc. A*, (1966) 1095.
106 M.A. Bush and G.A. Sim, *J. Chem. Soc. A*, (1970) 605.
107a M.O. Visscher and K.G. Caulton, *J. Amer. Chem. Soc.*, 94 (1972) 5923.
b K.G. Caulton, private communication.
108 S. Rabitz, *Ph.D. Thesis*, University of Wisconsin, 1972.
109 R.F. Fenske, private communication.
110 B.I. Swanson and S.K. Satija, *Chem. Commun.*, (1973) 40.
111 J. Chatt, G.A. Heath and R.L. Richards, *Chem. Commun.*, (1972) 1010.
112 J. Chatt and G.J. Leigh, *Chem. Soc. Rev.*, 1 (1972) 121.
113 Yu.G. Borodko, I.N. Ivleva, L.M. Kachapina, S.I. Salienko, A.K. Shilova and A.E. Shilov, *Chem. Commun.*, (1972) 1178.
114 M. Cooke, private communication.
115 C.K. Jørgensen, *Orbitals in Atoms and Molecules*, Academic Press, New York, 1962, p. 59.
116 J.S. Griffith, *The Theory of Transition-Metal Ions*, Cambridge University Press, Cambridge, England, 1964.
117 K. Nakamoto, *Infrared Spectra of Inorganic and Coordination Compounds*, Wiley, New York, 1963, pp. 113 and 118.
118 F. Hund, *Z. Phys.*, 40 (1927) 742; 42 (1927) 93; 51 (1928) 759.
119 R.S. Mulliken, *Phys. Rev.* 32 (1928) 186; *Rev. Mod. Phys.*, 4 (1932) 1.
120 R.B. Woodward and R. Hoffmann, *The Conservation of Orbital Symmetry*, Verlag Chemie, Weinheim, Germany.
121 B.F.G. Johnson and S. Bhaduri, *Chem. Commun.* (1973) 651.
122 L.H. Jones, R.S. McDowell and B.I. Swanson, *J. Chem. Phys.*, 58 (1973) 3757.
123 J.H. Enemark and R.D. Feltham, in *Summer Symp. on Inorg. Chem., Buffalo, N.Y., June 19–21, 1972.*
124 P.L. Picinto and W.R. Scheidt, *167th National Meeting of the American Chemical Society, Los Angeles, Calif., April 1974, Abstracts*, INOR-24.
125 B.B. Wayland, L.W. Olson, J.V. Minkiewitz and E.F. Smith, *167th Meeting of the American Chemical Society, Los Angeles, Calif., April 1974, Abstracts*, INOR-62; B.B. Wayland and L.W. Olson, *J. Chem. Soc., Chem. Commun.*, (1973) 897.
126 E. Miki, K. Mizumachi, T. Ishimori and H. Okuna, *Bull. Chem. Soc. Jap.*, 46 (1973) 3779.